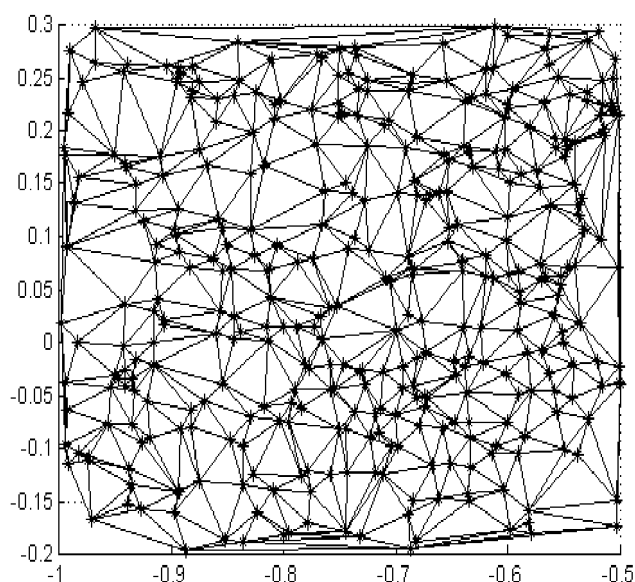


U K R A I N E

K h a r k i v

Spacetime & Substance

International Physical Journal



Volume 2, No. 5 (10), 2001

© 2001 Research and Technological Institute of
Transcription, Translation and Replication
JSC

Spacetime & Substance

International Physical Journal

Certificate of the series AB, No. 4858, issued by the State Committee for Information Policy, TV and Broadcasting of Ukraine (February 12, 2001).

The Journal is published by Research and Technological Institute of Transcription, Translation and Replication, JSC, under Licence of the series DK, No. 184, issued by the State Committee for Information Policy, TV and Broadcasting of Ukraine (September 18, 2000).

It is a discussion journal on problems of theoretical and experimental physics in the field of research of space, time, substance and interactions. The Journal publishes:

- the theories combining space, time, gravitation and others interactions (including the Einstein's SR and GR);
 - application of theories for description and/or explanations of properties of the Universe and microcosmos;
 - mathematical models and philosophical bases, which touch the description of a physical reality;
 - description of set-ups aimed at the realization of fundamental physical experiments and the forthcoming results;
 - discussion of published materials, in particular, those questions, which still have not a correct explanation.
-

The volume of one issue includes 48 pages. Format is A4. Periodicity of the publication: quaterly in 2000; monthly since 2001. The language is English. The equivalent versions: paper and electronic (*.TEX, *.PS, *.PDF).

Editorial Board:

N.A. Zhuck (Kharkiv, Ukraine) — <i>Editor-in-chief</i>	P. Carlos (Rio de Janeiro, Brazil) M.J.F.T. Cabbolet (Eindhoven, Holland)	P.G. Niarxos (Athens, Greece) V.I. Noskov (Moscow, Russia) V.L. Rvachev (Kharkiv, Ukraine) S.S. Sannikov-Proskurjakov (Kharkiv, Ukraine)
V.V. Krasnoholovets (Kyiv, Ukraine) — <i>Vice Editor</i>	P. Flin (Krakow, Poland)	
M.M. Abdildin (Almaty, Kazakhstan)	J. Gil (Zielona Gora, Poland)	V. Skalský (Trnava, Slovakia)
L.Ya. Arifov (Simferopol, Ukraine)	N.D. Kolpakov (Kharkiv, Ukraine)	R. Triay (Marseilles, France)
Yu.A. Bogdanov (Kharkiv, Ukraine)	I.Yu. Miklyaev (Kharkiv, Ukraine)	V.Ya. Vargashkin (Oryol, Russia)
B.V. Bolotov (Kyiv, Ukraine)	V. Mioc (Bucharest, Romania)	Yu.S. Vladimirov (Moscow, Russia)
M. Bounias (Le Lac d'Issarlès, France)	Z.G. Murzakhanov (Kazan, Russia)	<i>(The list is not finished)</i>
J.L. Buchbinder (Tomsk, Russia)	Lj. Nešić (Niš, Yugoslavia)	

Technical assistants: V.V. Moroz (\LaTeX), A.M. Varaksin (Internet)

Subscription information:

The price of one paper unit (in US Dollars) is 2.0 in Ukraine; 2.4 in NIS* states; 10.0 in all other countries. The electronic version price is 25 % of the paper version price.

*) NIS (New Independent States without Ukraine) are Azerbaijan, Armenia, Byelorussia, Georgia, Kazakhstan, Kirghizia, Moldova, Russia, Tadjikistan, Turkmenistan, Uzbekistan.

Accounts:

In US Dollars
Correspondent: THE BANK OF NEW YORK
Eastern Europe Division
One Wall Street, New York, NY 10286
Account No. 890-0260-610
Beneficialry Bank: UKRSIBBANK of Ukraine
In favour of ZEMELNY BANK JSC
Account No. 1600-8-50174-01-00
SWIFT: KHAB UA 2K
Beneficiary: NTI TTR JSC
Account No. 26009011415

In UA Hryvnyas
Account No. 26009011415
in KHAB ZEMELNY BANK,
MFO 351652,
AO NTI TTR,
Cod 24473039,
Kharkov, Ukraine
*(for Ukraine subscribers,
at the rate of the
National Bank)*

The corresponding conformation as to the paying should be sent to the Editorial Office by E-mail.

Editorial Office: Zhuck N.A., RTI TTR, 3 Kolomenskaya St., Kharkov 61166, Ukraine
Tel.: +38 (0572) 19-55-77, (044) 265-79-94. Tel./fax: +38 (0572) 409-298, 409-594, 141-164, 141-165
E-mail: zhuck@ttr.com.ua, spacetime@ukr.net, krasnoh@iop.kiev.ua. <http://spacetime.narod.ru>

© 2001 Research and Technological Institute of Transcription, Translation and Replication, JSC

QUASARS AND THE LARGE-SCALE STRUCTURE OF THE UNIVERSE

N.A. Zhuck,¹ V.V. Moroz, A.M. Varaksin

*Research and Technological Institute of Transcription, Translation and Replication, JSC
Box 589, 3 Kolomenskaya St., Kharkov 61166, Ukraine*

July 23, 2001²

Regularity in quasars allocation earlier unknown revealing that the quasars are grouped in thin walls of meshes with the medial size about 50–100 Mps, which like a foam homogeneously fill all apparent part of the Universe is determined. For investigation the database on 23760 quasars was used, in which two angular coordinates (Θ, φ) and redshift of radiation spectrum (z) for each quasar are submitted. Distance up to each quasar by redshift was determined by formula $r = R_0 \ln(1+z)$, where R_0 is the constant for the Universe, which equal about 10^{26} m. Next, investigation of quasars spatial distribution in spherical and cartesian co-ordinates is carried out. The Universe part most explored with the help of telescopes and radio telescopes were chosen for this purpose. Delone triangulation is carried out for laminas which thickness is appreciably less than the revealed meshes of large-scale quasar structure. The statistical processing of the finding distances between quasars is executed. The investigations have shown that: for large distances (noticeably are more than 100 Mps) quasars in the chosen part of the Universe without dependence from distances and angular standing in space have averages of distribution, root-mean-square diversion and correlation factors, typical for a uniform distribution of random quantities; in smaller gauges the quasars are grouped in thin walls of meshes (size about 100 Mps), reminding the lather; the quasars allocation in meshes correlates with galaxies allocation; the Universe has no precise boundaries even on distance in 30–40 billions light years. General scientific and weltanschauung significance of discovery that it is cardinally changes our representation about global structure and development dynamics of the Universe as a single whole to confirm the concept of the stationary inconvertible Universe and to reject concept dynamic dilating Universe which erroneously formed in the XXth century and taking the beginning from a so-called the Big Bang, which ostensibly has taken place of 12–15 billions years ago.

1. Introduction

At present, the official science adheres to the commonly accepted concept that the Universe appeared 12–15 billion years as a result of the Big Bang of the substance which had been in tremendously dense and hot state. After that the substance expanded, cooled down, split into the matter and the electromagnetic field and formed galaxies which are believed to continue moving farther apart until now.

Such a model is based on the non-steady solutions of the Einstein equations obtained by Soviet geophysics and mathematician Fridman at the beginning of the 1920s and the concept of the exploding commencement in the dynamics of the Universe advanced by American physicist Gamov at the end of the 1940s.

The objective properties of the Universe, which allegedly confirm this model, are the discovery of the red shift in the spectra of galaxies by American astronomer Hubble in 1929 and the Cosmic Microwave Background

Radiation at the temperature 2.7 K by American radio astronomers Wilson and Pansias in 1965. It is considered that the allocation of quasars in the Universe confirms the Big Bang too (see Appendix I).

The first discovery was interpreted by scientists as the result of the motion of galaxies away from each other and the second discovery was construed as the remainder (relic) of the electromagnetic radiation which had segregated from the initial substance and then cooled down to the said temperature during the expansion of the Universe.

The above-mentioned properties of the Universe, incidentally, are not the direct evidence of its expansion. For instance, the decrease in the frequency of light can be the result of either the expansion of the Universe or the dissipation of the energy of light when it spread at great distances, while the osmic Microwave Background Radiation can be either the remainder of the high-temperature explosion of the super dense substance or the total radiation of all stars of the stationary Universe with the said dissipation of the energy of light.

As a result of many errors, the modern official cosmology, in opinion of the authors, has reached the dead-

¹e-mail: zhuck@ttr.com.ua

²Report at the scientific seminar in the Kharkiv National Technical University of Radioelectronics (Kharkiv, UKRAINE)

lock in the development. In works [18]–[40], N.A. Zhuck (the co-author of this work) has attempted to construct alternative cosmology by digging around the foundations of physics and re-shaping its superstruction. As a consequence, a new stationary model of the Universe, which takes into account the more refined laws of physics (or their new interpretation), has been constructed (see Appendix II).

The Universe represents a giant physical laboratory, in which fundamental physical theories are verified. Cosmology is one of the tools of this laboratory. The subject of study of cosmology is the General Relativity is one of the two theories, on which the construction of modern physics (the second theory is quantum theory) is based. Perhaps it is this major role that cosmology plays in the life of mankind.

The new cosmological model is confirmed by 40 properties of the actual Universe (observations or results of experiments). The quasars are the farthest visible objects of the Universe (Appendix I). They are excellent object for investigation by means of the new stationary model of the Universe.

2. Initial database on quasars and transformation of their coordinates

The researches of quasars were carried out not only through telescopes. The considerable interest for researches was represented the fixed coordinates of already discovered quasars. The statistical researches of quasar distribution in space in increase process of quantity of discovered quasars gave the more and more interesting results.

The database on 23760 quasars was used for our investigation, in which two angular coordinates (Θ, φ) and redshift of radiation spectrum (z) for each quasar are presented [41]. The fragment of an initial database is presented in Tab. 1.

Distance up to each quasar by redshift was determined by formula

$$r = R_0 \ln(1 + z), \quad (1)$$

where R_0 is constant typical for the Universe approximately equal in 10^{26} m (see Appendix II). $R_0 = 1$ is assigned for calculating of distances up to quasars and for build-up of figures.

The formula (1) is derived out of the distribution law of light at a large distance

$$\nu = \nu_0 e^{-\frac{r}{R_0}}. \quad (2)$$

It is the very important formula. We presented two derivation of this formula in Appendix III and Appendix IV.

Table 1: Fragment of the initial database

No.	RAJ2000 "h:m:s"	DEJ2000 "d:m:s"	z
1	00 00 01.3	-02 02 00	1.356
2	00 00 02.8	-35 03 33	0.508
3	00 00 05.6	-27 25 10	1.930
4	00 00 09.9	-30 55 30	1.787
5	00 00 10.2	-31 59 50	1.638
6	00 00 12.0	+00 02 24	0.479
7	00 00 12.9	-02 10 25	1.450
8	00 00 16.3	-31 44 38	1.452
9	00 00 17.4	-08 51 23	1.250
10	00 00 20.2	-32 21 01	1.275
11	00 00 22.9	-02 27 15	0.590
12	00 00 23.7	+02 12 41	0.810
13	00 00 24.4	-12 45 48	0.200
14	00 00 24.8	-30 50 49	1.465
15	00 00 36.0	-31 19 25	2.013
...
23760	23 59 59.3	+08 33 54	0.084

Calculation of quasars coordinates in spatial spherical coordinates is carried out by the formulas (in radians; the corner φ_1 is measured from North Pole)

$$\Theta = \left(\Theta_h + \frac{\Theta_m}{60} + \frac{\Theta_s}{3600} \right) \cdot \frac{\pi}{12}; \quad (3)$$

$$\varphi_1 = \frac{\pi}{2} - \varphi \cdot \frac{\pi}{180}, \quad (4)$$

where

$$\varphi = \begin{cases} \varphi_d + \frac{\varphi_m}{60} + \frac{\varphi_s}{3600} & \text{if } \varphi_d \geq 0; \\ \varphi_d - \frac{\varphi_m}{60} - \frac{\varphi_s}{3600} & \text{if } \varphi_d < 0. \end{cases} \quad (5)$$

Calculation of quasars coordinates in spatial cartesian coordinates is carried out by the formulas (in R_0)

$$X = r \cos \Theta \sin \varphi_1; \quad (6)$$

$$Y = r \sin \Theta \sin \varphi_1; \quad (7)$$

$$Z = r \cos \varphi_1. \quad (8)$$

In further, the database was sorted for spherical coordinates by increment of distance up to quasars and for cartesian coordinates by increment of coordinate Z (for convenience of investigations).

The preliminary investigations have shown that the observed quasars locate on the coelosphere non-uniformly. Especially it concerns those places where North Pole, South Pole and the oceans are located (Fig. 1).

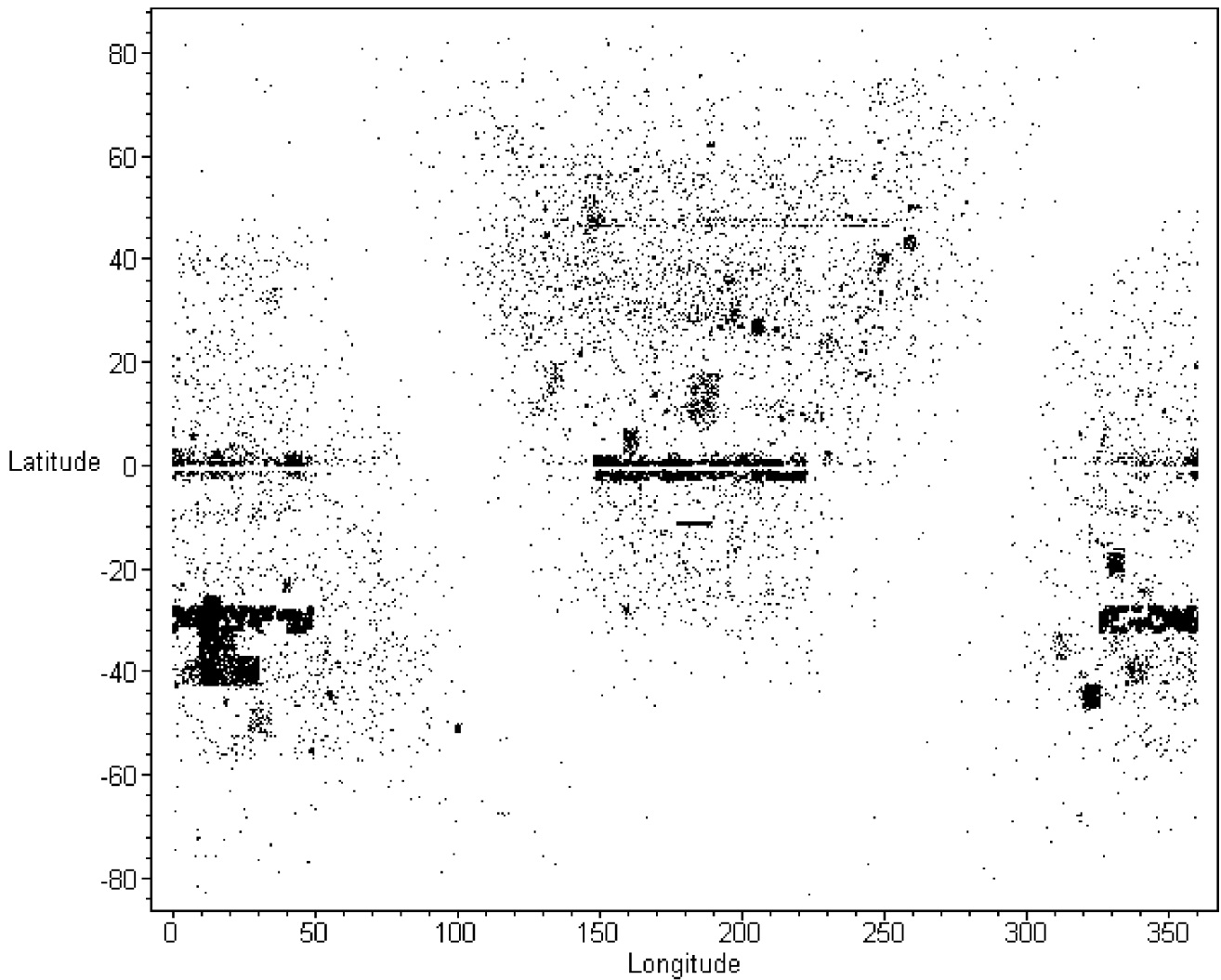


Figure 1: Allocation of discovered quasars on the coelosphere

3. Estimation of global homogeneity of quasars allocation

It is considered that density of a spatial distribution of quasars is fast incremented in range of values $z \cong 2 - 3$, and then is sharply reduced for large values of redshift (see Appendix I). Below we shall show that it not so.

Investigation of quasars spatial distribution in spherical and cartesian co-ordinates is carried out. The Universe part most explored with the help of telescopes and radio telescopes were chosen for this purpose. Delone triangulation is carried out for laminas, its thickness is appreciably less than the revealed meshes of large-scale quasars structure (the multitude of lines pairing each quasar to its nearest neighbors without their mutual crossing is constructed). Thus the particular set of distances between quasars has turned out. Further the statistical processing of set of these distances was

carried out.

In the beginning we have separated a thin layer of the Universe in a plane of the Earth equator (plane OXY, the axis OZ is directed to the North Pole, Fig. 2). Further we chose the most explored areas of the Universe for the analysis. Here we shall show two typical areas for an example (see Fig. 3).

The area 1 has the following sizes: $X = -1.0... - 0.5$, $Y = -0.2...0.3$, $Z = -0.03... - 0.01$ (in R_0). About 379 quasars are in this area.

The area 2 has the following sizes: $X = -0.9... - 0.7$, $Y = -0.6... - 0.4$, $Z = 0.03... - 0.1$. About 132 quasars are in the area 2.

Allocation of the quasars in the area 1 is shown in Tab. 2 and allocation of the quasars in the area 2 is shown in Tab. 3.

As have shown these investigations, average values, standard deviations and correlation factor practically

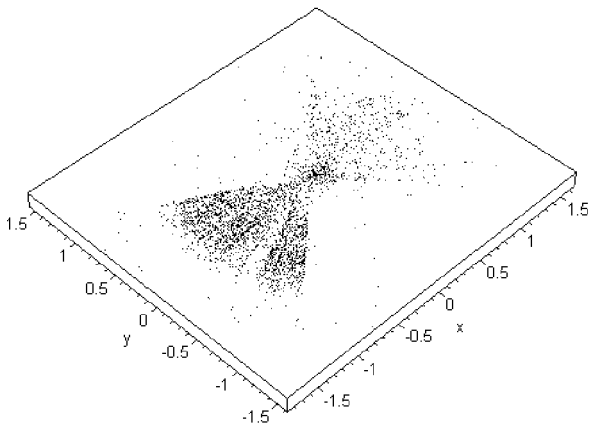


Figure 2: Thin layer of the Universe in a plane of equator

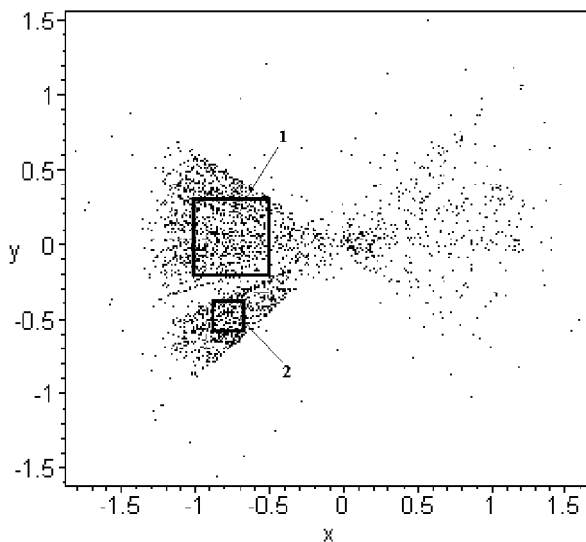


Figure 3: Standing of the areas 1 and 2

Table 2: Allocation of the quasars in the area 1

Description	Calculation	Theory
Mean m_x	-0.7307693464	-0.75
Mean m_y	0.05896529208	0.05
Standard-deviation σ_x	0.1415179730	0.1443375673
Standard-deviation σ_y	0.1364377974	0.1443375673
Linear-correlation k_{xy}	0.1089561031	0

Table 3: Allocation of the quasars in the area 2

Description	Calculation	Theory
Mean m_x	-0.8062837008	-0.8
Mean m_y	-0.4992200605	-0.5
Standard-deviation σ_x	0.05747427049	0.0577350269
Standard-deviation σ_y	0.06059568292	0.0577350269
Linear-correlation k_{xy}	-0,1016258970	0

coincide with similar parameters of uniform distribution of random quantities, i.e. with the theory. It is impossible to term these results and results of other similar investigations as ordinary accidental coincidence. Obviously that we have the facts confirming that the quasars are distributed uniformly in the Universe, and the Universe is stationary.

Next, the investigation of quasars allocation within the concept of the Big Bang of the Universe was carried out with determining of distances to each quasar in accordance with redshift but the method generally accepted in cosmology.

The investigations have shown that at the second method of distances definition:

a) quasars density grows to the Universe boundary which restricted by radius 12–15 billions of light-years, it correspond to the theory of Universe expansion from more its dense state in the past;

b) meshes in which walls the quasars are concentrated not only change in size, but also that most important, are deformed (are flattened) as approaching to the Universe boundary that cardinaly contradict to the theory of the explosion for which is typical the homogeneous expansion of a substance and, accordingly, proportional expansion of the sizes of the indicated meshes.

Thus, the second method of distances definition to the quasars and theory of the dilating Universe, from which this method follows, is necessary to consider erroneous, not relevant to the laws of physics and the observed phenomena of nature.

4. Estimation of local inhomogeneities in quasars allocation

The Delone triangulation is a set of lines pairing each quasar with its nearest neighbouring quasars. These lines not intersect and to form the delta circuits. From here the name of the triangulation method was formed.

The Delone triangulation allows to determine all distances between quasars in thin area of the Universe (i.e. practically on a plane). Further the statistical

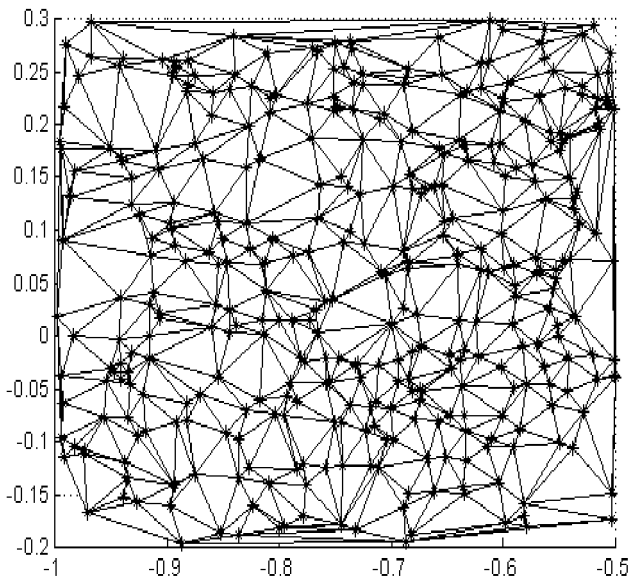


Figure 4: Delone triangulation in the area 1

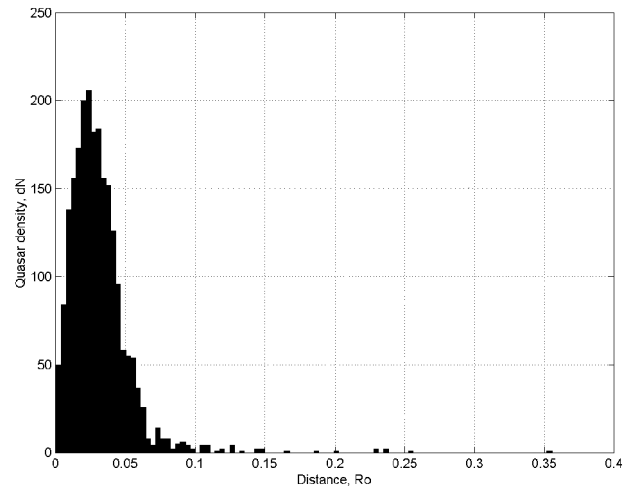


Figure 5: Histogram of the interquasars distances

handling of multitude of these distances is carried out that allows to obtain objective appraisal of large-scale allocation of quasars in the Universe, and also to determine structure of the Universe as a whole. After that the initial model of the Universe is confirmed or rejected.

We shall show for example how the Delone triangulation method for area 1 was used. We shall remind that about 380 quasars are in this area. Thus about 750 distances between quasars is formed provided that the lines between quasars are not intercrossed (see Fig. 4).

Further we have constructed a histogram (Fig. 5). Here density of quasars dN is put aside on a vertical axis. Distance between the nearest quasars is put aside on a horizontal axis. The histogram shows that the distances $r_{dNmax} = 0.024R_0$ come across most frequently. Taking into account that $R_0 \approx 10^{-26}$ m, $1 \text{ ps} = 3.1 \cdot 10^{16}$ m, this distance is equal about 77.4 Mps. It practically is equal to diameter of Universe honeycomb, which is estimated approximately in 50–100 Mps.

It is obvious, that on the obtained histogram the greatest distances (more than 0.1–0.15 radiuses of gravitational interactions) should generally be excluded from the analysis, as they are interlinked with edge effects, i.e. that the isolated part of the Universe without the taking into account of presence of neighboring quasars was considered.

5. Discussion

The analysis of the received results has allowed to decide that:

I. The new method of distances definition (1) up to quasars does not contradict observed phenomena

and common sense, quasars in cosmological gauges distributed uniformly, and in smaller gauges form a foam mesh structure of the Universe with the size of meshes about 100 megaparsecs.

II. The old method of distances definition up to quasars gives the results, which contradict known standings of the explosion theory and common sense. Therefore, concept of the Big bang of The Universe is also untrue.

III. The accepted results of the astrophysicists are untrue asserting that the quasars concentrate on particular distances and are typical for a particular period of the Universe life, as in their investigations the general dependence of quantitative density of quasars on distance was considered, but their spatial distribution, inhomogeneity observation of sky both on corners, and on distance up to quasars was not taken into account.

6. Conclusion

The investigations have shown that:

a) for large distances (noticeably are more than 100 Mps) the quasars in the chosen part of the Universe without dependence from distances and angular standing in space have averages of distribution, root-mean-square diversion and correlation factors, typical for a uniform distribution of random quantities;

b) in smaller gauges the quasars are grouped in thin walls of meshes (size about 50–100 Mps), reminding the lather;

c) the quasars allocation in meshes correlates with galaxies allocation;

d) the Universe has no precise boundaries even on distance in 30–40 billions light years;

e) asserting that the quasars concentrate on particular distances and are typical for a particular period of the Universe life is untrue;

d) the Universe is stationary system.

General scientific and weltanschauung significance of discovery is that, it cardinally changes our representation about global structure and development dynamics of the Universe as a single whole to confirm the concept of the stationary inconvertible Universe and to reject concept dynamic dilating Universe which erroneously formed in the XXth century and taking the beginning from a so-called the Big Bang, which ostensibly has taken place of 12–15 billions years ago.

The discovery confirms revealed earlier by one of the co-authors N.A. Zhuck the physical laws of the Universe functioning and competence of their practical use for cognition of the world and practical needs of a man.

Appendix I

GENERAL INFORMATION ABOUT QUASARS

Investigations of the Universe through radio telescopes have resulted in discovery such surprising objects as quasars. The increased resolving ability of radio telescopes has served as the background of quasars discovery. It has allowed defining the coordinates and angular sizes of objects emitting radio waves with more accuracy than earlier.

Quasars discovery

Two 27-meter antennas of the California technology institute which locate in Owens valley represented in pair with each other the radio interferometer have begun coordinates measurement of the radio emission sources which have been recorded in the 3rd Cambridge catalogue (3C) in 1960. The accuracy of coordinate determination has reached $\pm 5''$ and as result measurements was discovered that some sources have the very small angular sizes.

September 26, 1960. T. Met'juz and A. Sandage have photographed on a 200-inch telescope of the sky area containing one of such sources 3C 48. Within a rectangle of coordinates errors in this area there were no objects except for the star $16^m, 2V$. Around the star there were tracks of feeble nebula but the object looked star-shaped. October 22, 1960. A. Sandage has investigated a spectrum of the discovered object, in which there was a strong combination of broad emission lines, which was impossible to identificate. Any of spectral lines was not possible to know in its spectrum, lines was not possible to identify no with one chemical element. The color indexes 3C 48 were unusual too, they

corresponded to very hot objects with ultra-violet excess.

By 1962 T. Met'juz and A. Sandage have identified with star-shaped objects the radio emission sources 3C 196 and 3C 286. 1963 became decisive, to this time of K. Hazard, M. Makkej and A. SHimins with record accuracy determined the coordinates of radio emission source 3C 273. The object has appeared double with distance between components in $19''$ and diameter of each source less $10''$. One of source components coincided with "feeble star" ($m_V = 13^m$). Young Dutch astrophysicist Maarten Schmidt on observatory Mt. Palomar has investigated the spectrum 3C 273, in which again there were incomprehensible emission lines. Just he has supposed that these lines can be identified with the Balmer hydrogen line if to admit redshift equal 0.158.

The correctness of line identification offered by Schmidt was proved by Dj. Ouk, which has found in the infrared spectrum 3C 273 line H_α in accuracy on that place where it should be with offered value of redshift. After the specified event T. Met'juz and Dj. Grinstejn identified lines in the spectrum 3C 48 having supposed redshift $z = 0.367$.

Nine such objects became known to the end of year and then the flow of discovery has gushed when became clear on what attributes is possible them to search. By 1967 was already found about 150 quasi-sidereal radio emission sources (quasistellar source, QSS), in 1977 them became 370 and very soon the name quasar (for such objects) was coined.

Basic observed properties of quasars

The quasars at observation through a telescope look like as star-shaped objects, which besides are strong sources of radio emission. They have excess of radiation in ultra-violet and infrared area of a spectrum. Spectrum contains broad lines of radiation, always strongly shifted in the red side.

The quasars have a number of surprising properties:

a) The power of their electromagnetic radiation is extremely great from 10^{37} up to 10^{40} W. For comparison we shall specify that the power of radiation of our Galaxy amount approximately 10^{37} W. It is supposed, that this high-power radiation can arise at a gravitational collapse of huge weight from 10^6 up to 10^{10} Solar weight;

b) The spectrum of radiated light finds out strong redshift characterized in parameter $z = \Delta\lambda/\lambda$, where λ - wavelength of observation light, and $\Delta\lambda$ - its redshift in the side of long waves. This redshift is so great that, for example, the line α of series Lyman in a hydrogen spectrum, at standard conditions observed in ultra-violet area, appears in a visible part of a spectrum;

c) The quasars change their brilliance, at some the oscillation frequency of brilliance reaches up to 3^m and more. For example, the quasar 3C 279 has the amplitude amount almost 7^m and in a maximum of brilliance it is one of the brightest objects of the Universe, its $M_B = -31^m, 4$;

d) Feeble nebula ambient quasars were discovered, radiation of nebula so feeble, that for their ephemeral view the English and American astronomers named them beautifully as “fuzz”. So, in the center of such “fuzz” which is the size of a giant galaxy, a quasar like dense, tiny corn of a poplar in its shell is located.

The energy-release of quasars is huge. The luminosity of our Galaxy as was already mentioned amounts to about 10^{37} W; the quasar luminosity on some orders is higher. Total energy emitted by quasars is estimated in 10^{54} watt-second. It is in 10 billions times more than the Sun has emitted for all time of its existence. Variability of quasars radiation is found out both in optical and in a radio-frequency range. The oscillations of luminosity occur in times by an irregular mode about one year and less (up to several days). Therefore, it is possible to make a conclusion, that the sizes of quasars do not exceed a route transited by light during essential change of luminosity otherwise variability would not be observed. Hence, it is indirectly possible to estimate the sizes of quasars, their diameters do not exceed one light year, i.e. the quasars are smaller even of single galaxies (For comparison the diameter of our Galaxy about 100 thousand light years). From here follows that all the huge energy of a quasar is generated in an insignificant small volume.

Starting from such observed quasars properties several guesses were made:

Either

1) Or these objects located very much far outside a Galaxy and luminosity of objects in 100 and more time exceeds a luminosity of giant galaxy,

2) Or the quasars are objects thrown out from a kern of a Galaxy with tracks of explosive activity of kerns and moving with huge velocity, then distance up to them can be estimated by value about 106–107 parsecs, hence, and these objects radiate much less energy.

In the beginning the observed redshift tried to explain at the expense of Doppler effect. Then the quasars should flee from us with huge velocity. Quite often therefore it is possible to meet in the literature the identification of the parameter z with the relativistic Doppler shift $z = \sqrt{(1+u/c)/(1-u/c)}$, which comes on change to nonrelativistic Doppler shift $z = u/c$, when the relative velocity u becomes close to velocity of light in vacuum c . Thus, the quasars should flee from us with velocity, close to velocity of light in vacuum. Such explanation, however, looks rather doubtful. Besides, the guess suggested in this connection that the quasars represent objects thrown out by kerns of galaxies of a Local galactic congestion with almost velocity

of light removed from us no more than on 10 millions a parsec (1 parsec = 3.26 light years = $3.1 \cdot 10^{16}$ m), puts many new problems.

Today almost everyone recognizes that the shift of quasar spectra in the side of long waves is explained not by Doppler effect, and it generates the cosmological redshift. According to this explanation, the further from us is located a quasar, the more its spectrum is shifted in full conformity with cosmological effect of Hubble.

Cosmological models of the Universe

Any hypotheses and guesses explaining observed properties of the Universe always are formulated on the basis of definite cosmological model. Now in a cosmology there are two main models. The first model is based on a General Relativity (GR) and named as the model of observed Einstein-Fridman Universe. The second model was offered by such scientists as Bondy, T. Gold, F. Hoil and named as the model of the stationary Universe.

In both models is recognized that the large-scale structure of the Universe is identical everywhere and in all directions, i.e. the Universe is homogeneous and isotropic. But “the Perfect cosmological principle” the theory of the stationary Universe says that, besides that the Universe is identical not only everywhere, but also always. In the theory of observed Einstein-Fridman Universe there are solutions of two types. According to first, the Universe is dynamic and is continuously dilating after a so-called The Big Bang (the moment of the Universe birth). In the second version the expansion slows down more and more, and then will be replaced by squeeze and the Universe will be squeezed to a condition of extreme large density (condition of a singularity), and then again expansion will begin.

Today, the cosmological model of Einstein-Fridman is traditional and universally recognized and all explanations of observed properties of the Universe are created, as a rule, on the basis of the specified model.

Hypotheses about a quasars nature within the framework of conventional cosmological model

Quasars as defined stage of the Universe development

The statistical analysis of quasar redshift has shown that the values z in general do not exceed defined value $z \approx 5.5$ and shows the tendency to concentrate in an interval from $z = 1$ up to $z = 3$. In the beginning this is explained that because of absorption of light in interstellar gas the farther objects are inaccessible to modern telescopes. However, later the other explana-

tion was put forward.

According to it even with the help of more perfect telescopes dilating horizons by the observed Universe which allow to glance in its farther past, it is impossible to discover new more remote quasars since before the defined moment they simply did not exist. And this moment already now is within the reach of our telescopes. According to this cosmological interpretation since the radiation received by us from quasars today goes up to us about 10 billions years then the researchers observing the quasars is looking in the past of the Universe on 10 billions years back. The Universe then was at earlier stage of development and the processes taking place in its, differed by huge energies. It also explains unusual power of quasar radiation.

Starting from such guess, it is possible to consider, that the quasars correspond to a defined phase of development of the Universe as a whole, and are a characteristic feature for its, far past. Accordingly, up to quasars existing on early phases of the Universe development there should be huge distances, which the observations confirm.

Confluence of galaxies as the reason of a quasars phenomenon

Observations and researches of the “fuzz” images around quasars have resulted in new discovery. It is discovered that many of the “quasars” galaxies interact with other galaxy. Percent of such pairs is rather high and it reaches 30 % in the systems with small redshift [11]. Such facts observed allow to suppose that phenomenon of a quasar in many cases can be aroused by the galaxies interaction.

The specified hypotheses are that the interaction of galaxies strongly perturbs motion of gas in a system, and it falls to the center of a galaxy. There, a supermassive black hole “gobble up” it and this process is accompanied by liberation of huge quantity of energy, which we observe as a phenomenon of a quasar.

The modern researches show that the processes of confluence galaxies and the processes of activity of galactic kerns correlate among themselves. In this connection it is possible to suppose, that the epoch of quasars formation can be simultaneously by epoch of formation of massive galaxies at the expense of merging less massive units (dwarf galaxies). Straight observations of master’s galaxies (galaxies, which swallow up other galaxy) the nearest quasars through the Hubble telescope have given confirmation of straight connection the activity with interaction and confluence of galaxies. In particular, in case of master’s galaxy of quasar PKS 2349 is discovered that the satellite galaxy of a scale BMO is immersed in its.

According to the above-stated the quasars represent a rather complicated accretion system around a supermassive black hole located in the center of a mas-

ter’s galaxy. It is so-called accretion disk and a shaded disk or thick disk on which axis the radiolet is directed in case of radioloud objects, the system of fast flying clouds, which shape broad optical emission lines, and on large distances behind a disk give narrow optical emission lines.

Similar “assembly” of galaxies is observed with the help of the Hubble telescope on redshift about 2–3. Such process can explain both as fast decrease of number of quasars from the past to the present and well-known rupture in their distribution on large redshift. The radioloud quasars in model of confluence communicate with the rotation of a black hole, which is initiated or recent “strong” confluence of a comparable weight galaxies or rather small quantity of “feeble” confluence of a massive galaxy with dwarfs. Besides it is considered, that the confluence lead to occurrence of activity of galactic kerns.

Quasars as a defined phase of a galaxy life

Many characteristics of quasars are observed and at galaxies, i.e. between quasars and galaxies there is a continuous connection. Such galaxies reveal in the spectrum strong ultra-violet excess, some have appreciable redshift and are not sources of radio emission. The brightness of galaxies are much less than quasars. The radio emission was also found in some galaxies they were named by N-galaxies.

The spectra of quasars are similar to spectra of kerns Seyfert galaxies that in the field of the kern have broad emission lines indicating on the motion of large mass of gas. The energy distribution in a spectrum is also similar. The characteristics both radio emission and polarization of quasars light and galaxies differ from each other a little. The high-power flows of infrared radiation are observed both from quasars and from kerns Seyfert and radio galaxies. Therefore, hypotheses were put forward that the quasars are active and superpower kerns of remote, young galaxies.

Especially important and convincing evidence of nature unity of quasars and galaxies was the detection in 1967 by Dj. Ouk of brilliance variability of a unobstructive radio galaxy 3C 371 with amplitude about 2^m . The brilliance variability of several N-galaxies and Seyfert galaxies soon also were discovered. It turned out, that the brilliance variability is not a unique property of quasars, and this property is peculiar to galaxies with an active kern.

The likeness of quasar properties with properties of kerns Seyfert galaxies has given the basis to assume that the quasars are kerns of young galaxies.

More late observations in the beginning of 70’s and in 80’s years of XX century have shown that the discovered feeble nebulas around quasars in color are similar to late blue spiral galaxies and sometimes are even bluer. The blue color of galaxy indicates upon plenty

of young massive stars. It can mean that a nebula represents a young galaxy in which there is a high-power process of star formation.

In 1982 the American astronomers T. Boroson, Dj. Ouk, K. Grinss could found a good spectrum of nebula around quasar 3C 48 and have found in it, a narrow, typically stellar line of magnesium absorption. It was the first direct proof that the quasars are surrounded by stellar component and they are possibly considered as kerns of born galaxies.

Conventional representations about quasars distribution in space

Detection chronology of new quasars, a ways of their search

Since the moment of discovery the quantity of the detected quasars is constantly increased. In process of perfection of technical and methodological means of search and identification it is discovered more and more far quasars. But if to analyse the detection chronology of these objects then the next feature of quasars comes to light.

From the moment of quasars discovery in 1963 the process of detection of new quasars went very fast, but after achievement by redshift of value $z = 2$ dynamics of this process was considerably slowed.

If to analyse technical ways of quasars detection, it is possible to see, that at first mainly the radioloud quasars are discovered then since 1965 radiosilent quasars are discovered. They are discovered as blue objects, using the test of "ultra-violet excess". But such technique of quasar detection becomes inefficient at values of redshift exceeding 2 and this fact could explain slowing down the rates of discovery of new quasars.

At the end of 80's of XX century new more effective optical techniques of quasar detection have appeared. It has allowed in the first time, to discover quasars with large value of redshift. But, despite of large-scale researches with application of modern tests of detection and identification it was very difficult to find quasars with redshift exceeding 5.5. The question emerges whether it is possible to discover quasars with large value of redshift. Despite of limitations in modern methods of detection the quasars in general should be discovered at values $z > 5.5$. Such situation has resulted in the guess that on farther distances the quasars practically do not meet. And density of a spatial distribution of quasars is fast incremented in range of values $z \cong 2 - 3$, and then is sharply reduced for large values of redshift (see Fig. I.1).

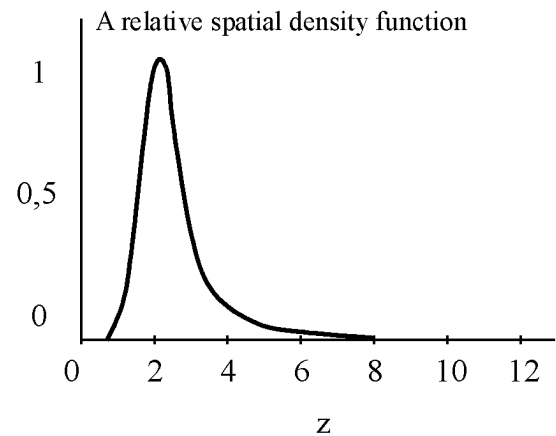


Figure I.1: A relative spatial density function of quasars

Periodicities in quasars spectra

The researches of quasars were carried out not only through telescopes. The considerable interest for researches was represented the fixed coordinates of already discovered quasars. The statistical researches of quasar distribution in space in increase process of quantity of discovered quasars gave the more and more interesting results.

The researches of quasar distribution were carried out on different parameters including on value of redshift z . Thus in general, histograms of distribution are built, explored peaks in quasar distribution especially nearby $z = 1.95$, but the further statistical analysis, as a rule, was not carried out.

The correlation analysis of a histogram of quasar distribution was carried out in 1971 by Carlsson [9, 10], who has revealed qualitatively new feature of distribution of quasars in space, the periodicity of distribution on argument $\ln(1+z)$. Calculation of an auto correlation function has confirmed presence of the specified periodicity. The sample of 166 objects was explored, and the period P on argument $\ln(1+z)$ has made 0.205.

Such fact, in a spatial distribution of quasars on redshift required an explanation, and originally reason of occurrence such irregularity was seen in techniques of quasars detection (effects of selection). But in the further the conclusion about strong influence of effects of selection was doubted and the objections against non-uniformity in distribution of quasars on $\ln(1+z)$ were rejected.

The statistical researches of coordinates of discovered quasars were continued, the more and more new samples, for a lot of objects were under construction, but the result remained the same, the redshift of discovered quasars tended to avoid some intervals z .

Today, the researches of periodicity in a spatial dis-

tribution of quasars are continued, but precise physical interpretations within the framework of conventional cosmological model of the Universe have not obtained.

Conclusion

Any facts observed should be liable to careful understanding and what obvious was this or that fact always there should be a defined shadow of doubt in the validity of interpretation of this fact.

As it was possible to see, within the framework of the traditional cosmological model there are enough of difficulties and contradictions at interpretation of discovered properties of the actual world.

Appendix II

MODEL AND PHYSICAL LAWS OF THE UNIVERSE

Introduction

The Universe is the study subject of cosmology. Cosmology is the general part of mathematics, physics, astronomy and philosophy, which studies the structure, evolution, and physics laws of the Universe as a whole.

The integral notion about the Universe puts cosmology in a special position in relation to other sciences. Indeed, if any other science can study its subject fully and comprehensively the investigator of the Universe can only examine part of the subject. Since the whole can exhibit such characteristics which are not present in its parts, the difficulties cosmology has been facing at all times can be understood.

The essence of the difficulties has always been as follows: any physical theory could not fully explain the observed properties of the Universe. If the theory was somehow adjusted to describe some properties of the Universe, the consequence that emerged did not agree with other known features or fell outside the common sense.

The situation is also aggravated by the fact that the Minkowski space-time in the General Relativity [2, 3], which represents the theoretical foundation of modern classic cosmology, is described by ten variables, while the theory itself offers only six independent equations. Therefore, it is no wonder that no one could construct an objective pattern of the world yet based only on the equations of the General Relativity.

As a result of discrepancies in the theory, particular hypotheses needed to be advanced to explain certain properties of the Universe. For this reason, many different models of the Universe have appeared. Unfortunately, no one of them fully satisfies all the requirements of the laws of logic or conforms to the real world.

At present, the official science adheres to the commonly accepted concept that the Universe appeared 12–15 billion years as a result of the Big Bang of the substance, which had been in tremendously dense and hot state. After that the substance expanded, cooled down, split into the matter and the electromagnetic field and formed galaxies, which are believed to continue moving farther apart until now.

Such a model is based on the non-steady solutions of the Einstein equations obtained by Soviet geophysics and mathematician Fridman [4, 5] at the beginning of the 1920s and the concept of the exploding commencement in the dynamics of the Universe advanced by American physicist Gamov [6] at the end of the 1940s.

The objective properties of the Universe, which allegedly confirm this model, are the discovery of the redshift in the spectra of galaxies by American astronomer Hubble [8] in 1929 and the Cosmic Microwave Background Radiation at the temperature 2.7 K by American radio astronomers Wilson and Penzias in 1965 [16].

The first discovery was interpreted by scientists as the result of the motion of galaxies away from each other and the second discovery was construed as the remainder (relic) of the electromagnetic radiation which had segregated from the initial substance and then cooled down to the said temperature during the expansion of the Universe.

The above-mentioned properties of the Universe, incidentally, are not the direct evidence of its expansion. For instance, the decrease in the frequency of light can be the result of either the expansion of the Universe or the dissipation of the energy of light when it spread at great distances, while the Cosmic Microwave Background Radiation can be either the remainder of the high-temperature explosion of the super dense substance or the total radiation of all stars of the stationary Universe with the said dissipation of the energy of light.

The question about the model and the laws of the Universe is comparable with a problem of what is prime: an egg or a hen. So if we define cosmology as the science about the Universe, we are immediately facing the problem of what is initial: the model of the Universe from which the law of physics of the Universe follow, or the laws of physics of the Universe, on the basis of which the model of the Universe is constructed?

Apparently, the problem does not need a direct answer. However, a third question, which is as if a quasi-superstructure over the dilemma about the primacy of the model or the laws of the Universe, requires resolving. The point is about the proportion and interrelation of such philosophical categories as the “whole” and the “part” and also the philosophical law of quantitative changes passing into qualitative changes. Here again, strictly parallel movement is needed.

To study the whole by its part, it is important to have continuous integration of notions on the subject of

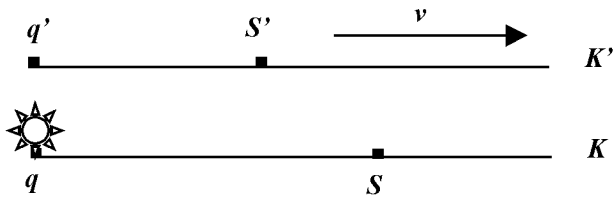


Figure II.1: Systems of readout

the investigation from different points of view at every stage of its investigation and continuous coordination of outcomes of the theory under development with the objective reality. Non-observance of the principle of conformity, occurrence of internal contradictions, singularities and paradoxes while applying the given theory for the description of the whole indicates to the falsity of the way taken by the investigators. It is the very situation, which has developed in cosmology nowadays, its official theoretic ground being based on the idea of Big Bang.

Light speed is a tensor

Any observer can not simultaneously be in several systems of readout. This fact guesses viewing all the natural phenomena only in one inertial system of readout. Thus there is a problem what is the speed of light of rather propellent objects.

Correctly to answer this problem, we shall consider two inertial systems of readout K , K' and bound with them two rulers, as it is shown in a Fig. II.1.

Let at that moment, when the beginnings of rulers q and q' coincide with each other, the bulb in a point q , bound with a fixed ruler, will light up. In time t light will reach a point S on this ruler. For the same time the relative frame ruler will move and on the contrary point S there will be a point S' . Thus distance, which light has passed along a relative frame ruler on quantity vt will be less than distance which it has passed on a fixed ruler. Hence, observer who is taking place in a point S (that is in fixed system of readout) on the gauges of space and time should make a deduction, that the front of a light wave catches up a point S' along a propellent ruler with velocity $c' = c - v$. At a motion in the opposite direction will be received $c' = c + v$.

All above-stated does not contradict a postulate of a special theory of relativity, as the speed of light is constant only in inertial systems of readout, and c' is a speed of light in one inertial system of readout measured on gauges of space and time of other inertial system of readout. Let's term it as a local velocity of light.

Thus, from this point of view the local velocity of light represents a tensor of the second rank (naturally,

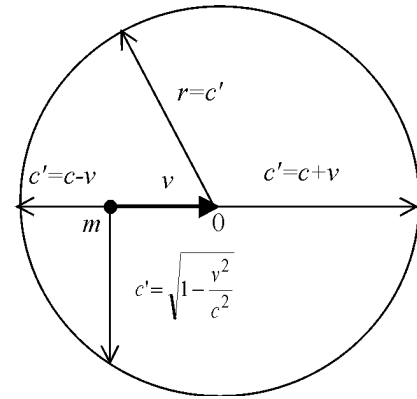


Figure II.2: The tensor of light speed

in three-dimensional space) which all builders by the ends contour a ball of radius $r = c$ displaced in relation to propellent object forward on quantity of velocity v of its motion (Fig. II.2). This ball is a geometrical fashion of a tensor of a local velocity of light [28].

The gravitation law

As it is known, Einstein has offered two views of the equations of the General Theory of Relativity which differ from each other on an addend with the cosmological term λ :

$$R_{ik} - \frac{1}{2}Rg_{ik} = -\varkappa T_{ik}, \tag{II.1}$$

$$R_{ik} - \frac{1}{2}Rg_{ik} - \lambda g_{ik} = -\varkappa T_{ik}, \tag{II.2}$$

where R_{ik} is the Ricci tensor, convolution of the Riman-Cristoffel curvature tensor R^l_{ijk} ; T_{ik} is the energy-momentum tensor of a substance without a substance of gravitational field; g_{ik} is the metric tensor of four-dimension spacetime; R is the curvature scalar, convolution of the Ricci tensor; $\varkappa = 8\pi G/c^4$ is Einstein's constant; c is the light speed; G is Newton's gravitational constant; $i, j, k, l = 1, 2, 3, 4$.

For a unique select of the equations it is necessary to take into account some performance of the Universe. Such performance is global flatness of the Universe which mathematical expression is equality

$$R^l_{ijk} = R_{ik} = R = 0. \tag{II.3}$$

As for the actual Universe filled with substance with deflection density, $\varkappa T \neq 0$, with the account (II.3) the fact of omission of equality (II.1) becomes obvious. Thus, the flat in global gauges Universe can be featured only with the equations (II.2). And, the diversions from flat space-time under activity of material masses can be

presented precisely (precisely!) only in a composition of the total which corresponds to the assignment of a tensor gravitational field h^{ik} on a background of the flat material world in arbitrary coordinates with the metric γ^{ik} [7, 12, 13, 14]:

$$\sqrt{-g}g^{ik} \equiv \sqrt{-\gamma}(\gamma^{ik} + h^{ik}), \quad (\text{II.4})$$

The other, not less important property of the Universe is its homogeneity and isotropy in great gauges. Mathematically this property can be reflected as equality to zero of a covariant derivative(derivative) of tensor density $\sqrt{-g}g^{ik}$ and corollaries of this equality (in Lorentz's coordinates):

$$(\sqrt{-g}g^{ik})_{;i} = (\sqrt{-g}g^{ik})_{;i} = (\sqrt{-g}h^{ik})_{;i} = 0, \quad (\text{II.5})$$

where the point with comma designates a covariant derivative, and the comma is usual derivative.

After that the equations (II.2) with the help of transformation (II.4) and requirement (II.5) are given in the field equations of the General Theory of Relativity

$$\square h_{ik} - \frac{2}{3}\lambda h_{ik} = 2\kappa T'_{ik}, \quad (\text{II.6})$$

where T'_{ik} is an energy-momentum tensor of a substance together with a substance of gravitational field which is oozed from the left-hand part of the Einstein's equations. Under the same requirements in [1, 4] the identity of Lagrangians for a deduction (II.2) and (II.6) is proved also.

Taking into account homogeneity and isotropy of the Universe (that is symmetry of a problem), for a spherical-symmetrical material body of mass m the equations (II.6) give the exterior solution as Yukawa potential

$$\varphi = -\frac{Gm}{r}e^{-\frac{r}{R_0}}. \quad (\text{II.7})$$

The constant R_0 is termed as radius of gravitational interactions and is determined under the formula

$$R_0 = c' \sqrt{\frac{3}{4\pi G \rho_0}}. \quad (\text{II.8})$$

For two of material bodies with masses m_1 and m_2 the following law of gravitation is gained

$$F = G \frac{m_1 m_2}{r^2} e^{-\frac{r}{R_0}} \left(1 + \frac{r}{R_0}\right). \quad (\text{II.9})$$

From the analysis of the obtained law follows that in the actual Universe all the material bodies (planets, stars, galaxies) interreact with each other more feebler than it follows from the law of Newton gravitation.

Identity of inertial and gravitational masses

It is necessary to note that in linear approach the actual law of gravitation (II.9) becomes:

$$F \approx G \frac{m_1 m_2}{r^2} \left(1 - \frac{r^2}{R_0^2}\right), \quad (\text{II.10})$$

which shows, that all material bodies in the Universe interreact with each other practically only in limits of radius of gravitational interactions equal approximately 10^{26} m (or 20 billions of light years).

On the other hand, if to compare an actual law of gravitation and law of gravitation of Newton, it appears that the area under a curve of force of the actual law on an interval from $\mathbf{0}$ up to ∞ is precisely equal the areas under a curve of the law of gravitation of Newton on an interval from $\mathbf{0}$ up to R_0 . Hence, law of gravitation (II.9) valid for the actual Universe, from the energy point of view by the law of Newton gravitation can be replaced restricting radius of activity of forces by quantity R_0 . The given approach allows to decide a series of remarkable problems promptly and obviously.

In view of above-stated we shall analyse, how the area of interaction of a material point of mass m with the Universe will vary at its dispersal up to velocity v and in what all this will give. It is to show that the new area of interaction of a point with medium also will represent a ball of radius R_0 , but moved forward on a course of its motion on quantity r (as in expression for R_0 it is necessary to substitute c'). It is possible also to show that the relation is valid

$$r = \frac{v}{c} R_0, \quad (\text{II.11})$$

Thus, the area of interaction of a propellent mass point displaces forward on a course of a motion proportionally velocities of its motion. In a limit, that is when the velocity of a motion is equal to speed of light the propellent point should be on a surface of its area of interactions. But it just and probably only for light.

At dispersal the point m loses gravitational connection with a part of space u behind of itself and will enter gravitational connection with a part of space w ahead of itself (Fig. II.3). The sizes of the areas both are identical and depend only on velocity v , but the situation of a point m concerning them is unsymmetrical. Hence, the aggregate operation on overcoming forces of a gravitation of area u and forces of a gravitation of area w is not equal to zero.

The author managed to find receptions of definition of this operation. If to take into account a probable initial velocity v_0 a material point, for low speeds the operation has appeared to equal quantity

$$A = \frac{mv^2}{2} - \frac{mv_0^2}{2}. \quad (\text{II.12})$$

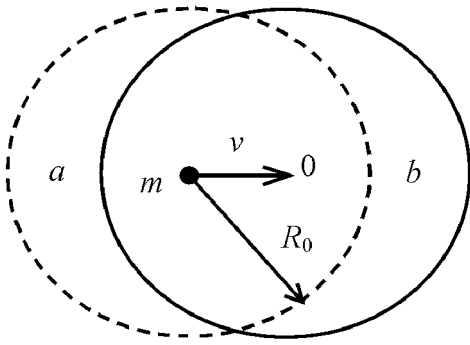


Figure II.3: Change of the interactions area at acceleration of a point

Thus, we have received, known from mechanics the theorem, of change of a kinetic energy of a body. If the obtained expression to differentiate on velocity and on time, the second Newton's law will be received. All this is valid in a relativistic case.

Characteristic feature of the obtained results is that both in the theorem of change of a kinetic energy, and in the second Newton's law not inertial, but gravitational mass enters so long as only such mass considered from the very beginning. So the identity of inertial and gravitational masses spirit of the Mach's principle [15] is proved and the mechanism of interaction of material bodies with the Universe is uncovered.

Gravitational viscosity and geodetic curvature of the Universe

After dispersal (cancellation of local force) of material body along coordinate X its free motion is featured by the equation

$$\frac{d^2 X}{dt^2} + H \frac{dX}{dt} = 0, \quad H = \sqrt{\frac{4\pi G \rho_0}{3}}, \quad (\text{II.13})$$

where H is the Hubble's constant, which has absolutely other physical sense, as it is accepted in a conventional cosmology.

By presence of the second (dissipative) addend the new law of a free motion differs from the first Newton's law. As a whole one of the most prime statements of this law can be such: if the local forces do not act on a body, the standing of its interaction area from the Universe (on the level R_0) in due course does not vary, and it aims asymptotically to the centre of this area.

The new property of the Universe is termed as gravitational viscosity. As the stationary value of Hubble has the order 10^{-18} s^{-1} , the gravitational viscosity practically has no an effect for local processes (for example, in gauges of Solar system). In a distance equal

to half of medial distance between galaxies the forces of the gravitational viscosity become comparable with the centrifugal forces and answer for shaping of the medial-gauge structure of the Universe, that is for shaping of galaxies.

The concept of the gravitational viscosity of the Universe adjoins by a tight fashion to the concepts of affinities (parallel transport of vector) in a non-Euclidean geometry of multivariate spaces. For a motion of the nonconservative systems — that is in the general view — there is a relation for the curvature of space

$$K^j(t) = \frac{d^2 X^j}{dt^2} + \Gamma_{ik}^j \frac{dX^i}{dt} \cdot \frac{dX^k}{dt} = \varphi(t) \frac{dX^j}{dt}. \quad (\text{II.14})$$

The medial addend with Christoffel's figures of the first kind (affine compendency) Γ_{ik}^j indicates a degree of normal curvature of space (we shall term it as geometrical) in which the parallel transport of vector and the letter on change of the length of the vector, that is on the existence of a dissipation of energy. It determines so-called geodetic curvature of space

$$K = \sqrt{g_{ij} K^i(t) K^j(t)}. \quad (\text{II.15})$$

For the actual Universe the geodetic curvature is equal

$$K = K_0 \sqrt{1 - \frac{v^2}{c^2}}, \quad (\text{II.16})$$

where $K_0 = Hc$ is constant for the Universe coefficient equal approximately 10^{-10} m/s^2 .

In the whole the analysis of all the results shows that the motion concerning the Universe has a character of a terrain clearance motion, but on activity of the local physical laws it cannot be noted (except for inertia and red bias in spectrums of radiation of other galaxies).

The propagation law of light and the Hubble's diagram

The analysis of interaction of light with the Universe has shown that gravitational potential ($-c^2$) acts on it, giving power loss and, as a corollary, change frequency ν in relation to initial ν_0 under the law.

$$\nu = \nu_0 e^{-\frac{r}{R_0}}. \quad (\text{II.17})$$

The given law completely permits photometer paradox, explains a nature of red bias in spectrums of radiation of other galaxies without engaging a Doppler effect and gives a new formula of definition of distances up to galaxies

$$L = R_0 \ln(1 + z), \quad (\text{II.18})$$

where z is parameter of red bias of light frequency.

In view of the new law of distribution of light dependence “visual stellar magnitude m — red bias z ” (the Hubble’s diagram) gains a view:

$$m = 5 \lg \{ \sqrt{1+z} \ln(1+z) \} + 21.68. \quad (\text{II.19})$$

In a gamut of apparent values of stellar magnitudes the given dependence practically is linear and completely coincides experimental datas.

The law (II.17) completely explains a nature, numerical performances and character of allocation of background microwave radiation. Actually, it is not a relic of the Big Bang, and aggregate radiation of all radiants of electromagnetic radiation (stars, galaxies etc.) of the Universe. If to integrate the whole radiation impinging on a single site on space from zero to infinitum the temperature of this radiation will be determined by the formula

$$T_0 = \sqrt[4]{\frac{L_s \rho_0 R_0}{4\sigma M_s}}, \quad (\text{II.20})$$

where M_s , L_s is medial mass and complete radiation flow of a medial star (or galaxy); σ is the Stefan-Boltzmann constant.

The evaluations show, that temperature of integrated radiation is equal to several degrees above terrain clearance zero (more precisely to calculate it is impossible), as it is observed actually. And its spectrum corresponds to a radiation spectrum of an absolute black body.

Large-scale structure of the Universe

The actual law of gravitation has a series of pleasant features. So, the evaluation of a binding energy of a material body of mass m from the Universe gives quantity

$$E_0 = -mc^2, \quad (\text{II.21})$$

which is equal precision to an internal energy of a body taken with an inverse. In contrast to it, the law of Newton gravitation gives a minus perpetuity. That is why with application of a Newton’s laws to the infinite Universe the gravitational paradox also has appeared. In the actual Universe with the actual law of gravitation such paradox does not exist, and the mass appears a measure of connection of the given material body with the whole Universe.

The actual law of gravitation gives one more important corollary: with mass shown in interactions with a material body depends on a relation of radius of a body R to radius of gravitational interactions R_0

$$M = \frac{R^2 c^2}{2GR_0} \left(1 - e^{-\frac{2R}{R_0}} \right). \quad (\text{II.22})$$

At $R \ll R_0$ the mass of a body is proportional to its volume, and at $R \gg R_0$ (or that is the same when $R \rightarrow +\infty$) to surface area of a body. It gives in a deduction about ability of a substance to create screen effect. It is capable to explain virial paradox and existence of gravitational-makes of areas of the Universe.

The interesting physical sense has also radius of gravitational interactions (II.8). It appears that it corresponds in precision to radius of a black hole on which surface the speed of light is equal to the first solar escape velocity. Thus, it is possible to tell that we live at in the centre of a black hole, but it is not our privilege, and the property of the Universe to form around of any point gravitational-makes area. By the way acceleration due to gravity on a surface of such black hole is equal only 10^{-10} m/s².

On the other hand, if to unit two identical material objects in one, not changing density the mass of the obtained object shown in interactions will be less than total masses of builders. It also should be expected, as the formally given law is similar to the law of nuclear interactions in the field theory of nuclear forces.

In classical physics there is a special theorem proving that inside a spherical-symmetrical material shell the gravitational field misses or, more precisely, that resultant of force, all the gravitational forces is equal to zero. Using of the actual law of gravitation it has appeared that the closer point is to a shell the stronger it is attracted to it. Differently, any spontaneous obturating of a material medium of the Universe as a shell conducts to the further shaping of such shell. That is why the Universe has cellular structure in major gauges where the aggregations of galaxies are in thin walls of these meshes and superaggregation and on crosses of meshes.

It is necessary to note, that in 1971 Karlsson has found out for the first time a cyclic change of a spectral radiant density of quasars proportional argument $\ln(1+z)$, where z is red bias of their spectrums. Such allocation of quasars correlates with allocation of galaxies forming in the Universe homogeneous thin-walled aggregations as meshes.

In view of the formula (II.18) cyclic changes of a spectral radiant density of quasars are conversed to cyclic dependence of allocation of quasars on distances indicating homogeneity of the Universe not only in space, but also in time, that is on its stationarity for the last a minimum of 40 billions years (so much time the electromagnetic waves went to us from the farthest quasars).

Thus, the author has designed the new stationary model of the Universe which approximately on 40 parameters is compounded with the properties of the actual Universe and has the same right on existence as well as model of Big Bang.

Appendix III

THE FIRST DEDUCTION OF THE PROPAGATION LAW OF LIGHT

From the regularities of the interaction of moving objects with the substance of the Universe, which have been considered in Appendix II, the conclusion is drawn that the gravitational potential should permanently act on a moving photon, i.e., quantum of light. Let us determine the said potential

$$\begin{aligned} \Phi_0 &= -\frac{GM_0}{R_0} = -\frac{G4\pi R_0^3 \rho_0}{3R_0} = -\frac{4\pi G \rho_0 R_0^2}{3} = \\ &= \left| R_0 = c \sqrt{\frac{3}{4\pi G \rho_0}} \right| = -c^2. \end{aligned} \tag{III.1}$$

The result obtained is evidence of a lack of infinite gravitational potentials in a homogeneous and isotropic space. It is in this way that a so-called gravitation paradox is solved. This is first. Second, the photon, when propagating in the space should lose its energy. In fact, the acceleration of gravity on the surface of the range of gravitational interaction is determined by expression

$$g_0 = -Hc, \tag{III.2}$$

in which abbreviation

$$H = \sqrt{\frac{4\pi G \rho_0}{3}}. \tag{III.3}$$

is introduced.

Then, taking into consideration expressions for the energy

$$\left. \begin{aligned} E &= h\nu, \\ E &= mc^2, \end{aligned} \right\} \tag{III.4}$$

which determine the equivalent mass of a photon

$$m_\nu = \frac{h\nu}{c^2}, \tag{III.5}$$

and the energy conservation law, we can write the equality

$$h\nu = \frac{h\nu}{c^2} g_0 dr + h\nu', \tag{III.6}$$

where ν, ν' are frequencies of light before and after the light has passed the distance dr . Planck's constant cancels out the expression. Then allowing that $\nu - \nu' = d\nu$, we get the equation

$$\frac{d\nu}{dr} + \frac{H}{c}\nu = 0. \tag{III.7}$$

Having regard to the relation $c/H = R_0$, we finally obtain

$$\frac{d\nu}{dr} + \frac{1}{R_0}\nu = 0. \tag{III.8}$$

Thereby, we have derived the law of propagation of light for the Universe. It can also be expressed in an integral form, if we integrate equation (III.8),

$$\nu = \nu_0 e^{-\frac{r}{R_0}}. \tag{III.9}$$

As a first approximation expression (III.9) becomes

$$\nu = \nu_0 \left(1 - \frac{r}{R_0} \right) \tag{III.10}$$

or in other presentation

$$\frac{\nu - \nu_0}{\nu_0} = -\frac{H}{c}r. \tag{III.11}$$

Considering the Doppler effect for the source and the receiver of light, which move away one from the other

$$\frac{\nu - \nu_0}{\nu_0} = -\frac{v}{c}, \tag{III.12}$$

(it will be clear later why we use such a presentation), we come to dependency

$$v = H \cdot r. \tag{III.13}$$

This is just the Hubble law. Thus in the linear approximation the law of propagation of light can be easily confused the Doppler effect. This was the case when the redshift in the radiation spectra of outlying galaxies was interpreted as the galaxies bouncing apart, i.e., the universal extension of the Universe. It was no wonder (though also revolutionary), as the Doppler effect had been studied very well and the properties of the Universe as a nonconservative system did not follow from anywhere. Note that the general relativity in its conventional formulation rules out this property of the nonconservative Universe.

The law of propagation of light (III.9) is yet more evidence that the Universe does not expand at all and that the light, when spreading in the space, loses its energy since the light is permanently forced to break away from gravitating masses behind.

The numerical value of Hubble's constant is approximately equal to $1.67 \cdot 10^{-18} \text{ s}^{-1}$, which corresponds to the equivalent speed of 51.6 km/s·Mps of the extension of the Universe.

Presently, the redshift in the spectra of galaxies serves as an instrument to calculate the distance to the galaxies. For this purpose the variable z is used which is expressed via the wavelength of light

$$z = \frac{\lambda - \lambda_0}{\lambda_0}, \tag{III.14}$$

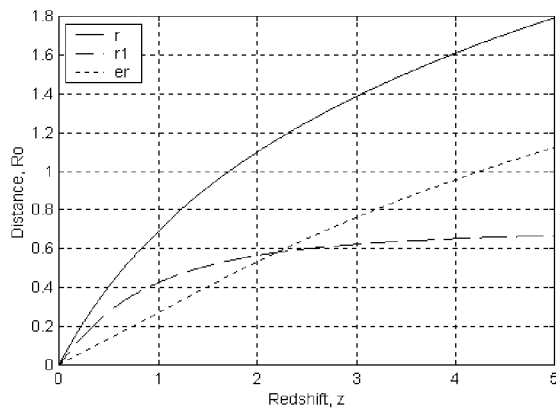


Figure III.1: Diagrams of distances to galaxies and quasars

and the calculated formula [55]

$$r1 = \frac{(1+z)^2 - 1}{(1+z)^2 + 1} \cdot \frac{c}{H}. \quad (\text{III.15})$$

If we utilize the deduced law of propagation of light (III.9), we reveal that the calculated formula should be quite different

$$r = R_0 \ln(1+z). \quad (\text{III.16})$$

In Fig. III.1 diagrams of distances to galaxies are presented: the dash curve $r1$ corresponds to calculations by formula (III.15); the solid curve r corresponds to calculations by formula (III.16); the dotted curve er shows the dispersal of errors if one uses formula (III.15). (When drawing the diagrams, we set $R_0 = c/H = 1$).

It is easy to see from this figure, that when determining the distance to a galaxy by the conventional method, errors become conspicuous starting from $z = 1$. When z arrives at 5...6 the value of the error reaches the magnitude of the measurable parameter itself, i.e., the distance. This leads to errors in the description of the general pattern of the world, though the premises to doubts the correctness of formula (III.15) have existed for a long time.

Appendix IV

THE SECOND DEDUCTION OF THE PROPAGATION LAW OF LIGHT

The unrestricted motion equation of material body in the line of arbitrary coordinate X for free cosmic space (ether) is represented in Appendix II

$$\frac{d^2X}{dt^2} + H \frac{dX}{dt} = 0, \quad (\text{IV.1})$$

where H is the Hubble constant, which evaluate through the gravitation constant G and the average density of the Universe ρ_0 by formula

$$H = \sqrt{\frac{4\pi G \rho_0}{3}}. \quad (\text{IV.2})$$

The equation (IV.1) shows that the ether has viscosity. Also it was shown that the bearer both gravitational, and electromagnetic interactions is the medium (ether) consisting of particles (amer) μ by a mass about 10^{-69} kg.

Considering, that the equation (IV.1) is valid for material body of any nature we apply it for description of motion these particles. On the other hand, taking into account a polarizability of an ether, i.e. the presence in it of elastic properties (that is been confirmed by spread of wavelike processes as electromagnetic waves) in the obtained equation it is necessary to add one more item $\mu\omega_0^2 X$ named the recovery force (here ω_0 is the ether particles oscillations eigenfrequency). As a result the motion equation will be obtained

$$\mu \frac{d^2X}{dt^2} + \mu H \frac{dX}{dt} + \mu\omega_0^2 X = 0, \quad (\text{IV.3})$$

where X is a shift of ether particle at any moment of time.

As the mass of ether particle is been a member of all items of the obtained equation then it is possible to exclude its and to simplify the equation to a view

$$\frac{d^2X}{dt^2} + H \frac{dX}{dt} + \omega_0^2 X = 0. \quad (\text{IV.4})$$

The equation (IV.4) is a desired equation of ether particles motion. We shall search its solution in the form of

$$X = e^{-\frac{t}{2\tau}} \cos(\omega t + \varphi), \quad (\text{IV.5})$$

where τ , ω and φ are unknown quantities. By direct substitution is determined that (IV.5) is a solution of the equation (IV.4) for any φ provided that

$$\tau = \frac{1}{H}, \quad (\text{IV.6})$$

$$\omega^2 = \omega_0^2 - \frac{H^2}{4}. \quad (\text{IV.7})$$

The most common solution of the equation (IV.4) is a superposition of two linearly independent solutions with two initial conditions for shift $X(0) = X_0$ and velocity $(dX/dt)_0 = \dot{X}(0) = \dot{X}_0$ of ether particles by $t = 0$. For example, we shall take $\varphi = 0$ and $\varphi = -\pi/2$. Then common solution of the indicated equation is possible to present as

$$X = e^{-\frac{Ht}{2}} (C_1 \sin \omega t + C_2 \cos \omega t), \quad (\text{IV.8})$$

where C_1 and C_2 are integration constants. For their definition at first we shall determine derivative of expression (IV.8)

$$\frac{dX}{dt} = e^{-\frac{Ht}{2}} (C_1\omega \cos \omega t - C_2\omega \sin \omega t) - \frac{H}{2} e^{-\frac{Ht}{2}} (C_1 \sin \omega t + C_2 \cos \omega t). \quad (IV.9)$$

At $t = 0$ from (IV.9) and (IV.8) we shall have

$$C_1 = \frac{1}{\omega} \left(\dot{X}_0 + \frac{H}{2} X_0 \right), \quad (IV.10)$$

$$C_2 = X_0. \quad (IV.11)$$

After that the expression (IV.8) becomes [1]

$$X = e^{-\frac{Ht}{2}} \left[\frac{1}{\omega} \left(\dot{X}_0 + \frac{H}{2} X_0 \right) \sin \omega t + X_0 \cos \omega t \right]. \quad (IV.12)$$

For feeble attenuation (and it is real so, as $H \approx 10^{-18} \text{ s}^{-1}$ is negligible quantity) exponential factor $\exp(-Ht/2)$ is possible to consider as stationary value during one cycle of oscillations. Under such conditions it is possible to neglect an augend in (IV.9) and easily to show, that the total energy of a particle E (the sum both kinetic and potential) is equal

$$E = \frac{\mu \dot{X}^2}{2} + \frac{\mu \omega_0^2 X^2}{2} = E_0 e^{-Ht}, \quad (IV.13)$$

where the initial value of particle energy E_0 is determined by expression

$$E_0 = \frac{\mu}{4} (\omega^2 + \omega_0^2) (C_1^2 + C_2^2). \quad (IV.14)$$

As in a microworld there is a quantization of energy proportionally by Plank constant h , the energies E and E_0 will be proportional to frequencies ν and ν_0 by the formulas

$$E = h\nu, \quad (IV.15)$$

$$E_0 = h\nu_0. \quad (IV.16)$$

Then from expression (IV.13) we have dependence for decrease of particle oscillation frequency in the time

$$\nu = \nu_0 e^{-Ht}. \quad (IV.17)$$

Being aware of Ref. [28] that the Hubble constant H is bound to radius of gravitational interactions R_0 by dependence (c is velocity of light)

$$H = \frac{c}{R_0}, \quad R_0 = c \sqrt{\frac{3}{4\pi G \rho_0}}, \quad (IV.18)$$

and that $ct = r$ is a distance into which the oscillatory process in space can be spread, we obtain familiar from a cosmology dependence for decrease of frequency of electromagnetic waves with distance

$$\nu = \nu_0 e^{-\frac{r}{R_0}}. \quad (IV.19)$$

On a basis (IV.19) an expression for definition of distances up to far space objects (galaxies and quasars) is obtained

$$r = R_0 \ln(1+z), \quad (IV.20)$$

where

$$z = \frac{\nu - \nu_0}{\nu_0} \quad (IV.21)$$

is a redshift of their radiation spectrums.

The law (IV.19) have been completely proved by observations [28]:

- by real presence of redshift in radiation spectrums of galaxies and quasars;
- by the missing of bright luminescence of the sky at night (contrary to a known photometer paradox of classical physics);
- by presence of microwave background radiation of space which is aggregate radiation of all stars of the Universe with taking into account the law (IV.19);
- by Hubble diagram which in a linear part coincides with the diagram obtained on the basis of the law (IV.19);
- by allocation of galaxies and quasars in space of the Universe (this discovery is still developed).

References

- [1] Crowford F. "The Berkeley course of physics. V. 3. Waves." McGraw-Hill Book Co., 1968.
- [2] Einstein A. "Die Feldgleichungen ger Gravitation. *Sitzungsber. preuss. Akad. Wiss.*, **48**, 2, 844–847 (1915).
- [3] Einstein A. "Die Grundlage ger allgemeinen Relativitätstheorie. *Ann. Phys.*, **49**, 769–822 (1916).
- [4] Friedmann A. "Über die Krümmung des Raumes." *Ztschr. Phys.*, **10**, 377–386 (1922).
- [5] Friedmann A. *Ztschr. Phys.*, **21**, 336–332 (1922).
- [6] Gamov G. *Phys. Rev.*, **70**, 572–573 (1946).
- [7] Grishchuk L.P., Petrov A.N., Popova A.D. "Exact Theory of the (Einstein) Gravitational Field in an Arbitrary Background Space-Time." *Comm. Math. Phys.*, **94**, 379–395 (1984).
- [8] Hubble E. "A relation between distance and radial velocity among extra-galactic nebulae." *Proc. NAS*, **15**, 168 (1929).
- [9] Karlsson K.G. "Possible discretization of quasar redshift," *Astron. and Astrophys.*, **13**, 333, (1971).

- [10] Khodjachich M.F. "Cosmological periodicities in radiospectrums of quasars," *Spacetime & Substance*, 1, 3, 120 (2000) (in Russian).
- [11] Kontorovich V.M., Krivitsky D.S., Kats A.V. "Explosive" evolution of galaxies (an analog of collaps) and appearance of quasars in the merger model." *Physica D* 87, 290 (1995).
- [12] Logunov A.A., Mestvirishvili M.A. *Progr. Theor. Phys.* 74, 31–50 (1985).
- [13] Logunov A.A., Mestvirishvili M.A. *Sov. Particles and Nucleas.* 17, 1–153 (1986).
- [14] Logunov A.A., Mestvirishvili M.A. "The Relativistic Theory of gravitation." Moscow, Nauka, 1989, 304 pp. (in Russian).
- [15] Mach E. "Die Mechanik in Ihrer Entwicklung, Historisch-Kritisch Dargestellt." Leipzig: Brokhaus, 1883.
- [16] Penzias A.A., Wilson R.W. *Astrophys. J.*, 142, 419–427 (1965).
- [17] Shaver P.A. "High Redshift Quasars." Seventeenth Texas Symposium on Relativistic Astrophysics and Cosmology. *Annals of the New York Academy of Sciences*, 759, 87 (1995).
- [18] Zhuck N.A. "On the some results following from the universal gravity law." Borisoglebsk, 1986, 58 pp. (in Russian).
- [19] Zhuck N.A. "Metamorphoses of cosmology." In "The Relativity Theory: for and against," FENID, Gomel, 3, 89 (1991) (in Russian).
- [20] Zhuck N.A. "The cosmological solutions of the Einstein equations." Kharkiv, KhVVAUL, 1995, 16 pp. (in Russian).
- [21] Zhuck N.A. "New overviews about the Universe and its laws." The 1-st RTI TTR scientific conference, RTI TTR, Kharkiv, 1998, 5–14 (in Russian).
- [22] Zhuck N.A. "The cosmological solutions of the Einstein equations," Kyiv, Author's Certificate of series PA, No 1718 with a priority of January 28, 1999 (in Russian).
- [23] Zhuck N.A. "The new stationary model of the Universe." The Gamov memorial international conference "The Universe of Gamov: original ideas in astrophysics and cosmology" (GMIC'99), Odessa, August 16–22, 1999, Abstracts, p. 37.
- [24] Zhuck N.A. "Cosmic equilibrium electromagnetic radiation," *Kharkiv Univ. Public.*, 456/2, 2000, p. 244 (in Russian).
- [25] Zhuck N.A. "The Microwave Background Radiation as aggregate radiation of all stars." The XVII international conference "Actual problems of extragalactic astronomy," Puschino, Moscow region, Russia, April 12–14, 2000 (in Russian).
- [26] Zhuck N.A. "The axiomatic theory of the Microwave Background Radiation." The Joint European and National Astronomical Meeting "European Astronomy at the Turn of the Millennium" (JENAM-2000), Moscow, Russia, May 29 – June 3, 2000, Abstracts, p. 48.
- [27] Zhuck N.A. "About identity of inertial and gravitational masses." The Joint European and National Astronomical Meeting "European Astronomy at the Turn of the Millennium" (JENAM-2000), Moscow, Russia, May 29 – June 3, 2000, Abstracts, p. 168.
- [28] Zhuck N.A. "Cosmology," Kharkiv, Model Vseleynoy Ltd, 2000, 464 pp. (in Russian).
- [29] Zhuck N.A. "Field formulation of the General Relativity and cosmology." The Ukrainian-Russian conference "Gravitation, cosmology and relativistic astrophysics" (GRAV-2000), Kharkiv, Ukraine, November 8–11, 2000, Abstracts, p. 37.
- [30] Zhuck N.A. "Cosmological effects in bulky Michelson-Morley interferometers." The Ukrainian-Russian conference "Gravitation, cosmology and relativistic astrophysics" (GRAV-2000), Kharkiv, Ukraine, November 8–11, 2000, Abstracts, p. 73.
- [31] Zhuck N.A. "The identity of inertial and gravitational masses is proved!" *Spacetime & Substance*, 1, 1, 23–28 (2000). <http://spacetime.narod.ru>.
- [32] Zhuck N.A. "The Microwave Background Radiation as aggregate radiation of all stars." *Spacetime & Substance*, 1, 1, 29–34 (2000). <http://spacetime.narod.ru>.
- [33] Zhuck N.A. "Gravitation viscosity and geotetic curvature of the Universe." *Spacetime & Substance*, 1, 2, 71–77 (2000). <http://spacetime.narod.ru>.
- [34] Zhuck N.A. "Gravitation viscosity and geotetic curvature of the Universe." *Spacetime & Substance*, 1, 3, 1–5 (2000). <http://spacetime.narod.ru> (in Russian).
- [35] Zhuck N.A. "Field formulation of the General Relativity and cosmology." *Spacetime & Substance*, 1, 4, 71–77 (2000). <http://spacetime.narod.ru>.
- [36] Zhuck N.A. "Cosmological effects in bulky Michelson-Morley interferometers." *Spacetime & Substance*, 1, 5, 71–77 (2000). <http://spacetime.narod.ru> (in Russian).
- [37] Zhuck N.A. "Field formulation of the General Relativity and problems of cosmology." *Spacetime & Substance*, 2, 1, 71–77 (2001). <http://spacetime.narod.ru>.
- [38] Zhuck N.A. "The Cosmos Microwave Background Radiation as aggregate radiation of all stars." *Physics of Consciousness and Life, Cosmology and Astrophysics*, 1, (2001). (In Russian).
- [39] Zhuck N.A. "Properties of the Yukawa potential and gravitational screening of a substance." *Spacetime & Substance*, 2, 3, 105 (2001). <http://spacetime.narod.ru>.
- [40] Zhuck N.A. "On the united nature of gravitational, electromagnetic and nuclear interactions." *Spacetime & Substance*, 2, 4, 165 (2001). <http://spacetime.narod.ru>.
- [41] Database on quasars (the basis is taken as of June 29, 2001). <http://cdsweb.u-strasbg.fr/cgi-bin/cat?VII/215>.
- [42] N.A. Zhuck, V.V. Moroz, A.M. Varaksin, "Quasars allocation in the Universe." Homepage, <http://quasars.narod.ru>.

ETHERAL WIND IN EXPERIENCE OF MILLIMETRIC RADIOWAVES PROPAGATION

Yu.M. Galaev¹

*The Institute of Radiophysics and Electronics of NSA in Ukraine,
12 Ac. Proskury St., Kharkov, 61085 Ukraine*

Received August 26, 2001

The phase method of anisotropic media parameters measurement of electromagnetic waves propagation is proposed. The experimental hypothesis check about the existence of such material medium of a radiowaves propagation in the nature, as Aether is executed in eight millimeter radiowaves range. The ethereal wind speed and this speed vertical gradient near the Earth's surface have been measured. The systematic measurement results do not contradict the initial hypothesis rules and can be considered, as experimental imagination confirmation about the Aether existence, as material medium, in the nature.

1. Introduction

The experimental researches of the ground channel phase characteristic of 8-mm range radiowaves propagation have revealed the problems, connected with its model elaboration [1–4]. The model [3] described the possible spatial effects influence, but this idea has not been developed further due to the quantitative divergence between demanded and measured atmosphere parameters. The interference model [4], as a whole, explained the observed effects, but in some cases the qualitative divergence between the calculation and measurement results took place. The further problem analysis has shown that the hypothesis engaging of the radiowaves propagation medium anisotropy has enabled to give the calculation results in conformity with the measurement results. It was supposed that the anisotropy is stipulated by the directional medium motion of radiowaves propagation and this medium flow has the space origin. Some information about such medium motion parameters was taken from the papers [5–7]. The works [5, 6] have been executed in order to the hypothesis experimental check about the Aether existence in the nature as the material medium, which fills the Global space and is the building stuff of all kinds of matter, the motions of which are revealed like physical fields and interactions. In due course the positive work results [5] were widely known, but they have been estimated by scientific community, as error because of some reasons. The hypothesis about the existence of such material medium, as Aether, in the nature wasn't accepted. We'll consider the major work results, which were executed in this direction tak-

ing into consideration the long-life and significance of the problem. We'll try to determine the reasons, which have made the physicists of that time consider the work results [5, 6] as error and refuse the Aether concept.

In 1877 D.K. Maxwell noticed, that while the Earth motion through Aether there should be an ethereal wind on the surface, which changes the light speed distributing in Aether. It is known that A.A. Michelson tried to find out an ethereal wind in 1881 for the first time [8, 7]. With the help of a cross shaped interferometer with the length of the optical path about 2.4 m, within the hypothesis of fixed Aether, he expected to receive the bands displacement of an interference pattern, conforming the orbital motion speed of the Earth by the value 30 km/s. However the measured displacement, which corresponded the speed by the value only 3–4 km/s. Michelson related this result to measurement errors and concluded about the initial hypothesis inaccuracy of stationary Aether. However, it is considered in physics almost since that time, that "Michelson experience" has shown in general the inaccuracy imagination about such medium existence as Aether in the nature. Many explorers didn't agree with such matters. The attempts to find out this medium continued, including Michelson himself.

In 1925 D.K. Miller received the optical path of the length about 64 m with a cross-shaped interferometer, as a result of long systematic measurements, that the suspected ethereal wind speed at the altitude 265 m above the sea level (Cleveland) has the value about 3 km/s, and at the altitude 1830 m (observatory Mount Wilson, Pasadena) is about 10 km/s. The motion apex coordinates of the Solar system were determined: the direct ascension 17.5^h , declination $+65^0$ [5].

¹e-mail: galaev@ire.kharkov.ua; Ph.: +38 (0572) 448742

The Miller works have attracted the great physicists' attention. The discussion has started about them, in which the influence of possible unaccounted factors on an optical interferometer was discussed first of all. In the work [10] S.I. Vavilov expressed, perhaps, the common opinion formed: "...the Miller's interferometer is so sensitive, that many local influences, considered hard, can be the cause of systematic bands displacement". Here again: "In any case, the experiments repetition in the other place and by the other device is necessary at this situation." It was clear, that the interferometer is required to save the environment parameters from the change affect. The solution seemed apparent - the interferometer should be placed into the thermostat and then into the pressurized chamber together with the thermostat. So it happened, but all the attempts in order to repeat Miller's experiment, except the experiment [11], were performed by the devices, which were placed in metallic chambers. R.D. Kenedy [12, 7] increased the interferometer sensitivity. The device was placed in the pressurized metallic chamber. The measurements were conducted at the same altitudes, as in [5]. The bands displacement was not observed. K.K. Illingwort [13, 7] improved Kennedy's device, but also these measurements showed a zero result. E. Stael [14, 7] placed an interferometer in the metallic chamber, i.e. thermostat, and raised it in an air balloon up to the altitude 2500 m. The required effect was not observed. In 1929 the work by A.A. Michelson, F.G. Peas, F. Pirson appeared [11]. In this experiment, at the same observatory Mount Wilson, the bands displacement of an interference pattern value no more than 1/50 of the expected effect was measured with the interferometer having the optical path length about 26 m, connected with the solar System motion having the speed 300 km/s. In other words, the speed of relative motion of the value 6 km/s was measured. The interferometer has been placed into a fundamental building of the observatory optical workshop for work temperature regime stabilization. The pressurized metallic chamber was not applied. Unfortunately, the problems, which the authors overcame at the experiment execution, were listed in general in this extremely laconic work (1 page). The measured results are presented only in such kind as they were given in the above mentioned work.

The experiment by G. Yoosa 1930 [15] was the last experiment on the ethereal wind detection, which was executed with an optical interferometer. The device was made on the quartz basis by the corporation Tseys, it was hanged in the vacuum-metallic chamber and supplied with photographic registration. The measurement results showed that the required ethereal wind, in any case, does not exceed the value 1 km/s (the device resolving capacity). Miller's measurements should be considered finally as the error ones and stipulated by outside causes after zero work result [15].

In 1933, Miller has marked the shielding property

of metal covers in his work [6]. However the scientific community did not react properly to such peculiarity, shown by him in this work, as, perhaps, the positive work results [11], as there was a lot of experiments with zero results obtained with the interferometers, screened by metallic chambers by that time. The physical shielding phenomenon interpretation was given by V.A. Atsukovsky [16] for the first time, having explained it by the fact, that the electrons in metals will create so-called "Fermi's surface".

After 1930 Michelson-Miller's experiment ceased to take a central place in physics. Only in 50 years, there was a capability of the experiment realization, which didn't repeat Michelson's scheme, but being its analogues in the results interpretation sense after the devices appearance, based on completely other ideas (resonators, masers, Mossbauer effect etc.). Such experiments were conducted [17-20]. And again, the common tool error of these experiments was the usage of ethereal wind effects detection of different metallic chambers. They were metallic resonators in [17, 18, 20], lead chamber in [19], since it was necessary to work with a gamma-radiation. The works' authors, perhaps, have not given the proper significance to Miller's conclusions 1933 [6] about the inapplicability of metal boxes in the experiments with an ethereal wind.

Thus, proper checks of Miller's experiments weren't conducted yet until nowadays, in spite of numerous physicists' attempts to repeat his experiments! All his followers carefully screened the devices from an ethereal wind by metal chambers, and, according to A.A. Atsukovsky's image expression, "...it's the same that to make the attempts to measure the wind, which blows outdoors, looking on the anemometer put in a densely close room" ([7], p. 4). The known works until nowadays cannot be ranked as experiments, which could confirm or deny Miller's results, confirm or deny the hypothesis about Aether existence in the nature. The measuring means, unsuitable for ethereal wind effects measurement, were applied in all these works.

The great job for work collecting and analysis, dedicated the ethereal wind problem, was performed by Atsukovsky [7]. The aether model is offered and the aether dynamic picture of the world was designed in his works [21, 22, 16]. The Aether is represented as a material medium, which fills in the global space and has the properties of viscous and compressible gas, it is a building stuff for all material formations. The element of Aether is an amer. The physical fields represent different forms of Aether motion, i.e. the Aether is a material medium of electromagnetic waves propagation. The gradient boundary layer is formed at mutual motion of the Solar System and Aether near the Earth surface, in which the Aether running speed (ethereal wind) increases with an altitude. The ethereal wind apex is northern. It is shown, that the metals have larger aether dynamic resistance and interfere the Aether

flows. Therefore metering devices arrangement in metal chambers is inadmissible. The reason of failures is due to it [12–14 etc.]. The work authors [7, 16, 21, 22] consider that the experiments [5, 11] are authentic.

However the positive work results [5, 11] couldn't be considered as final experiment currently, after which the doubts regarding the definite physical concept are removed. The matter is that within modern imagination about the light speed constancy, the fact finding of the Earth and Solar system motion in space availability is not enough to make a conclusion about Aether existence, as material medium, i.e. medium consisting of separate particles. So, Sanyak's known rotary effect and the relative movement, discovered with it, for example the Earth's diurnal rotation [23, 7], in modern physics is interpreted without engaging the Aether hypothesis existence [24]. Essentially, the attempt to show that the discovered motion is conditioned by the Earth relative movement and Aether material medium were made by two explorers: Miller [5] and Staal [14], but both made the essential methodical errors. Miller placed the interferometer at different altitudes and obtained that the speed of the discovered motion raised with the altitude increase over the Earth's surface. There shouldn't be such relation in case of movement in space, without Aether availability, as the material medium flow. However these major measurements, executed in [5], are methodically incorrect: the measurements are carried at different altitudes in time; the measurements are conducted in the environment various conditions (temperature, humidity, pressure, solar radiation, airflows, etc.), the interferometer is rather sensitive to the environment parameters variability; the measurements, strictly speaking, are conducted by miscellaneous devices, since Miller's huge interferometer was disassembled, assembled again and adjusted while moving from Cleveland to Mount Wilson observatory. Therefore, the technique, which Miller applied for speed dependence measurement of the discovered motion from an altitude above the Earth's surface, was unacceptable to make a final conclusion for the benefit of Aether existence, as material medium. Staal tried to apply more correct technique for this problem solution [14]. The optical interferometer mounted on an air balloon, rose up to the altitude 2500 m. The interferometer was placed into the pressurized metal chamber (the thermostat) for stabilization of the working conditions. As it has already been emphasized, the application of metal chambers is completely inadmissible at such measurements. This circumstance was not known at that time. It occurred, that the measured displacement of interference bands corresponds to the ethereal wind speed of 7 km/s with the error of the same magnitude order. The conclusion of the author's work [14]: "We can not discuss Miller's result on the basis of this experimental series, as our measurements accuracy is just on the border of Miller's observations. However we can ex-

clude Miller's effect, raised with the altitude increase." In other words, the motion could be found out, and high-altitude relation of this speed misses completely.

Thus, considering the work lacks [5, 11] and large number experiments availability with zero result, it is possible to understand the physicists disbelieving to the works at that time [5, 11], the results of which indicated the necessity of the fundamental physical concepts change.

Positive results of the data application [5, 6], at the experiments analysis [1-4], detected reasons of unsuccessful attempts to repeat Miller's experiments, showed, that it is necessary to make the experiment again in order of the hypothesis check of the electromagnetic waves propagation material medium — Aether existence in the nature. It is necessary to solve the following problems for this purpose. It is necessary to take into account the lacks, allowed in earlier conducted researches; to apply other measurement methods, which will enable to show the Earth's relative movement availability in the unified measurement act in a single experiment and that the motion is stipulated by the Earth relative movement and the material medium flow of electromagnetic waves propagation and this medium motion has a space parentage. The positive result of such experiment can be considered as the experiment hypothesis confirmation of Aether material medium existence in the nature.

2. Measurement method

The Aether model has been adopted as the initial hypothesis and offered in the works [21, 22, 16] while the experiment accomplishment. The following effects should be observed in this case at electromagnetic waves propagation near the Earth's surface. The anisotropy effect, i.e. wave propagation velocity depends on the radiation direction that is stipulated by the Earth and Aether relative movement, i.e. the medium of electromagnetic waves propagation. The altitude effect, i.e. the wave propagation velocity depends on the altitude above the Earth's surface that is stipulated by Aether viscosity, i.e. the material medium of electromagnetic waves propagation. The space effect, i.e. the wave propagation velocity along the Earth surface changes the value within one day, that is stipulated by the space origin of ethereal wind. Thus as a result of the Earth's diurnal rotation the altitude (astronomical coordinate) of the Solar System motion apex will change its value within sidereal dayowing as for any other aster. Therefore horizontal component of ethereal wind speed and, therefore, the rate of electromagnetic waves propagation along the Earth's surface will change their values within the same term. Therefore, according to the research problems, the measurement method should be responsive to the indicated effects, and provide their

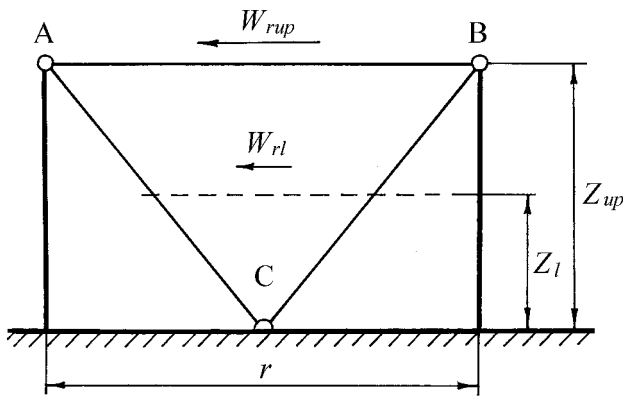


Figure 1: The experience scheme

observation in the unified measurement action.

The method of measurement is applied in the work, based on the reciprocity principle rules in electrodynamics [25], according to which the radiowaves propagation conditions from one point of a radio link to the other are completely those, as well as backwards and this symmetry does not depend on the interspace properties, which is only supposed to be isotropic. If the radiowaves propagation velocity depends on the radiation direction, such space is anisotropic and the reciprocity principle is not applied. The ground radio link of a line-of-sight with a counter radiowaves propagation of a millimeter-wave is used at the method implementation. In this case the main fields formation mechanism in the acceptance points is the interference of direct waves and waves, reflected from the Earth's surface, i.e. waves, which spread at miscellaneous altitudes from ground [26]. It enables, comparing the wave interference results to find out the development of anisotropic and altitude effects simultaneously in both points. The space effect was found out, as well as in [5, 6], by the results averaging of systematic measurements executed to scale the sidereal time S.

Let's consider the operational principle of the measurement method. The experience scheme is shown in the Fig. 1

The letters *A* and *B* indicate the transceiver points of the radio link. Two waves come there at each of these points: a straight line distributing on a pathway *AB* at the altitude Z_{up} above the Earth's surface, and the wave, reflected from the Earth's surface in the point *C*. The expansion of a pathway *AB* is r . The medium trajectory height *ACB* is Z_l . The arrows indicated as W_{rup} and W_{rl} , demonstrate the radial component direction of the ethereal wind speed, i.e. the component, which is operational along the radio link. Their lengths are proportional to ethereal wind speeds at the altitudes Z_{up} and Z_l . The radio link represents the

radio interferometer, which due to the Earth's diurnal rotation turns into the Aether flow. The characteristics measurement method of the radio tracts is applied for observation of the wave interference [27]. The method essence is in the following. The zonding modulation signal I with a carrier frequency f_0 and the frequencies lower ($f_1 = f_0 - F$) and upper ($f_1 = f_0 + F$) of the lateral components (F is a modulating frequency) emits from the transmitting point. At propagation each i signal component I receives the phase increment φ_i (the indexes $i = 1, 2$ correspond to the frequencies $f_{0,1,2}$). The adopted signal component with the frequency f_0 is multiplied separately from each of lateral components in the receiving device, and the phase shift $\Delta\varphi_i$ is measured between the multiplication results having differential frequencies. The expression for $\Delta\varphi_i$ looks like

$$\Delta\varphi = (\varphi_0 - \varphi_1) - (\varphi_2 - \varphi_0) \quad (1)$$

Such phases combination is invariant to the time zero change and received the name "a phase invariant" in the paper [28]. Let's find the value $\Delta\varphi_i$ at a wave interference in the radio link points, shown in the Fig. 1. In this case, the resultant oscillation phase with i frequency can be determined with the following known expression [29]

$$\varphi_i = k_i r + \arctg \frac{R \sin(k_i \Delta r + \Theta)}{1 + R \cos(k_i \Delta r + \Theta)} \quad (2)$$

where: $k_i = 2\pi/\lambda_i$ is the wave number; $\lambda_i = c/f_i$ is the wavelength; c is the radiowave propagation velocity in the fixed Aether ($W = 0$), in vacuum; R is the module of the reflection coefficient; Θ is the phase of the reflection coefficient; Δr is the propagation difference between direct and reflected waves. As in the experiment $Z_{up} \ll r$, it is possible to consider, that $\Theta \approx \pi$ [29]. Then (2) will be like

$$\varphi_i = k_i r + \arctg \frac{-R \sin(k_i \Delta r)}{1 - R \cos(k_i \Delta r)} \quad (3)$$

Let's designate

$$M_i = \arctg \frac{-R \sin(k_i \Delta r)}{1 - R \cos(k_i \Delta r)} \quad (4)$$

Let's record (3) as $\varphi_i = k_i r + M_i$ and we shall substitute φ_i into (1). Allowing, that

$k_{2,1} = k_0 \pm \Delta k$, $\Delta k = k_2 - k_1 = k_2 - k_0$, we shall receive

$$\Delta\varphi = (M_0 - M_1) - (M_2 - M_0) \quad (5)$$

We'll decompose (4) into Taylor rows in the point neighborhood $k_0 \Delta r$ according to the powers $(\Delta k \Delta r)$. Limiting by the first four decomposing members, we shall record:

$$M_1 = M_0 - \Delta k \Delta r M_0' + \frac{1}{2} \Delta k^2 \Delta r^2 M_0'' -$$

$$-\frac{1}{6}\Delta k^3\Delta r^3M_0''' + \dots, \quad (6)$$

$$M_2 = M_0 + \Delta k\Delta rM_0' + \frac{1}{2}\Delta k^2\Delta r^2M_0'' + \frac{1}{6}\Delta k^3\Delta r^3M_0''' + \dots \quad (7)$$

Let's substitute the values M_1 , M_2 , defined by the expressions (6), (7), into (5), we shall obtain

$$\Delta\varphi = -(\Delta k\Delta r)^2M_0'' \quad (8)$$

Let's calculate the second derivative M_0'' , then (8) will be like

$$\Delta\varphi = -(\Delta k\Delta r)^2 \frac{R(1-R^2)\sin k_0\Delta r}{(1+R^2-2R\cos k_0\Delta r)^2} \quad (9)$$

The expression (9) introduces the phase invariant value $\Delta\varphi$ in an interference case in the reception method point of direct waves and the waves, reflected from the Earth's surface distributing on the pathways AB and ACB . For problem solving of the research results of simultaneous values measurements $\Delta\varphi_A$ and $\Delta\varphi_B$, in the points A and B accordingly, we shall deduct one of the other

$$\Phi = \Delta\varphi_A - \Delta\varphi_B \quad (10)$$

In the considered method Φ is the measured value. According to the reciprocity principle, at the radiowaves propagation in the isotropic medium $\Delta\varphi_A = \Delta\varphi_B$. In this case

$\Phi = 0$. In case of the anisotropic medium the reciprocity principle is not applied and $\Phi \neq 0$.

It follows from (9), that at fixed values Δk and k_0 the value $\Delta\varphi$ depends on R and Δr . In the paper the data about actual values R , i.e. having a place in a radio link, selected for measurements, are obtained experimentally at this radio link characteristics analysis. The information about the value R change range can be found, for example, in the paper [26]. The propagation difference Δr is determined by the radio link geometry, but at the radiowaves propagation in atmosphere, owing to radiowaves refraction, as well the value Δr depends upon the gradient value g_n of the high-altitude profile of the atmosphere interception factor $n(Z)$ [29]. At the linear (and close to it) relation $n(Z)$ the value g_n in the atmospheric layer $\Delta Z = Z_{up} - Z_l$ can be determined as

$$g_n = (n_{up} - n_l) / \Delta Z, \quad (11)$$

where n_{up} , n_l is the index coefficient of air at heights Z_{up} , Z_l .

The direct wave propagation velocity is ($W_{up} = W_l = 0$) the velocity of propagation of a direct wave is equal $V_{up} = c/n_{up}$, the wave velocity, reflected from

the Earth's surface is $V_l = c/n_l$ in the isotropic case. Then (11), taking into account, that $V_{up}V_l \approx c^2$, can be written like

$$g_n = (V_l - V_{up}) / c\Delta Z. \quad (12)$$

In the anisotropic case ($W_{up} > W_l > 0$, that corresponds the positions of an initial hypothesis) the radiowave propagation velocity is V and its relation to the altitude $V(Z)$ depend on the radiation direction, that is stipulated by the gradient medium flow of radiowaves propagation, i.e. Aether (Fig. 1) available. In this case wave propagation velocities at altitudes Z_{up} and Z_l are

$$V_{up} = \frac{c}{n_{up}} \pm W_{rup}, \quad V_l = \frac{c}{n_l} \pm W_{rl}, \quad (13)$$

where the sign "+" is applied, when the radiowaves propagation direction coincides the ethereal wind direction, and the sign "-" is applied, when these directions are inverse. Let's put the values Z_{up} and Z_l in (12). If the propagation directions of radiowaves and ethereal wind coincide, we shall receive

$$g_{n+} = \frac{1}{c\Delta Z} \left(\frac{c}{n_l} + W_{rl} - \frac{c}{n_{up}} - W_{rup} \right). \quad (14)$$

Let's open brackets, then

$$g_{n+} = \frac{n_{up} - n_l}{\Delta Z n_l n_{up}} - \frac{W_{rup} - W_{rl}}{c\Delta Z}. \quad (15)$$

Allowing, that $n_l n_{up} \approx 1$, $(n_{up} - n_l) / \Delta Z = g_n$, and $(W_{rup} - W_{rl}) / \Delta Z = g_{Wr}$ is the gradient of the ethereal wind speed radial component in the layer ΔZ , the expression (15) can be written as

$$g_{n+} \approx g_n - g_{Wr} / c. \quad (16)$$

The first sum member (16) represents the high-altitude profile gradient of the atmosphere refraction coefficient g_n in the layer ΔZ . The second member represents the additional component to g_n , stipulated by the velocity gradient availability in the ethereal wind flow g_{Wr} . At the radiowaves propagation towards the ethereal wind motion, it is possible to receive

$$g_{n-} \approx g_n + g_{Wr} / c. \quad (17)$$

It follows from (16), (17) that if the Aether gradient flow is available, the wave refraction distributing in counter directions, will be different by virtue of $g_{n+} \neq g_{n-}$.

Let's consider the offered measurement method action with reference to a concrete experimental radiolink, taking into account the features of hardware implementation of this method now. Let's estimate the values of probable hardware and methodical measurement errors.

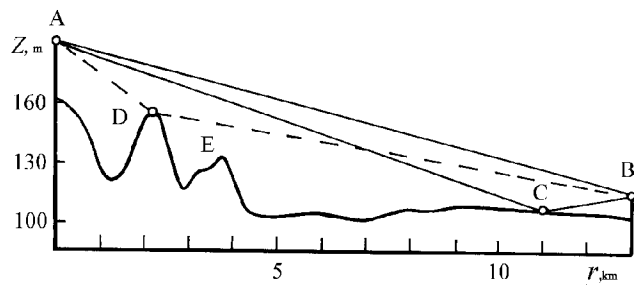


Figure 2: The experimental radiolink profile

3. Experimental radiolink

The measurements are conducted with the ground radiolink of direct visibility within 13 km. The radiolink profile is shown in the Fig. 2.

The points A and B are the final transceiver points in the figure. The point A was on the northern side of Kharkov, the point B was in the village Russian Tishky. The aerial of the point A was at the altitude 30 m from the Earth's surface, and the aerial of the point B was at the altitude 12 m. The hill top D, the terrain in the region of the point C and point B have the grass covering. The hill top E is occupied with forests. The medium trajectory height is AB overland $Z_{up} \approx 42$ m. The lumen value above the top D, defined by geodesic method, is $H_1 \approx 25.3$ m. The interval from the point A up to the top $Dr_1 \approx 2200$ m. The azimuth of a radio link, measured in the point A regarding the meridian, $\alpha \approx 45^\circ$. To specify the fields formation mechanism in radiolink points, the vertical field structure is measured in the point A. The measurements are executed in summer, in August. The radiation was conducted by the aerial of the point B on a carrier frequency of this point zonding signal. The vertical probing is executed by consequent rise of the auxiliary receiving device supplied with the aerial of rather broad directional diagram ($\approx 10^\circ$). The rise started from a aerial arrangement level of the point A. The measurement results are shown by the points on the left-hand piece of the Fig. 3. The continuous line approximates the view of measured field structure. The power P of the received signal in decibels regarding the reference level P_0 is plotted on an abscissa axis. The height of the auxiliary receiving device in meters is plotted on an ordinate axis.

As it is visible from the Fig. 3, the structure of a high-altitude profile contains two components mainly. The first structure is presented by several change terms, the second is presented only by the part of its term. The measured structure can be described by three waves interference: the direct wave (distributing on the paths

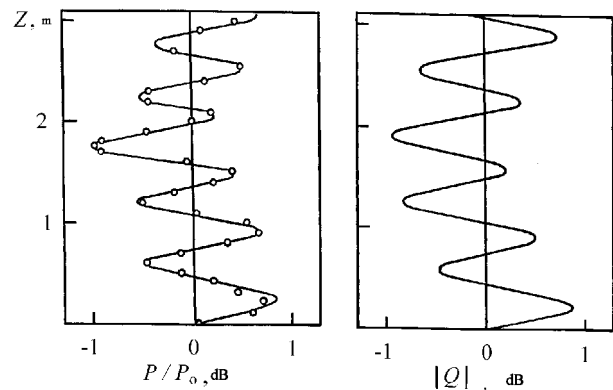


Figure 3: The high-altitude field profile

BA), the waves, reflected from the top D (on the path BDA), and the waves, reflected from the terrain in neighborhood of the point C (on the path BCA).

The problem solution of a field calculation at several waves interference is described in the work [29]. The factor attenuation module is determined by the following formula at vertical probing

$$|Q(Z_a)| = \left\{ \left[1 + \sum_{j=1}^J R_j \cos \gamma_j(Z_a) \right]^2 + \left[\sum_{j=1}^J R_j \sin \gamma_j(Z_a) \right]^2 \right\}^{1/2}, \quad (18)$$

where Z_a is the auxiliary device uprise height; J is the interfering waves quantity; j is the wave number, reflected from j point on the Earth's surface. The phase shift $\gamma_i(Z_a)$ between a straight line and j waves is

$$\gamma_j(Z_a) = 2\pi\lambda^{-1}\Delta r_j(Z_a) + \Theta_j. \quad (19)$$

The propagation waves difference at $g_n = 0$ is

$$\Delta r_{0j}(Z_a) = \frac{[H_j + \Delta H_j(Z_a)]^2}{2r q_j(1 - q_j)}, \quad (20)$$

where H_j is the lumen value above j reflection point at $g_n = 0$; $\Delta H_j(Z_a)$ is the additional element to the value H_j , which depends upon Z_a ; $q_j = r_j/r$ is the relative coordinate of j of the reflection point; r_j is the interval from the point A up to j reflection point. The lumen value at $g_n \neq 0$ is determined by the expression

$$H_j(g_n) = H_j - 0.25r^2 g_n q_j(1 - q_j). \quad (21)$$

The additional element value $\Delta H_j(Z_a)$ is

$$\Delta H_j(Z_a) = (1 - q_j) Z_a. \quad (22)$$

The calculation result is given on the right piece of the Fig. 3, executed on the formulas (18)-(22). The following parameters values of reflection points are adopted at calculations: $\Theta_{1,2} = \pi$; $r_1 = 2200$ m; $H_1 = 25.3$ m; $R_1 = 0.07$; $r_2 = 11000$ m; $H_2 = 24$ m; $R_2 = 0.04$; value $g_n = -5.5 \cdot 10^{-8}$ m $^{-1}$. The values R_1 and R_2 are obtained from the data of the field vertical probing (left-hand piece of the Fig. 3). Their rather small values (for example, in comparison with the work data [26]) are stipulated by the following features of reflected waves formation in an experimental radiolink (Fig. 2). It is: the waves divergence at reflection from the domed top D ; the segment C was irradiated with a side lobe of the antenna point B direction. It is visible from the Fig. 3, that the calculation results will be agreed with the measurement results as a whole. The differences available can be explained by those that the calculation is executed in the supposition about the independence g_n from Z_a .

At measurements realization, foreseen by this work problems, the probing signals transmission in the points A and B was implemented by the aerials with directional diagrams width $\approx 0.5^0$. In this case the top D was outside of the aerial chart main lobe of the point A . Therefore the signal values, received in both points from the top D directions, were much less (on 17...20 dB) signal values, received from the point C directions. (As it was marked, the auxiliary aerial with the directional diagram width about 10^0 was applied at vertical probing and the top D was in a main lobe of such aerial). Therefore further estimations were executed within the following supposition. The signals received in the points A and B , represent the wave interference results, which come to these points on the pathways AB and ACB . The following parameters of a reflecting segment are adopted for calculations: $r_2 = 11000$ m; $H_2 = 24$ m; $R_2 = 0.04$. (As only this segment is considered below, the indexes writing is omitted and considered, that $H_2 = H$; $R_2 = R$; $q_2 = q$; $\Delta r_{02} = \Delta r_0$).

We shall substitute the value H to (20), defined by (21) for the relation calculation Δr from g_n , we shall receive

$$\Delta r = \frac{H^2}{2rq(1-q)} - \frac{rH}{4}g_n + \frac{r^3g_n^2}{32}q(1-q). \quad (23)$$

The first member (23), according to (20), represents the value Δr_0 at $g_n = 0$, $Z_a = 0$. The second and third members depend on g_n . Thus within the change range g_n , peculiar for atmosphere [30-32], the value of the third member does not exceed 0.01 from the second value. The values Δr_0 and $rH/4$ are determined only in geometrical parameters of a radiolink. In this case, neglecting third member in the expression (23) and having designated $rH/4 = d$, we shall receive

$$\Delta r \approx \Delta r_0 - dg_n. \quad (24)$$

It follows, that anisotropic effects and altitudes result in the components occurrence to g_n by value $\pm g_{Wr}/c$ in an anisotropic case ($W_{up} > W_l > 0$), from (16), (17). Let's substitute values g_n , defined by (16), (17) in (24). Let's receive, that the propagation difference at propagation directions concurrence of radiowaves and etheral wind is

$$\Delta r_+ = \Delta r_0 - d(g_n - g_{Wr}/c). \quad (25)$$

It is at a radiowaves propagation towards the etheral wind motion

$$\Delta r_- = \Delta r_0 - d(g_n + g_{Wr}/c). \quad (26)$$

It follows, that $\Delta r_+ > \Delta r$, $\Delta r_- < \Delta r$ and $\Delta r_+ \neq \Delta r_-$ from (25), (26). The difference in these values is determined by the velocity gradient of the etheral wind value g_{Wr} .

We shall estimate the possible value g_{Wr} . The estimations will be executed for a case, when the horizontal component of the etheral wind speed receives the maximum value. It should be observed at the moment of the etheral wind lower transit apex (the apex crosses the meridian in the bottom point). In [5], the declination of the etheral wind apex $\delta_M = +65^0$ is determined in an equatorial system of astronomical coordinates. The index "M" means the measurement place, i.e. the observatory Mount Wilson. Its geographic latitude $\varphi_M = 34^0$ n.l., the altitude above the sea level $Z_M \approx 1830$ m. In [5] the etheral wind speed in the interferometer plane, i.e. horizontal component of this speed W_M , was measured, it is

$$W_M = W \cos h_M, \quad (27)$$

where W is the value of the etheral wind speed module at the altitude Z_M ; h_M is the apex height in a horizontal system of astronomical coordinates at the latitude φ_M . Resulting in the measured data, obtained by Miller on Mount Wilson and in Cleveland, the high-altitude relation of the etheral wind speed, presupposing the exponential nature of this relation, can be approximated by the expression

$$W_M(Z) = bW_M(1 - e^{-\beta Z}), \quad (28)$$

where $b = 1.136$; $\beta = 1.16 \cdot 10^{-3}$ m $^{-1}$ are proportional ratios; W_M is the speed values of the etheral wind, measured in [5, 6] at the altitude Z_M ; Z is the altitude above the sea level. The expression (28) enables by the results [5, 6], obtained at the altitude Z_M , to calculate high-altitude speed relation of the etheral wind $W_M(Z)$ at the latitude φ_M . The measurements were conducted near Kharkov, at the latitude $\varphi_K = 50^0$ n.l. The index "K," as well as above, means the measurement place. Supposing, that the nature of high-altitude speed relation of the etheral wind in this point of a

terrestrial globe looks like to the relation (28), we shall write

$$W_K(Z) = bW_K(Z_M)(1 - e^{-\beta Z}), \quad (29)$$

where $W_K(Z)$ is the horizontal speed component of the ethereal wind at the latitude φ_K , at the altitude Z_M , which can be determined as

$$W_K(Z_M) = W \cos h_K, \quad (30)$$

where h_K is the apex altitude of the ethereal wind at the latitude φ_K . It is possible to receive from the equations (27), (30), that

$$W_K(Z_M) = W_M \cos h_K / \cos h_M. \quad (31)$$

Let's write down h_K and h_M through the apex declination value δ_M and the latitude φ_K , φ_M . Let's take the ratio for transition from the first equatorial system of astronomical coordinates to horizontal ones, [33]

$$\cos h \cos A = -\cos \varphi \sin \delta + \sin \varphi \cos \delta \cos t. \quad (32)$$

Here A is the apex azimuth in a horizontal system of astronomical coordinates; t and δ is an hour angle, and the apex declination in equatorial coordinate system accordingly; φ is geographic latitude of the observation place. In a point of the lower apex transit, as well as for any aster, $A = 180^\circ$, $t = 12^h$ (in a degree measure $t = 180^\circ$) [33]. In this case (32) becomes

$$\cos h = \sin(\delta + \varphi). \quad (33)$$

Let's substitute the values $\cos h$, defined by the expression (33), in (31). Allowing the latitudes values are φ_K , φ_M and the value defined in [5] the apex declination δ_M , we shall receive

$$W_K(Z_M) = W_M \sin(\delta_M + \varphi_K) / \sin(\delta_M + \varphi_M). \quad (34)$$

Then, allowing (34), the expression (29) will be like

$$W_K(Z) = bW_M \frac{\sin(\delta_M + \varphi_K)}{\sin(\delta_M + \varphi_M)} (1 - e^{-\beta Z}). \quad (35)$$

The expression (35) allows to calculate high-altitude relation of the ethereal wind speed horizontal component for the latitude φ_K by the work results [5, 6], obtained at the altitude z_M . As the radio link is declined from a meridian with the angle α , the high-altitude relation of the ethereal wind speed radial component in the radio link location, at the moment of a lower apex culmination is

$$W_{rK}(Z) = bW_M \cos \alpha \frac{\sin(\delta_M + \varphi_K)}{\sin(\delta_M + \varphi_M)} (1 - e^{-\beta Z}). \quad (36)$$

We shall find the high-altitude gradient relation of this speed, differentiating (36) on a variable Z . We'll obtain

$$g_{W_{rK}}(Z) = b\beta W_M \cos \alpha \frac{\sin(\delta_M + \varphi_K)}{\sin(\delta_M + \varphi_M)} e^{-\beta Z}. \quad (37)$$

Let's calculate the anticipated value $g_{W_{rK}}$. The value $W_{Mmax} \approx 9000$ m/sec represents the average value of the ethereal wind maximum speeds in the work [5], measured during all months of observations. Having put in (37) $W_M = W_{Mmax}$ and $Z = Z_K = 150$ m (Z_K is the radiolink altitude over the sea level), we shall receive $g_{W_{rK}} = 6.4$ m/sec·m.

4. Instrumentation

The measurement method essence, adopted in this work, is described above. Let's notice the following. The expression (1) introduces a processing algorithm of the received signal I . It was shown in the work [27], that at such processing of the sources instability of the carrier and modulating frequencies do not enter in (1) and do not influence on the value $\Delta\varphi$ measurement accuracy. It has enabled to facilitate the creation and exploitation problem of the devices, intended for phase characteristics of radiolinks measurement, essentially. The self-excited generators with parametric stabilization of their frequencies are applied at the way implementation as emission sources. The way realised in radiowaves lengths range 8mm and earlier was probed in [1-4]. The final radiolink points were equipped with identical complete transceiver sets as well as the recording equipment. The transmission and sounding signals reception in each of the points were conducted with the same aerial. The aeriels of both points are identical and have mirrors of diameters 1,1m. The generators of carrier frequencies had the values frequencies about 37 GHz, and generators of modulating oscillations 0.5 GHz. The generators frequencies of carrier oscillations differed from each other in 50 MHz for radiated and received signals separation. The carrier frequency is $f_{0A} = 36.95$ GHz in the point A , and the carrier frequency is $f_{0B} = 37$ GHz in the point B . The resulting power of each transmission devices executed on Gunn's diodes, is about 70 mW. The generators of carrier and modulating oscillations with concomitant clusters are located in thermostats. The hardware complex contained the systems of the frequencies automatic tuning. The hardware has passed the comprehensive lab tests on a board and into the measuring complex structure within the environment temperatures $-25^\circ\text{C} \dots +35^\circ\text{C}$ in different meteorological conditions. One-channel recorders were used for registration in both final points. The additional recorder was used in the point A and for amplitude registration of a received signal. This information allowed to distinguish the time periods, during which the hydrometeors (rain, snow) settled out, that was not always possible to determine visually. As well the amplitude channel executed the function of the work continuous control of the measuring system. The analysis of the hardware actual characteristics and its test

results have shown, that sa is the hardware resulting root-mean-square measurement error of the values Φ does not exceed 2.4^0 .

5. The radiointerferometer work

In the accepted measurement method according to (10) the measured value Φ represents the difference of phase invariants values of radiolink probing signals, received simultaneously in radiolink points. Allowing (9), (25), (26), we shall write the expression for Φ as follows

$$\begin{aligned} \Phi = & -\Delta k^2 \Delta r_+^2 \frac{R(1-R^2) \sin k_{0B} \Delta r_+}{(1+R^2-2R \cos k_{0B} \Delta r_+)^2} + \\ & + \Delta k^2 \Delta r_-^2 \frac{R(1-R^2) \sin k_{0A} \Delta r_-}{(1+R^2-2R \cos k_{0A} \Delta r_-)^2}, \end{aligned} \quad (38)$$

where the indexes at k_{0A} and k_{0B} reflect the difference of probing signals carrier frequencies, received in the points A and B accordingly. The first member of the right part (38) represents the value $\Delta\varphi_A$, the second represents the value $\Delta\varphi_B$. The expression (38) is written to conformity with the initial hypothesis position of the ethereal wind northern apex. In this case the values Δr_+ , Δr_- are determined by the expressions (25), (26) accordingly and the measured value Φ should get the positive values. Let's consider the work features of the measurement method, which are stipulated by its specific technical implementation.

We shall consider the isotropic case ($W_{up} = W_l = 0$), that corresponds to radiowaves propagation in Aether, fixed regarding the observer (radiolink) at the presence of isotropic atmosphere within the adopted hypothesis. (It is adequate to such medium as Aether absence in nature within the modern generally accepted imaginations.) In this case the radiowave propagation velocity does not depend on the radiation direction, but depends on the altitude above the Earth's surface $V(Z) = c/n(Z)$. As $W_{up} = W_l = 0$ and $g_{Wr} = 0$, according to (25), (26), (24), we shall receive $\Delta r_+ = \Delta r_- = \Delta r$. Then, if in (38) to suppose, that $k_{0B} = k_{0A}$, we shall receive $\Phi = 0$ and this equalling, according to a reciprocity principle, does not depend on the interspace properties. However, the engineering solution was accepted at this method implementation, in which the carrier frequencies value of probing signals, emitted by each of radiolink points, differed. As $k_{0B} = k_{0A}$, $\Phi \neq 0$, that we shall consider $\Delta\Phi$ as the measurements error. We shall identify the values $\Delta\Phi$ depending on the parameters change such as g_n and R with (38), (24). We shall estimate probable ranges of the values change g_n and R for the calculations fulfilment. The average values g_n change from $-4.25 \cdot 10^{-8} \text{ m}^{-1}$ in winter up to $-5.95 \cdot 10^{-8} \text{ m}^{-1}$ in summer in the air layer 25–50 m above the Earth's surface according

to the work data [30–32]. Such data take intermediate values in spring and autumn. The values g_n change on the average during the day as follows $(-3,6 \dots -4,9) \cdot 10^{-8} \text{ m}^{-1}$ in winter and $(-5,5 \dots -6,4) \cdot 10^{-8} \text{ m}^{-1}$ in summer.

According to the work [26], on flat tracts with grass covering, the values change of the reflection coefficient module R is within the limits of $0.2 \dots 0.5$ on the wave 8 mm, in the season of active vegetation, up to $0.4 \dots 0.7$ after grass withering, remaining approximately the same if there is a friable snow cover. Thus the highest values of the reflection coefficient, reached $0.7 \dots 0.8$, were noticed in the season of snow melting.

In the work, at $\Delta\Phi$ errors calculating, the range of the value R change is taken within $0.03 \dots 0.07$, that is stipulated by the mentioned above features of the reflected wave formation in a radiolink. The selected change range R is matched to its change range as to the value, measured in the work [26], and includes the value $R = 0.,04$, which is determined in the work from the field vertical probing results in an experimental radiolink (left-hand piece of the Fig. 3). Such probing was executed at the end of summer, when the grass covering represented the withering green. It is possible to suppose on the basis of the work results [26] and vertical probing data, that the values $R \approx (0,04 - 0,05)$ are close to average value in a radiolink during the part of the year, since September till January, in which the measurements were executed. We shall use such change range R at fulfilment of the ethereal wind parameters estimations.

The calculation results of $\Delta\Phi$ error values and $\Delta\varphi$ values are presented on two pieces of the Fig. 4 depending on the gradient g_n values for three values R .

Abscissa axis for these pieces is common. The values g_n and the values, conforming to them $\Delta\varphi$, are given for visualization on it. The conformity between these values was established with the help (24). The values $\Delta\Phi$ and $\Delta\varphi$ in grades were taken on ordinate axes. On the lower piece, for $R = 0.05$, two curves are given, i.e. $\Delta\varphi_A(g_n)$ is the continuous line and $\Delta\varphi_B(g_n)$ is the broken line. As it is visible, the curves are shifted regarding each other. It was stipulated by the values difference of probing signals carrier frequencies, as the results in errors $\Delta\Phi$ occurrence. The curves $\Delta\varphi_A(g_n)$ and $\Delta\varphi_B(g_n)$ represent the maxima and minima position of interference patterns in the points A and B . (The analogue is the interference pattern in an optical interferometer). The radio interferometer working section, within which the measurements were conducted, is indicated by the heavy straight line section in the bottom part of the piece. The same relations for values $R = 0.03$ and $R = 0.07$ are reflected in the piece by the curves $\Delta\varphi_A(g_n)$, shown only within the radio interferometer working section. The errors $\Delta\Phi$ calculation results, executed for three values R are given on the upper piece of the Fig. 4. The value g_n change range is indicated by the broken line, i.e. the stroke

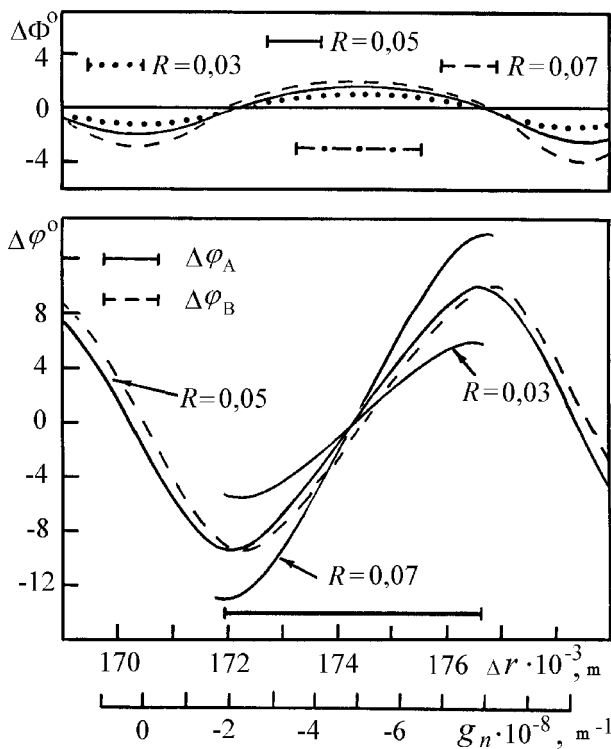


Figure 4: The measurement error relation to the vertical profile gradient of the refraction coefficient

section in this piece bottom, which was determined from the works [30–32]. It follows from the Fig. 4 and calculations results, that the value $\Delta\Phi$ changes in all the indicated gradient g_n change range in the following limits: at $R = 0.04$ from $\Delta\Phi_{min} = 0.870$ up to $\Delta\Phi_{max} = 1.180$; at $R = 0.05$ from $\Delta\Phi_{min} = 1.090$ up to $\Delta\Phi_{max} = 1.430$. The calculations have shown, that the error $\Delta\Phi$ is systematic and can be considered as the correction.

The diurnal and seasonal variations of ambient temperature can result in the radio link geometry change — the value Δr_0 change, and at $f_{0A} \neq f_{0B}$ the errors $\Delta\Phi_T$ occurrence is possible. It can be supposed, that the radiolink length remains invariable, since the radiolink final points are arranged on concrete buildings, the foundations of which are in an ice-free soil layer at almost constant temperature. Nevertheless, the errors calculation DFT was executed in the supposition, that the whole radiolink was located on concrete foundation with the length 13000 m. It has appeared, that the value $\Phi_T \leq 0.01^\circ$ in the temperature range $galaev.tex \Delta T = 50^\circ C$. A bit larger errors can occur at altitudes temperature change of radiolink final points. $\Delta\Phi_T \leq 0.05^\circ$ at $\Delta T = 50^\circ C$ in this case. The calculations are conducted at $R = 0.07$. As it is visible

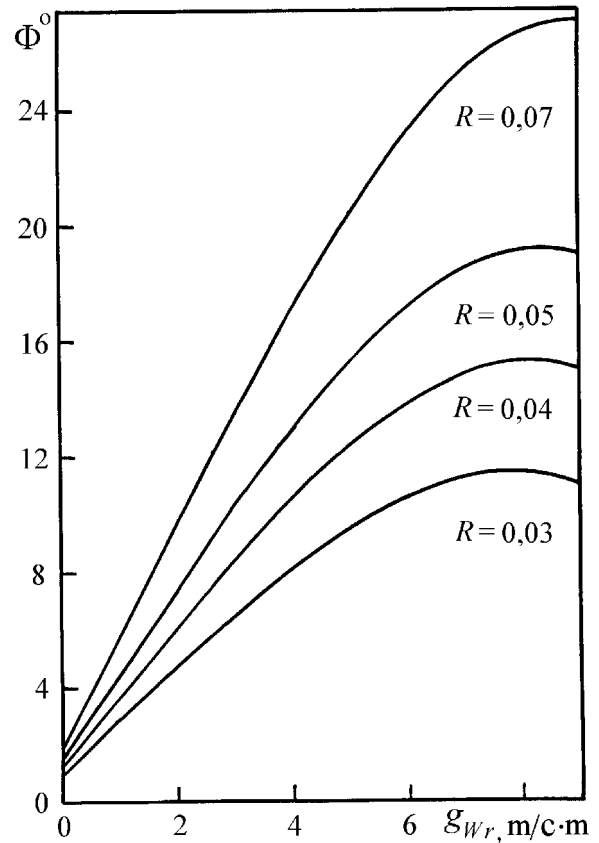


Figure 5: The measured value relation to the ethereal wind velocity gradient

the errors $\Delta\Phi_T$ are small, and they can be neglected. The executed analysis has shown, that the measurement method is tolerant practically in an isotropic case to change the environment parameters. The detected errors $\Delta\Phi$ are insignificant and represent systematic displacement, which we shall consider as the correction.

In an anisotropic case ($W_{up} > W_l > 0$, that corresponds to the positions of the initial hypothesis) from (38), (25), (26) follows, that the measured value Φ depends on a radial component gradient of the ethereal wind speed gWr and the value R . The calculation results of the relations $\Phi(gWr)$, executed at $g_n = -5 \cdot 10^{-8} m^{-1}$ are given for four values R in the Fig. 5.

The values Φ are put in grades on an ordinate axis. The curves family, given in the Fig. 5, allows to determine the values gWr by the value Φ measurement results. As the value gWr is determined as a profile derivative $W_r(Z)$, so the value Φ is proportional to the ethereal wind W_r speed.

The expressions (38), (25), (26) demonstrate the relevant property of the accepted measurement method, necessary for this research problem solving. The measured value is not equal to zero (the correction value is taken into account) only in the case, when two effects of the ethereal wind, i.e. the anisotropy effect and the

altitude effect, take place simultaneously. Really, it is easy to see, that $\Phi \neq 0$ only when $W_{rup} \neq W_{rl} \neq 0$. In other cases, when $W_{rup} = W_{rl}$ (i.e. $gW_r = 0$) or $W_{rup} = W_{rl} = 0$, the measured value $\Phi = 0$. In other words, the method is responsive to the Earth's relative movement and electromagnetic waves propagation medium — the Aether only in the case, if this medium will form a gradient layer near the Earth's surface at the motion, i.e. if the medium shows the viscosity property — the property intrinsic to material mediums, which are derivated from separate fragments. Therefore, the anisotropic effects and altitudes can be found out with the reviewed measurement method in the unified measurement act. The space effect also can be found in this unified measurement act, as the same measurements results should be subjected to the averaging procedure in the sidereal time scale for periodic components detection.

6. The measurement technique

The probing signals I_A and I_B were emitted towards one another from the points A and B accordingly. Simultaneously the probing signals reception and their processing according to the adopted measurement way were performed in each of the points. The measured values $\Delta\varphi_A$ and $\Delta\varphi_B$ were recorded on the recorders' tapes in both points. The time marks were performed in the point A and were transmitted with the signal I_A to the point B . These marks were recorded synchronically with both points of the recorders in such a way. The measurements were conducted continuously and around-the-clock. The instrumentation calibration and control of its operation implemented with the self-contained device, which performed the testing signal with controled parameters and the spectrum similar to the probing signal spectrum. Such operations were conducted at regular intervals, as a rule, 1 time for 1 operating hour.

7. The processing technique of measurement results

The measurement results processing of the values $\Delta\varphi_A$ and $\Delta\varphi_B$ included the calculation procedures of the measured value Φ ; its diurnal variation within separate sidereal day $\Phi_d(S)$; its diurnal variation within sidereal day, averaged for the whole measurements cycle of $\overline{\Phi(S)}$; root-mean-square deviations σ_Φ .

The values $\Delta\varphi_A$ and $\Delta\varphi_B$ were shown on separate chart tapes like continuous records. The signal amplitude record was used for the sites allocation, executed at hydrometeors falling. Such sites were removed from further processing. The sidereal time marks were synchro recorded on all tapes. The values $\Delta\varphi_A(S)$

Table 1: Distribution of measurement time on months of the year

Month of the year	IX	X	XI	XII	I
Common measurement time (hours)	278	193	165	300	352

and $\Delta\varphi_B(S)$ readouts were made, they were recorded in the table of the conforming observations date from these tapes with the separate slide scale, in one hour of the sidereal time. In the same table, the values of the measured value $\Phi(S)$ were recorded, calculated on the formula (10) for each of this sidereal day hours. The sequence of such numbers obtained for separate sidereal day, describes diurnal variation $\Phi_d(S)$. The calculated values were recorded in the other table. The average value of the measured one was calculated for each hour of this table sidereal day

$$\overline{\Phi(S)} = \frac{1}{\rho} \sum_{j=1}^{\rho} \Phi_j(S), \quad (39)$$

where ρ is the quantity of the value Φ readouts, made during the whole cycle of measurements, in the sidereal time equal to S . The root-mean-square deviations of values Φ from its average value were calculated for each hour of the sidereal time with the following known expression [34]:

$$\sigma_\Phi(S) = \left\{ \frac{1}{\rho} \sum_{j=1}^{\rho} [\Phi_j(S) - \overline{\Phi(S)}]^2 \right\}^{1/2}. \quad (40)$$

8. Measurement results

The results are considered in the work, which were obtained during 5 months, since September 1998 till January 1999. The measurements were conducted around-the-clock, except both weekends and holidays as well as the cases, when the electric power was not supplied to one of the measuring points for technical reasons. The general time of continuous measurements was 1288 hours. The measurement time distribution on months of the year is shown in the Tab. 1.

The distribution of readouts quantity of the measured value $\Delta\Phi$ on sidereal day time, for the whole measurement cycle (5 months), is shown in the Tab. 2.

In the Fig. 6 the examples of measurement result records, 9th November 1998 are shown.

The figure is composed from pieces mated in time of three chart tapes with the following values records: signal amplitudes, adopted in the point A (the upper curve); the phase invariant $\Delta\varphi_A$, the phase invariant

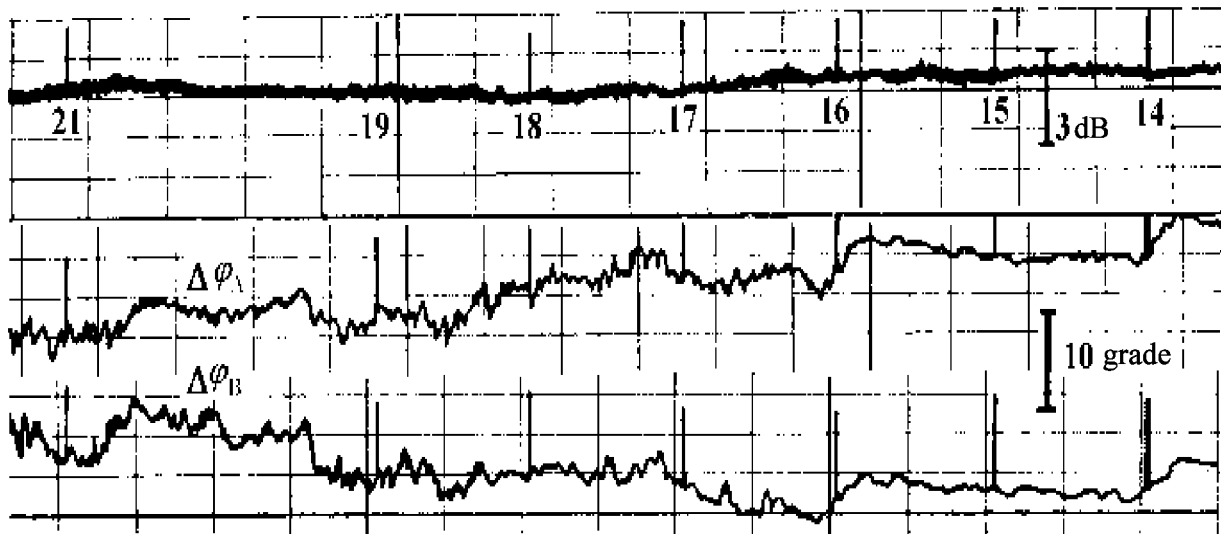


Figure 6: The example of registered values records

Table 2: Distribution of readouts quantity of the measured value on the sidereal day time

Sidereal time (hour)	1	2	3	4	5	6	7	8	9	10	11	12
Quantity of readouts	53	54	55	54	54	50	50	52	51	52	53	53
	13	14	15	16	17	18	19	20	21	22	23	24
	51	52	54	55	57	54	54	57	55	55	55	58

$\Delta\varphi_B$ (lower curve). The pieces illustrate the typical changes of the registered values. Speeds of the chart tapes drive are 20 mm/hour. The vertical strokes represent time marks in the figure. The digits under strokes indicate the sidereal time value in hours. The time flow direction is from right to left. The scale sections for a signal amplitude change estimation in decibels and phase invariant values change in degrees are marked in the figure right section. The change of time difference between the values $\Delta\varphi_A$ and $\Delta\varphi_B$, i.e. the change of the measured value $\Phi = \Delta\varphi_A - \Delta\varphi_B$ can be seen in the figure. From the moment $S = 14$ hour up to $S = 21$ hour, the value Φ has changed to $\approx 11^\circ$. The difference between values $\Delta\varphi_A$ and $\Delta\varphi_B$ fluctuations can be explained by the following. The radiowaves are propagated in counter directions in a radio link. According to the initial hypothesis, their propagation medium is the Aether — material medium, having the properties of viscous and compressible gas. The gradient speed layer is formed in the Aether flow at Aether motion near the rough surface, as well as at motion of any viscous and

compressible gas, and such motion can be accompanied by this flow parameters fluctuations. (Other causes of such fluctuations are possible also).

The ethereal wind speed fluctuations and this speed gradient g_W result in values fluctuations $\Delta\varphi_A$ and $\Delta\varphi_B$. It follows from (25), (26) and lower pieces of the Fig. 4, that such fluctuations are counter correlated. The radiowaves propagation in the Aether occurs in isotropic atmosphere available at the same time. Known atmosphere parameters fluctuations [29] also will result in fluctuations $\Delta\varphi_A$ and $\Delta\varphi_B$. It follows from (23) and lower piece of the Fig. 4, that the fluctuations g_n result in the correlated fluctuations of values $\Delta\varphi_A$ and $\Delta\varphi_B$. Therefore, the fluctuations of each values $\Delta\varphi_A$ and $\Delta\varphi_B$ within the adopted fluctuation hypothesis are the fluctuation superposition, stipulated by the indicated causes. Besides, it follows from (16), (17), that $g_{n+} \neq g_{n-}$ is at $g_{Wr} \neq 0$. In this case the radiowaves refraction, distributing in the driving Aether in counter directions, is various. The radiowaves pathways pass with the distinguished characteristics in the

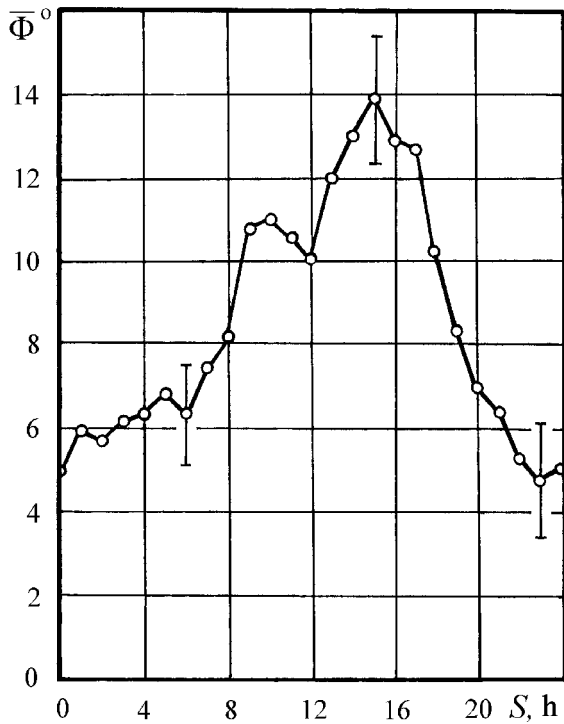


Figure 7: Mean diurnal variation of the measured value

space field, and the reflecting sites on the Earth's surface are shifted regarding each other. It can result in the values $\Delta\varphi_A$ and $\Delta\varphi_B$ fluctuation decorrelations. The reviewed features of the values $\Delta\varphi_A$ and $\Delta\varphi_B$ fluctuations formation illustrate the distinctions available, which are visible in the Fig. 6.

The systematic measurement results were subjected to statistical processing. The mean diurnal variation of the measured value within sidereal day $\overline{\Phi}(S)$ is given in the Fig. 7

The sidereal time S in hours is marked on an abscissa axis, the measured value in grades is marked on an ordinate axis. The vertical strokes indicate confidence intervals, defined as $\overline{\Phi}(S) \pm \sigma_{\Phi}(S)$. It follows from a Fig. 7, that the measurement results are not definitely zero and are not accidental observation errors. The relation $\overline{\Phi}(S)$ has the expressed form of the varied value with the period, equal to one sidereal day, i.e. the measured effect has a space parentage. It is shown above, that the measured value is not equal to zero point only in the case when two effects of the etheral wind, i.e. an anisotropies effect, stipulated by the Earth's relative movement and radiowaves propagation medium as well as the altitude effect, stipulated by the speed gradient layer in this medium flow available, take place simultaneously. The positive measurement results, given in the Fig. 7, demonstrate, that these both required etheral wind effects take place simultaneously. Therefore, the space effect development, the anisotropy effect and the

altitude effect are shown in the unified experiment, in the unified measurement act.

Let's compare the measurement results of the work to the results [5] and [11]. We shall use maximum ratings of the measured values at matching. We'll define the values g_{WrK} with the relations $\Phi(g_{Wr})$, which were given in the Fig. 5. We shall call such values g_{WrK} to be measured. The measured gradient values of the etheral wind speed horizontal component g_{WK} can be found as follows

$$g_{WK} = g_{WrK} / \cos \alpha, \quad (41)$$

that follows from the expressions (35) - (37) results. The expression (37) allows to compare the measurement results of the work to the data [5, 11]. Really, having put in (37) $Z = Z_K$ can be found, that

$$W_M = \frac{g_{WrK} e^{\beta Z_K} \sin(\delta_M + \varphi_M)}{b \beta \cos \alpha \sin(\delta_M + \varphi_K)}. \quad (42)$$

The expression (42) allows to calculate the values W_M with the measured values g_{WrK} . We shall designate the values W_M , calculated with (42), as W_{MK} and treat this value as follows: W_{MK} is the horizontal component of etheral wind speed on the geographic latitude φ_M , the altitude Z_M , calculated by the measurements results of the etheral wind velocity gradient at the latitude φ_M and the altitude Z_K .

Let's substitute the value W_M , defined by (42), in (36). Let's receive, that the radial component of the etheral wind speed in a radiolink can be determined with the following expression

$$W_{rK} = g_{WrK} (e^{\beta Z_K} - 1) / \beta. \quad (43)$$

This speed horizontal component is equal accordingly to

$$W_K = W_{rK} / \cos \alpha. \quad (44)$$

Calculated with (43), (44) we shall call also the values W_{rK} and W_K to be measured.

The parameters measurement results of the etheral wind and the work results [5, 11] are listed in Tab. 3.

The first column of the Tab. 3 represents the value measurements result $\overline{\Phi}(S)_{max}$ in grades. The columns 2,3,4 are the calculation results of the etheral wind parameters executed with the expressions (41), (44), (42) accordingly. The data about the etheral wind parameters are shown in the table like fractions. Multipair numerator corresponds to the parameter value obtained at $R = 0.04$, and denominator - at $R = 0.05$. Such form of the measurement results representation is stipulated by those, that the systematic values R measurement was not conducted during the experiments. The digit in the column 2, given in brackets, represents the calculated value g_{WK} with (37), (41), that we shall

Table 3: The ethereal wind parameters

1	2	3	4	5	6
Φ , grade	g_{WK} , m/s·m	W_K , m/s	W_{MK} , m/s	W_M , m/s [5]	W_M , m/s [11]
14	$\frac{8,63}{6,22}$; (9,05)	$\frac{1414}{1019}$	$\frac{8490}{6124}$	9000	6000

call as the anticipated ethereal wind velocity gradient value in Kharkov. The column 5 represents the maximal ethereal wind speed value, obtained by Miller at measurement results averaging, executed in the observatory Mount Wilson in April, August and September 1925 [5]. The column 6 represents the maximal ethereal wind speed value, measured in the observatory Mount Wilson in the experiment [11], 1929.

The executed estimations have shown, that the horizontal component of ethereal wind speed reaches the value $W_K \approx 1414$ m/s in Kharkov. This work measurement results are recalculated to the observatory Mount Wilson location with the expression (42). The obtained value $W_{MK} \approx 8490$ m/s, that is close to the result [5] $W_M = 9000$ m/s. A bit smaller values W_{MK} (allowing the estimations at $R = 0.05$), in comparison with the result [5], can be explained with different conditions of the experience realization. The cross-country terrains measurement are conducted on the slightly cross terrain. The ambient relief altitudes difference is about 20 m. The experiment [5] was executed at a mountain top and the ambient terrain was much below the measurement conducting place. It can be supposed, that in the first case the terrain ambient relief affect on the ethereal wind speed value is more, than in the case of the work [5]. Such supposition about the surface and local subjects influence (hills, buildings, located closely to the radiolink, etc.) has been confirmed at the results comparison [5] and [11]. So, the ethereal wind speed smaller values in [11] in comparison with the data [5] are explained in [7] by Aether flow deceleration with buildings walls, in which there was this work author's interferometer [11]. Miller [5] built a light wooden house for the measurements realization in the observatory Mount Wilson. There were continuous windows made of white canvas on all its sides. In 1929 Michelson, Peas, Pearson [11] conducted the similar experiment in a fundamental building of an optical workshop in Mount Wilson observatory. The ethereal wind measured speed was no more than 6000 m/s as a result.

The ethereal wind speed value, measured in a radio frequency band at the work, is close to the ethereal wind speeds values, measured in electromagnetic waves optical range in the experiments of Miller [5, 6], Michelson, Peas, Pearson [11]. Such comparison results can be considered as mutual confirmation of the research results veracity, the experiment [5, 6] and the experiment [11].

The ethereal wind velocity gradient measurements

were not performed in former works, we can compare the measured values g_{WK} with the anticipated (calculated) value. As we can see from the table 3 (column 2) the value g_{WK} measurement results are close to its calculated value.

The executed analysis has shown, that this work results can be explained by radiowaves propagation phenomenon in a space parentage driving medium with a gradient layer speed in this medium flow near the Earth's surface. The gradient layer available testifies that this medium has the viscosity — the property intrinsic material media, i.e. media consisting of separate particles. Thus, the executed experiment results agree with the initial hypothesis positions about the Aether material medium existence in the nature.

9. Conclusion

The parameters measurement method of anisotropic media of electromagnetic waves propagation was offered and realised in the range of millimeter radiowaves at the work. The systematic experimental research results, executed near the Earth's radiolink of a line-of-sight, have shown:

- the Earth's relative movement and radiowaves propagation medium available;
- the radiowaves propagation medium flow has a space origin;
- the radiowaves propagation medium has the viscosity — the property intrinsic to material media consisting of separate particles.

The work results can be considered as the experimental hypothesis confirmation about the existence of such material medium, as the Aether, in the nature.

References

- [1] Yu.M. Galaev, B.V. Zhukov, F.V. Kivva, "The pass-band variability of a ground communication circuit of millimeter radiowave range." Scientific instrument manufacture in mm. and sub. mm. radiowaves frequency bands: Digest of scientific works Kharkov: Institute of radiophysics and electronics engineering of NSA in Ukraine. 1992, pp. 63–72.
- [2] F.V. Kivva, Yu.M. Galaev, "Dispersion effects in frequency windows of mm wave range radio waves." Atmospheric Propagation Technical Exchange Proceedings: ARL, Orlando, FL, USA. 1993, pp. 509–517.

- [3] Yu.M. Galaev, "Model of radiowave dispersion in atmosphere." Atmospheric Propagation and Remote Sensing III: Edited by Walter A. Flood and Walter B. Miller, Proc. SPIE 2222. 1994, pp. 851–861.
- [4] Yu.M. Galaev, F.V. Kivva, "A wideband communication line of millimeter radiowaves band. Experiment. Model." 7-th International Crimean conference "Microwave technique and telecommunication technologies" (CrMiCo 97). The conference papers: Sevastopol, Crimea, Ukraine. 2, 1997, pp. 670–673.
- [5] D.C. Miller, "Significance of the ether-drift experiments of 1925 at Mount Wilson." *Science*, LXIII, No. 1635, pp. 433–443 (1926).
- [6] D.C. Miller, "The ether-drift experiment and the determination of the absolute motion of the Earth." *Rev. Modern. Phys.*, **3**, 203–242 (1933).
- [7] "Ethereal wind." Digest by Dr. in Sc. V.A. Atsukovsky. Moscow, Energoatomizdat, 1993, 289 pp.
- [8] A.A. Michelson, "The relative motion of the Earth and the Luminiferous ether." *The American Journal of Science*, III series, XXII, 128, 120–129 (1881).
- [9] D.C. Miller, "Ether-drift experiment at Mount Wilson." *Proc. Nat. Acad. Amer.*, **11**, 306–314 (1925).
- [10] S.I. Vavilov, "New "ethereal wind" searches." *Successes of physical sciences*, **6**, 242–254 (1926).
- [11] A.A. Michelson, F.G. Pease, F. Pearson, "Repetition of the Michelson - Morley experiment." *Journal of the Optical Society of America and Review of Scientific Instruments*, **18**, 3, 181–182 (1929).
- [12] R.J. Kennedy, "A refinement of the Michelson - Morley experiment." *Proc. Nat. Acad. Sci. of USA*, **12**, 621–629 1926.
- [13] K.K. Illingworth, "A repetition of the Michelson-Morley experiment using Kennedy's refinement." *Physical Review*, **30**, 692–696 (1926).
- [14] E. Stahel, "Das Michelson - Experiment, ausgefuhrt im Freiballon." *Die Naturwissenschaften*, Heft 41, **8**, 10, 935–936 (1926).
- [15] G. Joos, "Die Jenaer Wiederholung des Mihelsonversuchs." *Ann. Phys.*, **7**, 385–407 (1930).
- [16] V.A. Atsukovsky, "General etherdynamics. Simulation of the material and field structures on the basis of the imaginations about the gas like Aether." Moscow, Energoatomizdat, 1990, 280 pp.
- [17] L. Essen, "A new ether drift experiment." *Nature*, **175**, 793–794 (1955).
- [18] J.P. Cedarholm, G.F. Bland, B.L. Havens, C.H. Townes, "New experimental test of special relativity." *Phys. Rev. Letters*, **1**, 9, 342–349 (1958).
- [19] D.C. Cyampney, G.P. Isaac, M. Khan, "An ether drift experiment based on the Mssbauer effect." *Phys., Letters*, **7**, 241–243 (1963).
- [20] T.S. Jaseja, A. Javan, J. Murray, C.H. Townes, "Test of special relativity or of the isotropy of space by use of infrared masers." *Phys. Rev.*, **133a**, 1221–1225 (1964).
- [21] W. Azjukowski, "Dynamik des Athers." *Ideen des exakten Wissens*, Stuttgart, **2**, 48–58 (1974).
- [22] V.A. Atsukovsky, "The introduction into etherdynamics. Model imaginations of material and field structures on the basis of gas like Aether." Moscow, MOIP, physics dep., 1980. — Dep. in VINITI 12.06.80 No. 2760-80 DEP.
- [23] A.A. Michelson, H.G. Gale, Assisted by F. Pearson. "The effect of the earth's rotation on the velocity of light." Part II. *The Astrophysical Journal*, LXI, **5**, 140–145 (1925).
- [24] S.N. Stolyarov, "Sanyaka's experience." The Physical encyclopaedic dictionary. Moscow, The Soviet encyclopedia, 1965, **4**, 466 pp.
- [25] V.V. Nikolsky, T.I. Nikolskaya, "Electrodynamics and radiowaves propagation." Moscow, Nauka, 1989, 544 pp.
- [26] G.P. Kulemin, V.B. Razskazovsky, "Dissipation of millimeter radiowaves by the Earth's surface at small angles." Kiev, Nauk. dumka, 1987, 232 pp.
- [27] A.s. 1337829 USSR, MKI⁴ G01R29/00. "The measurement way of radiotracts characteristics." / Y.M. Galaev, B.V. Zhukov, *Bul. ed.*, **34**, 183 (1987).
- [28] V.A. Zverev, A modulation measurement method of ultrasonic dispersion." *The Reports of NSA USSR*, **91**, **4**, 791–794 (1953).
- [29] A.I. Kalinin, E.L. Cherenkova, "Radiowaves propagation and radiolinks operation." Moscow, Svyaz, 1971, 440 pp.
- [30] E.E. Vyaltseva, "Variability of the atmosphere refraction factor for a MWF in a boundary layer," *Meteorology and hydrogeology*, **2**, 8–14 (1972).
- [31] E.E. Vyaltseva, "Variability of the air refraction index for a MWF in a 300-m layer in winter." Ed. IEM, 1974. Iss. **6** (44), pp. 99–105.
- [32] G.N. Lipatov, O.Ya. Aksakova, "Some features of diurnal pass and vertical profile of radiowaves refraction index in lower 500m atmospheric layer." Ed. TSVG-MO, 1977, iss. **9**, pp. 71–78.
- [33] V.K. Abalakin, E.P. Aksenov, E.A. Grebennikov, etc. "Guide on a celestial mechanics and astronomy dynamics." Moscow, Nauka, 1976, 864 pp.
- [34] L.Z. Rumshisky, "Mathematical processing of the experiment results." Moscow, Nauka, 1971, 192 pp.

BROAD STATIC STARS CLASS MODELLING WITHIN ONE APPROACH

Alexandre Baranov¹ and Michael Lukonenko²

*Krasnoyarsk State University, Department of Theoretical Physics, 79 Svobodny Avenue, Krasnoyarsk
 660041, Russia*

Received November 30, 2000

A class of static spherical stars is considered. The Einstein equations with energy-momentum tensor in perfect fluid approximation and with the mass density distribution $\mu(x) = \mu_0(1 - x^{2\nu})^n$ are solved (μ_0 is a center density, $x = r/R$, R is the radius of star). By means a method of successive approximations with a small compactness parameter $\eta = 2M/R$ (M is mass of star) the analytical solution of approximative Einstein's equations for integer value of n parameter is received. Models of three fundamentally different astrophysical objects are considered. These are a neutron star ($n = 1$, $\nu = 1$, $\eta = 0.147$), the white dwarf Sirius B ($n = 5$, $\nu = 1$, $\eta = 1.3 \cdot 10^{-4}$), stars of main sequence such as the Sun ($n = 1$, $\nu = 1$, $\eta = 4.2 \cdot 10^{-6}$). Analysis of stability given models is conducted. Such critical parameters of considered star models as greatly possible mass, minimum star radius, greatly possible compactness is determined. Results of calculations with known observational data were correlated.

1. Introduction

At modelling of such astrophysical objects as stars, frequently it is possible to not take into account dynamic processes account into them running. The necessity of the account of changes arises then, when the star or rotates, or fast loses the mass at the expense of radiative sublimation of the matter [1] and radiation. In other cases the physical description of stars in the assumption of their static character is admissible.

In the present article the descriptive attempt of physical star properties for different types of stars within the framework of one approach is realized. At modelling except for static character of a star, it suggests its spherical symmetry. The space-time geometry of such object interior gravitational field we shall describe by a 4-interval

$$ds^2 = F(r)dt^2 + 2L(r)dtdr - r^2(d\theta^2 + \sin^2\theta d\varphi), \quad (1)$$

where functions $F(r)$ and $L(r)$ are metric coefficients. We use here a geometrical system of units in which velocity of light and gravitational constant are equal to unit. The Einstein equations are solved with a energy-momentum tensor in perfect non-viscous fluid approximation and with the mass density distribution inside a star as

$$\mu(x) = \mu_0(1 - x^{2\nu})^n, \quad (2)$$

where μ_0 is an energy (mass) density at the star centre; $x = r/R$; R is the star radius; n, ν are parameters.

We have chosen this type of mass density distribution not accidentally. For $n = 0$ and $\{\nu = 1, n = 1\}$ Einstein equations are solved analytically. If $n = 0$, we have the interior Schwarzschild solution [2], and if $\{\nu = 1, n = 1\}$, we have an exact solution for parabolic mass density distribution [3].

2. Mathematical model

For 4-interval (1) and energy-momentum tensor in perfect non-viscous fluid approximation, with mass density distributions (2), Einstein equations will look as follows

$$\varepsilon = 1 - \frac{\chi}{x} \int \mu(x)x^2 dx; \quad (3.1)$$

$$G'' + \frac{d}{dx} \left(\ln \frac{\sqrt{\varepsilon}}{x} \right) G' + \frac{\varepsilon'x + 2(1 - \varepsilon)}{2x^2\varepsilon}; \quad (3.2)$$

$$\tilde{p}' = -\tilde{p}^2 \frac{x}{2\varepsilon} + \tilde{p} \cdot \left(\frac{\varepsilon - 1 - \tilde{\mu}x^2}{2x\varepsilon} \right) + \frac{\tilde{\mu}(\varepsilon - 1)}{2x\varepsilon}, \quad (3.3)$$

where $\varepsilon = F/L^2$; $G = \sqrt{F}$; $\tilde{p} = \chi p$; $\tilde{\mu} = \chi \mu$; $\chi = 8\pi R^2$; $p(x)$ is a pressure; a prime means derivative on x .

The central of energy density μ_0 is connected with a central pressure p_0 by means the Fermi degenerated relativistic gas equation of state. The junction conditions together of an interior gravitational field of the

¹e-mail: bam@lan.krasu.ru

²e-mail: mvl@krw.ru

star with a field of an exterior solution Schwarzschild give following relations:

$$\varepsilon(x = 1) = 1 - \eta; p(x = 0) = 0 \quad (4.1)$$

$$G(x = 1) = \sqrt{1 - \eta}; G'(x = 1) = \frac{\eta}{2\sqrt{1 - \eta}} \quad (4.2)$$

where $\eta = 2M/R$ is the star compactness; M is the star mass.

Now we have system (3) with three equations and four unknown functions. These function are $\mu(x)$, $p(x)$, $\varepsilon(x)$, $G(x)$. For closing given system of equations we shall add to it the mass density distribution (2).

Thereby, expressions (2-4) describe the mathematical model of our problem. Given model has no analytical solutions under integer values of parameter $n > 1$.

3. Integration of Einstein equations

For integer values of parameter n we may multiply out of the expression (2) by means the formula of binomial theorem. Then equation (3.1) is integrated and we have relation

$$\varepsilon(x) = 1 - \eta \cdot \sigma(x)/\sigma(1) \quad (5.1)$$

with

$$\sigma(x) = \sum_{j=0}^n C_n^j \frac{(-1)^j}{2^{j\nu} + 3} x^{2j\nu+2} \quad (5.2)$$

and following equality

$$\eta = \chi\mu_0\sigma(1). \quad (6)$$

In the expression (5.1), constant of integration is put equal to zero for restriction of function $\varepsilon(x)$ in the star center. Equality (6) permits to introduce the parameter η in the system equations (2-4). For real stars $\eta \ll 1$ (for example, for the Sun $\eta_{\odot} = 4 \cdot 10^{-6}$) and we may construct an analytical approximate solution of system (2-4) by the progressive approximations method. It is a main idea of our paper.

We define function $\psi(x)$ for further calculations as $\psi(x) = \sigma(x)/(x^2\sigma(1))$.

Thus,

$$\varepsilon(x) = 1 - \eta \cdot x^2\psi(x). \quad (7)$$

On physical sense the function ψ is the ration of average mass density of the star interior part with radius $x > 0$ to the total star average mass density.

Substitution of equality (7) in equation (3.2) gives

$$(G'/x)' = \eta Q(x), \quad (8)$$

where

$$Q(x) = x\psi(x)G''(x) + x\psi'(x)G'(x)/2 + \psi'(x)G(x)/2.$$

We shall find the solution of equation (8) as series on compactness:

$$G(x) = \sum_{k=0}^{\infty} \eta^k G_k(x). \quad (9)$$

Using method to mathematical inductions, it is possible to prove validity of following formulas

$$(G'_{k+1}/x)' = \eta Q_k(x); \quad (10.1)$$

$$G_0 = 1, \quad (10.2)$$

where

$$Q_k(x) = x\psi(x)G''_k(x) + x\psi'(x)G'_k(x)/2 + \psi'(x)G_k(x)/2. \quad (10.3)$$

Expression for function $F(x)$ may be written now in the following form

$$F(x) = \sum_{k=0}^{\infty} \eta^k F_k(x) = G^2(x) \quad (11.1)$$

with

$$G^2(x) = \sum_{k=0}^{\infty} \left(\eta^k \cdot \sum_{j=0}^k G_j G_{k-j} \right). \quad (11.2)$$

Integrating twice expression (10.1), finally is obtained

$$F_k(x) = \sum_{j=0}^k \left[\tilde{Q}_j(x) + C_1^{(j)} x^2/2 + C_2^{(j)} \right] \times \left[\tilde{Q}_{k-j}(x) + C_1^{(k-j)} x^2/2 + C_2^{(k-j)} \right]; \quad (12.1)$$

$$F_0 = 1, \quad (12.2)$$

where

$$\tilde{Q}_j(x) = \int x \left(\int Q_j(x) dx \right) dx, \quad (12.3)$$

$C_1^{(j)}$ $C_2^{(j)}$ are constants of integration. These constants are defined on each step k of iterations from the functions $F_k(x)$ junction conditions on the star surface with external Schwarzschild field

$$F(x = 1) = 1 - \eta \Rightarrow F_k(x = 1) = \delta_k^0 - \delta_k^1; \quad (13.1)$$

$$F'(x = 1) = \eta \Rightarrow F'_k(x = 1) = \delta_k^1, \quad (13.2)$$

where δ_k^j is the Kronecker symbol.

Thus, the expressions (12) are the formulas of the function $F(x)$ progressive approximations method over small parameter η . That the integrand functions in (12.3) represent the sums of various real degrees x , we have no problems with calculation of analytical expression for k-approximation function $F_k(x)$ according to formula (12.1).

Table 1: Parameters of prototyped stars

Type	R	M	μ_0	n
of star	[cm]	[M_{\odot}]	[g/sm ³]	
A	$1 \cdot 10^6$	1	$1 \cdot 10^{15}$	1
B	$2.02 \cdot 10^9$	0.89	$1.3 \cdot 10^{10}$	5
C	$6.96 \cdot 10^{10}$	1	142.54	25

Table 2: Result of modelling

Type of star	p_0 [din/sm ²]	$V_{sound}(x=0)$ [c]
A	$5.84 \cdot 10^{33}$	0.21
B	$2.38 \cdot 10^{22}$	$6.68 \cdot 10^{-3}$
C	$3.46 \cdot 10^6$	$1.64 \cdot 10^{-3}$

We shall find an approximate expression for the second metric factor $L(x)$, using the relation $\varepsilon(x) = F(x)/L^2(x)$ and equality (7). Especially we shall mark that function

$$F(x) = \sum_{k=0}^{\infty} F_k(x) \quad (14)$$

is the exact solution of system equations (2-4) under choice of mass density as (2). This solution has approximate character then, when summation over k in (14) is produced up to a fixed value.

4. Real stars modelling

From boundary conditions (4.1) on function $\varepsilon(x)$ and equality (6) the relation follows

$$\sum_{j=0}^n \frac{(-1)^j}{2j\nu + 3} = \frac{2M}{8\pi\mu_0 R^3}. \quad (15)$$

One allows to coordinate parameters n and ν in the left-hand part with physical characteristics of the star.

We obtained the following values of parameter n (at $\nu = 1$) for different three types of stars. Type **A** is a neutron star, type **B** is a white dwarf (the Sirius B) and type **C** is a star of main sequence (the Sun).

The values of parameter n in Tab. 1, have some inaccuracy, connected with properties of the equality (15). The left-hand part of this equality is discrete, but right part is continuous. Therefore not always there is a possibility to select for a concrete star an integer value of parameter n , satisfying (15).

Under the formula (12) the analytical expression of an approximate solution of the system of equations (2-4) for three types of stars was obtained (Tab. 1). Central values of pressure and sound velocities V_{sound} were obtained as the result of our modelling.

Results of calculations were correlated with known observational data. For example, for the Sun model we have following facts, described in [4]:

1. value p_0 from Tab. 2 differs from known on 2% ;

Table 3: Limiting values of compactness

n	0	1	2	3	4	5
η_{max}	0.14	0.21	0.20	0.18	0.16	0.14

Table 4: Critical parameters of stars

$\{n, \nu\}$	$M^*[M_{\odot}]$	R^* [km]
{0.2, 1}	1.65	16.69
{1.4, 1}	0.85	9.58
{2.6, 1}	0.62	7.43
{3.8, 1}	0.52	6.39
{1.0, 1}	0.46	5.78
{20, 1}	0.30	3.66
{1, 0.2}	1.65	16.69
{1, 1.4}	0.85	9.58
{1, 2.6}	0.62	7.43
{1, 3.8}	0.46	6.39
{1, 1.0}	0.42	5.78
{1, 20}	0.30	3.66

2. value of pressure on boundary of the solar kernel ($x = 0.25$) on the order is less central value;
3. value of the mass density on boundary of the solar kernel on the order is less central value.

5. Stability of model

We investigated of the model stability domain in the space of parameters $\{n, \eta, \nu\}$ with using following criterions of stability:

1. Oppenheimer–Volkoff criterion of stability [5]: $dM/d\mu_0 < 0$;
2. principle of the energy domination: $p/\mu < 1/3$;
3. principle of the causality: $V_{sound} < 1$.

Thus, we have got restriction on maximum of compactness η_{max} for fixed values of parameters n and ν . These restrictions are in Tab. 3. $\{\nu = 1, 0 \leq n \leq 5\}$.

The stability criterion

$$dM/dR < 0, \quad (16)$$

is equivalent to Oppenheimer–Volkoff criterion. This criterion allows to find maximum of star masses M^* and minimum of star radii R^* , which characterized by fixed values of parameters ν and n . These restrictions for $\{\nu = 1, 0 \leq n \leq 5\}$ and $\{n = 1, 0.2 \leq \nu \leq 20\}$ are located in Tab. 4.

Comparing modelling data (Tabs. 1, 2) and restriction on use of model (Tabs. 3, 4, 5) we may conclude about applicability of this approach to broad class of

stars – from neutron stars and white dwarves up to the main sequence of stars.

Let's note that in paper [6] the star models with the energy density distribution of the type (2), however consideration was limited by $\{\nu = 1, n = 1, 2, 3\}$.

6. Conclusion

In summary, it is necessary to note that the choice of the mass density distribution as type (2) does not restrict applicabilities of our method. For realization of successive approximations method it is necessary to integrate the expressions (3.1) and (12.3) only.

The paper is realized in framework of the Federal program of Russia "Astronomy."

References

- [1] A.M. Baranov, N.N. Paklin, *Izv. Vuz. (Fizika)*, 10, 13-17 (1994). (in Russian)
- [2] J.L. Singe, "Relativity: the General Theory," Foreign Literature, Moscow, 1963, p.244 (in Russian).
- [3] A.M. Baranov, *Dep. in VINITI* 13.07.76, 2626-76 (in Russian).
- [4] "Physical encyclopedic dictionary," eds. A.M. Prohorov, *Soviet encyclopedia*, Moscow, 1983 (in Russian).
- [5] J.R. Oppenheimer, G. Volkoff in: "Albert Einstein and general relativity," Mir, Moskow, 1979, p.337 (in Russian).
- [6] H. Knutsen, *Gen. Rel. and Grav.*, **22**, 925-946 (1967).
- [7] A.M. Baranov, M.V. Lukonenko, S.F. Tegai, *Abstracts of Intern. Confer. "Geometrization of Physicis III"*, "Hater", Kazan, 1997, 6 (in Russian).

ON FIXED SINGULARITIES IN KERR-SCHILD SPACES

Alexandre Baranov¹ and Sergei Tegai¹

Krasnoyarsk State University, Department of Theoretical Physics, 79 Svobodny Avenue, Krasnoyarsk 660041, Russia

Received November 30, 2000

Kerr theorem is used to obtain possible kinds of fixed singularities in Kerr-Schild spaces with geodesic and shear-free null congruence. Function $F(G, \tau_1, \tau_2)$ determining implicitly the null congruence is chosen in the general form of square polynomial. The discriminant of the polynomial describes common singularities of the electromagnetic and gravitational fields. It is shown that all fixed singularities are intersections of two second order surfaces. For example the ring singularity of Kerr-Newman solution is an intersection of a sphere and a plane passing through the center of the sphere. With the square form of function F the Kerr-Newman solution is the only one with fixed singularity finite in the three-space.

1. Introduction

The Kerr-Schild space is described by

$$g_{\alpha\beta} = \eta_{\alpha\beta} - 2Hk_{\alpha}k_{\beta}, \quad (1)$$

where $\eta_{\alpha\beta}$ is Minkowskian metric; H is a scalar function; k_{α} is a null vector for both metrics $g_{\alpha\beta}$ and $\eta_{\alpha\beta}$:

$$g_{\alpha\beta}k^{\alpha}k^{\beta} = \eta_{\alpha\beta}k^{\alpha}k^{\beta} = 0. \quad (2)$$

Consider only the spaces assuming geodesic and shear-free null congruence with tangent vector \mathbf{k} . By Kerr theorem [1] a geodesic and shear-free null congruence can be given by

$$-k_{\alpha}dx^{\alpha} = \bar{G}d\zeta + G\bar{\zeta} + G\bar{G}dv + du, \quad (3)$$

where $u, v = x^0 \pm x^3; \zeta, \bar{\zeta} = x^1 \pm ix^2$ and $G(u, v, \zeta, \bar{\zeta})$ is implicitly determined by

$$F(G, \tau_1, \tau_2) = 0. \quad (4)$$

$F(G, \tau_1, \tau_2)$ is an arbitrary analytic function of three complex variables $G, \tau_1 = \zeta G + u, \tau_2 = vG + \bar{\zeta}$.

Common singularities of the electromagnetic and gravitational fields are given by $dF/dG = 0$. Solutions with singularities bounded in three-space are of the most interest for star exterior modelling.

2. Linear case

General linear form of function $F(G, \tau_1, \tau_2)$ is

$$F = a_1\tau_1 + a_2\tau_2 + a_3G + b_1. \quad (5)$$

The condition for singularity

$$dF/dG = a_1\bar{\zeta} + a_2v + a_3 = 0 \quad (6)$$

is a system of two real linear equations. Both describe three-dimensional hyperplanes in four-space. So the singularity can't be finite in linear case.

3. Square case

General square form of function $F(G, \tau_1, \tau_2)$ is

$$F = b_1\tau_1^2 + b_2\tau_1\tau_2 + b_3\tau_1G + b_4\tau_2^2 + b_5\tau_2G + b_6G^2 + c_1\tau_1 + c_2\tau_2 + c_3G + d_1. \quad (7)$$

The condition $dF/dG = 0$ is equivalent to the equation $D = 0$, where D is a discriminant of square polynomial $F(G)$.

Only fixed singularities are considered later. This means that D must not depend on x^0 . As D is a fourth degree polynomial all its terms with $x^{04}, x^{03}x^i, x^{02}x^{i2}$ and others containing x^0 must be equal to zero. All the discriminant's terms of fourth degree can be written in the form $(b_2^2 - 4b_1b_4)(x^{02} - x^{12} - x^{32} - x^{42})^2$. And the terms of the third degree can be written in the form

$$(x^{02} - x^{12} - x^{22} - x^{32}) \times \\ \times [(2b_2(b_3 + c_2) - 4b_1b_5 - 4b_4c_1)x^0 - \\ - (2b_2(b_5 + c_1) - 4b_3b_4 - 4b_1c_2)x^1 - \\ - i(2b_2(b_5 - c_1) - 4b_3b_4 + 4b_1c_2)x^2 + \\ + (2b_2(b_3 - c_2) - 4b_1b_5 + 4b_4c_1)x^3].$$

So the demand of fixed singularity leads to the discriminant of only the second degree. This complex discriminant gives the intersection of two real second order surfaces with additional requirements

$$b_2^2 - 4b_1b_4 = 0; \quad (8)$$

¹e-mail: bam@lan.krasu.ru

$$b_2(b_3 + c_2) - 2b_1b_5 - 2b_4c_1 = 0; \tag{9}$$

$$b_2(b_5 + c_1) - 2b_3b_4 - 2b_1c_2 = 0; \tag{10}$$

$$b_2(b_5 - c_1) - 2b_3b_4 + 2b_1c_2 = 0; \tag{11}$$

$$b_2(b_3 - c_2) - 2b_1b_5 + 2b_4c_1 = 0; \tag{12}$$

$$-4b_1b_6 - 4b_4d_1 + b_3^2 + c_2^2 + 2b_2c_3 - 4b_5c_1 + 2b_3c_2 = 0; \tag{13}$$

$$-2b_2(d_1 + b_6) + 2(b_1 + b_4)c_3 - (b_3 - c_2)(c_1 - b_5) = 0; \tag{14}$$

$$i[2b_2(d_1 - b_6) + 2(b_1 - b_4)c_3 - (b_3 - c_2)(c_1 + b_5)] = 0; \tag{15}$$

$$-4b_1b_6 + 4b_4d_1 + b_3^2 - c_2^2 = 0; \tag{16}$$

$$-4c_1b_6 - 4b_5d_1 + 2(b_2 + c_2)c_3 = 0, \tag{17}$$

where (13)-(17) are the coefficients with x^{0^2} , $2x^0x^1$, $2x^0x^2$, $2x^0x^3$, x^0 correspondingly. These constraints lead to the following cases:

- 1 $b_2 = b_1 = b_4 = 0$.
 - 1.1) $b_3 - c_2 = 0$.
 - 1.2) $b_3 - c_2 = 1$.
- 2 b_2, b_1, b_4 are not equal to zero at the same time.
 - 2.1) $b_3 \neq 0, b_5 \neq 0, b_3c_2 = b_5c_1 \neq c_3$.
 - 2.2) $c_1 \neq 0, c_2 \neq 0, b_3c_2 = b_5c_1 \neq c_3$.
 - 2.3) $b_3 = b_5 = c_1 = c_2 = 0$.
 - 2.4) $b_3c_2 = b_5c_1 = b_2c_3$.

3.1. $b_2 = b_1 = b_4 = 0$

With the notation $a_0 = b_3 - c_2$, $a_1 = b_5 - c_1$, $a_2 = i(b_5 + c_1)$, $a_3 = b_3 + c_2$ equations (13) - (16) take the simple shape of

$$a_1^2 + a_2^2 + a_3^2 = 0 \tag{18}$$

and

$$a_0a_1 = a_0a_2 = a_0a_3 = 0. \tag{19}$$

1.1 If $a_0 = 0$ the characteristic quadric form \tilde{D} of the discriminant has the shape of

$$\tilde{D} = a_1^2x^1^2 + a_1a_2x^1x^2 + a_1a_3x^1x^3 + a_2^2x^2^2 + a_2a_3x^2x^3 + a_3^2x^3^2. \tag{20}$$

The singularity described by it is a line. The linear part of the discriminant influence only on the location of the line and can be easily eliminated by linear substitution of coordinates.

1.2 In this case we get the Kerr-Newman solution [2]. The discriminant has the form of

$$D = (x^{1^2} + x^{2^2} + x^{3^2}) + c_3^2 - 4b_6d_1 + 2((b_6 - d_1)x^1 + i(b_6 + d_1)x^2 + c_3x^3). \tag{21}$$

It's real part is a sphere and it's imaginary part is a plane passing through the center of the sphere. Their intersection is a ring singularity of the Kerr-Newman solution.

3.2. $b_2 \neq 0, b_1 \neq 0, b_4 \neq 0$

The equations (9)-(12) are linear and homogeneous on variables b_2, b_1, b_4 . So b_2, b_1, b_4 are not simultaneously equal to zero only when the rank of the system is less than three. This is equivalent to

$$4(b_3c_2 - b_5c_1) = a_0^2 - a_1^2 - a_2^2 - a_3^2 = 0. \tag{22}$$

The equations (13) - (17) are also the system of linear equations on variables b_2, b_1, b_4 . The solution of this system exists only if

$$c_3^2 - 4b_6d_1 = 0. \tag{23}$$

With (8) and (22) this gives us the degenerate complex quadric form \tilde{D} . The singularity in this case is a line.

2.1 For $b_2 \neq 0, b_3 \neq 0, b_5 \neq 0$ we obtain from (9) - (12), (22)

$$b_1 = \frac{b_3}{2b_5}, b_4 = \frac{b_5}{2b_3}, c_2 = \frac{b_5c_1}{b_3}; \tag{24}$$

$$2b_6 = 2c_3b_4 + (b_3 - c_2)b_5; \tag{25}$$

$$2d_1 = 2c_3b_1 - (b_3 - c_2)c_1. \tag{26}$$

Characteristic quadric form \tilde{D} of the discriminant is proportional to

$$\begin{aligned} \tilde{D} \sim & (b_3^2 - b_5^2)^2x^1^2 - 2i(b_3^2 - b_5^2)(b_3^2 + b_5^2)x^1x^2 - \\ & - 4b_3b_5(b_3^2 - b_5^2)x^1x^3 - (b_3^2 + b_5^2)^2x^2^2 + \\ & + 4ib_3b_5(b_3^2 + b_5^2)x^2x^3 + 4b_3^2b_5^2x^3^2. \end{aligned} \tag{27}$$

Both real and imaginary parts of it have eigenvalues

$$[0, (b_3\bar{b}_3)^2 + (b_5\bar{b}_5)^2, -(b_3\bar{b}_3)^2 - (b_5\bar{b}_5)^2]. \tag{28}$$

2.2 Analogously with 2.1 we obtain

$$b_1 = \frac{c_1}{2c_2}, b_4 = \frac{c_2}{2c_1}, b_5 = \frac{c_2b_3}{c_1}. \tag{29}$$

With equations (25), (26) this gives us the quadric form

$$\begin{aligned} \tilde{D} \sim & (c_1^2 - c_2^2)^2x^1^2 - 2i(c_1^2 - c_2^2)(c_1^2 + c_2^2)x^1x^2 - \\ & - 4c_1c_2(c_1^2 - c_2^2)x^1x^3 - (c_1^2 + c_2^2)^2x^2^2 + \\ & + 4ic_1c_2(c_1^2 + c_2^2)x^2x^3 + 4c_1^2c_2^2x^3^2 \end{aligned} \tag{30}$$

and it's eigenvalues

$$[0, (c_1\bar{c}_1)^2 + (c_2\bar{c}_2)^2, -(c_1\bar{c}_1)^2 - (c_2\bar{c}_2)^2], \tag{31}$$

2.3 In this case we can assume $b_1 = f_1d_1, b_2 = f_1c_3, b_4 = f_1b_6, c_3 = 2f_2^2d_1, b_6 = f_2d_1$, where $f_1 \neq 0$ because all of b_i are not equal to zero, and we have

$$\begin{aligned} \tilde{D} \sim & (1 - f_2^2)^2x^1^2 - 2i(1 - f_2^2)(1 + f_2^2)x^1x^2 - \\ & - 4f_2(1 - f_2^2)x^1x^3 - (1 + f_2^2)^2x^2^2 + \\ & + 4if_2(1 + f_2^2)x^2x^3 + 4f_2^2x^3^2. \end{aligned} \tag{32}$$

2.4 In this case D is identically equal to zero.

$$F = ((b_5v + b_3\bar{\zeta} + b_3b_5)G + b_3u + b_5\zeta + b_5c_1)^2. \tag{33}$$

Singularity is infinite by the same reasons as in linear case. For fixed singularity $b_5 = 0$.

4. Conclusion

We see that for square form (7) of function $F(\tau_1, \tau_2, G)$ there are two kinds of singularities. First is the ring singularity of the Kerr-Newman solution and the second one is a line. So we can conclude that for obtaining of nonstationary solutions by Kerr-Schild method we need to choose higher degree of F or consider the singularities depending on time.

The paper is realized in framework of the Federal program of Russia "Astronomy."

References

- [1] D. Cramer, H. Shtefany, M. McCallum, E. Herlt, "Exact solutions of Einstein equations," Energoizdat, Moscow, 1982 (in Russian).
- [2] R.P. Kerr, W.B. Wilson *Gen. Rel. and Grav.*, **10**, 273 (1979).

ALGEBRAIC CLASSIFICATION OF 5D KRISHNA RAO WAVE SOLUTION

Alexandre Baranov¹ and Nikolai Bardushko²

*Krasnoyarsk State University, Department of Theoretical Physics, 79 Svobodny Avenue, Krasnoyarsk
660041, Russia*

Received December 14, 2000

The Krishna Rao 5D generalized solution's wave properties by means of the Weyl curvature tensor algebraic classification which was introduced earlier by one of authors are investigated. It was shown that 5D metric belongs to the algebraic class similar to Petrov's type II of 4D space-time algebraic classification while the initial 4D metric is type N.

1. Introduction

In general relativity wave solutions investigation is one of the most important problems. The same metric in various coordinates looks differently. Sometimes it is difficult to say, whether the solution of the Einstein equations belongs to a wave type or not. As a rule on this problem there can not be an answer basing only on appearance of the metric. So it is necessary to use special invariant methods for detection of wave properties of space-time.

Petrov's algebraic classification of gravitational fields is such method in 4D space-time [1]. Here we consider space-time as space with a time-like direction both 4D and 5D space-times. Using a symmetry of the curvature tensor subscripts the Riemann tensor of 4D space-time into symmetrical traceless complex 3×3 the Weyl matrix may be mapped. An eigenvalues problem of such Weyl matrix solves the task of algebraic classification of gravitational fields in 4D space-time. Depending on Weyl matrices' eigenvalues and eigenvectors we have seven matrix canonical subtypes, i.e. in 4D space-time only seven various algebraic subtypes of gravitational fields exist or total three types by Petrov [1].

It is known that gravitational fields of various types on Petrov have different the Segre characteristics of the Weyl matrix. The analysis of wave criterions in 4D space-time was investigated in details in [2]. In that classification wave solutions correspond to algebraically special types N and III as rule. The Segre characteristics of the Weyl matrices are [(2 1)] and [(3)] respectively and type N describes pure gravitational wave. Sometimes type II is considered as a wave algebraic type. In

reality the type II describes mixed gravitational fields with wave properties and has the Segre characteristic of the Weyl matrix [2 1]. The Weyl matrix canonical form of the type II is a sum of two canonical Weyl matrices: type D and type N.

2. On 5D algebraic classification

Maximum data on the space-time structure can be obtained from the curvature tensor of Riemann. That is why it is so important to extend the 4D Petrov's algebraic classification onto 5D space-time of Kaluza. An attempt of such extension and algebraic classification of some solutions was undertaken in [3]. According to this approach the conformal curvature tensor of Weyl from the Kaluza space-time is mapped to symmetrical traceless 10×10 Weyl matrix and the 5D space-time is mapped to 10D manifold of bivectors. Then it is solved the matrix eigenvalue problem in general case to classify the Kaluza space.

3. Krishna Rao generalized solution

Metric element of the 5D space-time we will take as

$$ds^2 = e^{2k}(dt^2 - d\rho^2) - \rho^2 d\varphi^2 - dz^2 - e^{2m} du^2, \quad (1)$$

where

$$k = k(t - \rho), \quad m = m(t - \rho).$$

This metric element generalizes Krishna Rao wave solution [4] onto 5D Kaluza-Klein theory. Let us to classify corresponding Weyl tensor by means of ideas from [3].

¹e-mail: bam@lan.krasu.ru

²e-mail: cut_cut@mail.ru

At first we have got to use orthonormalized 1-form basis to follow the method [3]. So we construct it as

$$\begin{aligned} \theta^{(0)} &= e^k dt, & \theta^{(1)} &= e^k d\rho, \\ \theta^{(2)} &= \rho d\varphi, & \theta^{(3)} &= dz, \\ \theta^{(5)} &= e^m dt. \end{aligned} \tag{2}$$

Nonzero conformal curvature Weyl tensor components in basis (2) are

$$\begin{aligned} W_{(0)(1)(0)(1)} &= W_{(2)(3)(2)(3)} = W_{(3)(5)(3)(5)} = \dot{m}A; \\ W_{(0)(2)(0)(2)} &= A(-B + 4\dot{k} - \dot{m}); \\ W_{(0)(2)(1)(2)} &= A(B - 4\dot{k}); \\ W_{(0)(3)(0)(3)} &= -A(B + 2\dot{k} - \dot{m}); \\ W_{(0)(3)(3)(1)} &= A(B + 2\dot{k}); \\ W_{(3)(1)(3)(1)} &= -A(B + 2\dot{k} + \dot{m}); \\ W_{(1)(2)(1)(2)} &= A(B - 4\dot{k} - \dot{m}); \\ W_{(0)(5)(0)(5)} &= -A(B - 2\dot{k} - \dot{m}); \\ W_{(0)(5)(1)(5)} &= A(2B - 2\dot{k}); \\ W_{(1)(5)(1)(5)} &= A(2B - 2\dot{k} + \dot{m}); \\ W_{(2)(5)(2)(5)} &= -3\dot{m}A, \end{aligned} \tag{3}$$

where

$$A = \frac{\epsilon^{-2k}}{6\rho}, \quad B = 2(\ddot{m} + \dot{m}^2 - 2\dot{k}\dot{m})\rho.$$

Weyl tensor may be mapped onto 10D bivector manifold by following manner. Each pair of antisymmetrical subscripts is represented as a new subscript. This subscript rule of mapping is

$$\begin{aligned} 01 \rightarrow 1, & \quad 02 \rightarrow 2, & 03 \rightarrow 3, & \quad 23 \rightarrow 4, \\ 31 \rightarrow 5, & \quad 12 \rightarrow 6, & 05 \rightarrow 7, & \quad 15 \rightarrow 8, \\ & & 25 \rightarrow 9, & \quad 35 \rightarrow 10. \end{aligned} \tag{4}$$

The mapping reduces the Weyl tensor to symmetrical traceless 10×10 Weyl matrix

$$\mathbf{W} = \tag{5}$$

w_1	w_2	w_3	w_4	w_5	w_6	w_7	w_8	w_9	w_{10}	w_{11}
w_2	w_4	w_5	w_1	w_6	w_7	w_8	w_9	w_{10}	w_{11}	w_1
w_3	w_5	w_6	w_7	w_8	w_9	w_{10}	w_{11}	w_1	w_2	w_3

Here only nonzero components are shown and

$$\begin{aligned} w_1 &= W_{(0)(1)(0)(1)}, & w_2 &= W_{(0)(2)(0)(2)}; \\ w_3 &= W_{(0)(2)(1)(2)}, & w_4 &= W_{(0)(3)(0)(3)}; \\ w_5 &= W_{(0)(3)(3)(1)}, & w_6 &= W_{(3)(1)(3)(1)}; \\ w_7 &= W_{(1)(2)(1)(2)}, & w_8 &= W_{(0)(5)(0)(5)}; \\ w_9 &= W_{(0)(5)(1)(5)}, & w_{10} &= W_{(1)(5)(1)(5)}; \\ w_{11} &= W_{(2)(5)(2)(5)}. \end{aligned}$$

The matrix (5) has a box structure according to [3]. Each box of matrix (5) represents different physical fields in 4D space-time: $W\{1..6, 1..6\}$ describes the gravitation; $W\{1..3, 6..10\}$ corresponds to the electric field; $W\{3..6, 6..10\}$ corresponds to the magnetic field; $W\{6..10, 6..10\}$ corresponds to a scalar field.

Now we set up an eigenvalue problem for the Weyl matrix (5),

$$\det|\mathbf{W} - \lambda\mathbf{I}| = 0, \tag{6}$$

where matrix

$$\mathbf{I} = \text{diag}(-1, -1, -1, 1, 1, 1, -1, 1, 1, 1)$$

is a mapping of the tensor $g_{(\alpha)(\beta)}g_{(\gamma)(\delta)} - g_{(\alpha)(\gamma)}g_{(\beta)(\delta)}$ according to the subscript rule(4).

Elementary transformations of λ -matrix are rotations of basis (2) in 5D. By means of such elementary transformations λ -matrix may be reduced to canonical form

$$\mathbf{W}(\lambda) = \text{diag}(1, 1, p_1, p_1, -p_1, -p_1^2, -p_1^2, p_2, p_3, p_4), \tag{7}$$

where diagonal components of λ -matrix (7) are the elementary divisors of eigenpolynomial (6) with their multiplicity and

$$p_1 = \lambda - \lambda_1 = \lambda - \dot{m}A;$$

$$p_2 = \lambda - \lambda_2 = \lambda - (-3\dot{m}A);$$

$$p_3 = \lambda - \lambda_3 = \lambda - (-\dot{k} - \dot{m} - \sqrt{17\dot{k}^2 + 8B\dot{k}})A;$$

$$p_4 = \lambda - \lambda_4 = \lambda - (-\dot{k} - \dot{m} + \sqrt{17\dot{k}^2 + 8B\dot{k}})A;$$

Segre characteristic in this case is

$$[(11)(122)111]. \tag{8}$$

A metric with the characteristic (8) belongs to algebraically special metric types. Our λ -matrix (6) has elementary divisors with double multiplicity.

As well as in the Petrov algebraic classification let us call it as II type. In this case every elementary divisor has its eigenvector. Eigenvectors are lightlike if they belong to the elementary divisors with double multiplicity or more. Eigenvectors in the 10D manifold define invariant directions in 5D space-time. The lightlike bivectors correspond to light-like invariant directions. So the algebraic classification may be used to determine wave structure of space-time. If a space-time is described by the Weyl matrix (5) with elementary divisors of double multiplicity or more then it has wave structure.

The considered 5D space-time with the metric element (1) has the Weyl matrix's (5) elementary divisors of double multiplicity (see (5)). These divisors correspond to following lightlike bivectors

$$\begin{aligned} \mathbf{e}_1 &= \theta^{(0)} \wedge \theta^{(2)} + \theta^{(1)} \wedge \theta^{(2)}, \\ \mathbf{e}_2 &= \theta^{(0)} \wedge \theta^{(5)} + \theta^{(1)} \wedge \theta^{(5)}. \end{aligned} \tag{9}$$

Bivectors (9) define lightlike directions in 5D space-time

$$\begin{aligned} \mathbf{l}_1 &= \theta^{(1)}, \\ \mathbf{l}_2 &= \theta^{(5)}. \end{aligned} \tag{10}$$

Thus 5D space-time with metric (1) has wave structure and the Krishna Rao generalized solution preserves its wave structure, but it is more general solution.

In 4D space-time the Krishna Rao metric belongs to the type N of Petrov’s algebraic classification. For this type of space-time the Weyl matrix has elementary divisors with double multiplicity and eigenvalues which are equal to zero.

To have complete correspondence in 5D space-time with the 4D algebraic classification we should require

$$\lambda = \frac{\dot{m}}{6\rho} e^{-2k} = 0. \tag{11}$$

The equation (11) determines N-type for the 5D space-time with metric element (1).

4. Energy-momentum tensor

It is easy to see that in 5D space-time the Ricci tensor for the metric (1) is not equal to zero. Using the generalized 5D Einstein’s equations

$$R_{(\mu)(\nu)} - g_{(\mu)(\nu)}R = -kT_{(\mu)(\nu)}, \tag{12}$$

we may write nonzero components of the energy-momentum tensor for the Krishna Rao generalized solution (1) in the orthonormalized basis (2) as

$$T_{(\mu)(\nu)} = \begin{pmatrix} T_{(0)(0)}T_{(0)(1)} & & & & \\ T_{(0)(1)}T_{(1)(1)} & & & & \\ & 0 & & & \\ & & T_{(3)(3)} & & \\ & & & 0 & \end{pmatrix}, \tag{13}$$

where R is scalar curvature; μ, ν run 0, 1, 2, 3, 5 and

$$T_{(0)(0)} = (B - 2\dot{m} + k)/\rho;$$

$$T_{(0)(1)} = -(B + \dot{k})/\rho;$$

$$T_{(1)(1)} = -(B + 2\dot{m} + k)/\rho;$$

$$T_{(3)(3)} = 2\dot{m}e^{-2k}/\rho.$$

It is seen that the energy-momentum tensor has wave structure, i.e. it has lightlike eigenvectors. According to an algebraic classification of symmetric second rank tensors the tensor (13) belongs to the class II of such classification.

5. 4D projection

To investigate observable properties of 5D space-time with metric element (1) let us produce a 4D projection, i.e. a projection on 4D space-time. This 4D-projector may be easily written in 5D form as

$${}^4g_{\mu\nu} = g_{\mu\nu} - \frac{g_{5\mu}g_{5\nu}}{g_{55}^2}, \tag{14}$$

or using the equation (1) we have 4D metric element

$${}^4ds^2 = e^{2k}(dt^2 - d\rho^2) - \rho^2 d\varphi^2 - dz^2, \tag{15}$$

which is the Krishna Rao 4D metric for the pure radiation.

6. Conclusion

The wave properties of the 5D Krishna Rao’s generalized solution have been investigated. We used an approach which is written in [3] and permits to generalize the 4D Petrov algebraic classification on 5D Kaluza space-time. It was shown that new 5D metric belongs to algebraically special type (in the sense of the 5D algebraic classification), analogous to the type II of the Petrov classification. The research of physical meaning of the 5D energy-momentum tensor is a problem of following investigation. The algebraic classification of 5D spaces may be used to systematize space-times, to analyze and to search new solutions.

References

- [1] A.Z. Petrov, “New methods in general relativity,” Nauka, Moscow, 1966, 495 p. (in Russian).
- [2] V.D. Zakharov, “Gravitational waves in the Einstein theory of gravitation,” Nauka, Moscow, 1972, 199 p. (in Russian).
- [3] A.M. Baranov, *Izv. Vuz. (Fizika)*, No.3, 73-78 (1995) (in Russian).
- [4] D. Cramer, H. Shtefany, M. McCallum, E. Herlt, “Exact solutions of Einstein equations,” *Energoizdat*, Moscow, 1982, p. 211-212 (in Russian).

Spacetime & Substance

Contents of issues for 2000–2001 years

Vol. 1 (2000), No. 1 (1)

ADDRESS TO THE READERS (1).

A. Einstein. ON THE ELECTRODYNAMICS OF MOVING BODIES (2).

Yu.S. Vladimirov. THE GRAVITATION AND BINARY GEOMETROPHYSICS (15).

N.A. Zhuck. THE IDENTITY OF INERTIAL AND GRAVITATIONAL MASSES IS PROVED! (23).

N.A. Zhuck. THE COSMIC MICROWAVE BACKGROUND AS AGGREGATE RADIATION OF ALL STARS (29).

N.D. Kolpakov. THE DISCOVERY OF POLARIZATION WAVES AND PROBLEMS OF PHYSICS (35).

V.E. Kats, A.V.Pashkov. ABSOLUTE SIGN SYMMETRY (41).

DISCUSSION (44).

THE QUESTIONNAIRE (44).

THE UKRAINIAN-RUSSIAN GRAVITATIONAL CONFERENCE (45).

RESEARCH AND TECHNOLOGICAL INSTITUTE OF TRANSCRIPTION, TRANSLATION AND REPLICATION (47).

Vol. 1 (2000), No. 2 (2)

THE EDITORIAL BOARD (49).

A. Einstein. THE EQUATIONS OF THE GRAVITATIONAL FIELD (51).

Bijan Saha. SOLITONS OF INDUCED SCALAR FIELD AND THEIR STABILITY (53).

V. Ya. Vargashkin. ANALYSIS OF *HIP* #54268 PHENOMENON AS THE EARLIEST FROM CANDIDATES TO GRAVITATIONAL MICROLENS (60).

N.A. Zhuck. GRAVITATIONAL VISCOSITY AND GEODETIC CURVATURE OF THE UNIVERSE (71).

Vasile Ureche and Rodica Roman. THE KEPLER'S THIRD LAW IN GRAVITATIONAL MANEFF'S FIELD (78).

V.A. Smirnov, G.I.Kuzjmenko. COSMOGONY AND EVOLUTION OF COMET AND METEOR SUBSTANCE IN THE SOLAR SYSTEM (81).

A.V. Snagoschenko and S.V.Bondarenko. PHILOSOPHICAL PROBLEMS OF FUNDAMENTAL CONCEPTS: "PERPETUITY", "GRAVITATION" (86).

THE UKRAINIAN-RUSSIAN CONFERENCE "GRAVITATION, COSMOLOGY AND RELATIVISTIC ASTROPHYSICS" (90).

DISCUSSION (96).

NEW BOOKS (96).

Vol. 1 (2000), No. 3 (3)

**The 1-st Scientific Conference
“NEW CONCEPTS ABOUT WORLD AND STRUCTURE OF SUBSTANCES”
(October 30, 1998, RTI TTR, Kharkov, Ukraine)
The Conference Proceedings (In Russian)**

INTRODUCTION (97)

N.A. Zhuck. NEW CONCEPTS ABOUT THE UNIVERSE AND ITS LAWS (98).

N.D. Kolpakov. NEW PHYSICS (105).

V.V. Balyberdin, N.A. Zhuck. PROSPECTS OF EXPERIMENTS ORGANIZATION ON DEFINITION OF MEDIAL DENSITY OF THE UNIVERSE AND VELOCITY OF POLARIZATION WAVES (110).

V.M. Kontorovich. MERGINGS OF GALAXIES AS THE CAUSE OF QUASARS PHENOMENON (114).

M.F. Khodjachich. COSMOLOGICAL PERIODICITIES IN RADIOSPECTRUMS OF QUASARS (121).

A.V. Archipov. ARCHAEOLOGICAL RECONNAISSANCE OF MOON (126).

A.P. Volchenko. ABOUT THE NEW APPROACH TO CONSTRUCTION OF THE SPECIAL RELATIVITY (130).

Yu.A. Bogdanov. PRACTICAL RESULTS OF FIELD INTERACTION OF NATURAL OBJECTS (135).

V.I. Balabay. THE CHARACTERISTICS OF A PHYSICAL VACUUM AND METHODS OF THEIR MEASURING (138).

Vol. 1 (2000), No. 4 (4)

**The Ukrainian-Russian Conference
“GRAVITATION, COSMOLOGY AND RELATIVISTIC ASTROPHYSICS” (GRAV-2000)
(November 8-11, 2000, Kharkov, Ukraine, Kharkov National University)
Part 1. The separate reports in English**

SCIENTIFIC PROGRAM (145).

S.A. Belousova. THE DESCRIPTION OF THE HADRON SPIN POLARIZABILITIES BY THE COVARIANT LAGRANGIAN AT LOW ENERGIES (151).

Justin Chashihin. DIMINUTION OF COSMIC DISTANCES SOLVES PROBLEMS OF SOLAR NEUTRINOS, SUPERLUMINAL EXPANSION AND GALACTIC HALOS (153).

Justin Chashihin. QUANTUM SOLUTION OF SINGULARITIES PROBLEM IN GENERAL RELATIVITY (157).

Justin Chashihin. AN IDEA FOR DIRECT EXPERIMENTAL MEASUREMENT OF THE SPEED OF GRAVITATIONAL INTERACTION (161).

A.K. Guts. THE RELATION OF UNCERTAINTY FOR RADIUS OF THE UNIVERSE (163).

D.V. Kattzyn, E.V. Saveljev. CONFORMITY IN THE SOLUTIONS OF EINSTEIN EQUATIONS FOR MODELS OF THE MULTIVARIATE UNIVERSE, FILLED WITH SUBSTANCE (165).

- D.L. Khokhlov.** ON THE FLATNESS AND HORIZON PROBLEMS (168).
- Doris Kiekhöven.** GRAVO-INERTIAL FIELD THEORY (170).
- Volodymyr Krasnoholovets.** SPACE STRUCTURE AND QUANTUM MECHANICS (172).
- Rasulkhozha S. Sharafiddinov.** ON THE GRAVITATIONAL FIELD OF THE ELECTRIC CHARGE (176).
- K.N. Sinitsyn.** THE "BLACK HOLES" AND NATURE OF "DARK MATTER" IN THE BINARY MODEL OF DISTRIBUTION OF THE DENSITY SUBSTANCE AND NATURE OF GRAVITY (179).
- K.N. Sinitsyn.** THE BINARY MODEL OF DISTRIBUTION OF THE DENSITY SUBSTANCE AND NATURE OF GRAVITY (182).
- N.A. Zhuck.** FIELD FORMULATION OF THE GENERAL RELATIVITY AND COSMOLOGY (186).
- V.A. Zykunov.** SPIN EFFECTS OF THE W-PRODUCTION IN HADRON-HADRON COLLISIONS (191).

Vol. 1 (2000), No. 5 (5)

The Ukrainian-Russian Conference

"GRAVITATION, COSMOLOGY AND RELATIVISTIC ASTROPHYSICS" (GRAV-2000)

(November 8-11, 2000, Kharkov, Ukraine, Kharkov National University)

Part 2. The separate reports in Russian

- M.M. Abdildin, M.S. Omarov, M.E. Abishev.** ON THE ORBITAL STABILITY OF THE MOTION PROBLEMS IN GR (193).
- M.M. Abdildin, M.E. Abishev.** INTEGRATION OF THE EQUATION OF ROTATION MOTION IN PROBLEM OF TWO ROTATED BODIES IN GR (194).
- A.S. Bogdanov.** PROBLEM OF THE SEARCH OPTICAL CANDIDATES ON THE IDENTITY WITH GRB (196).
- A.A. Chernitskii.** THE POSSIBILITY OF UNIFICATION FOR GRAVITATION AND ELECTROMAGNETISM IN NONLINEAR ELECTRODYNAMICS (199).
- S.S. Sannikov-Proskurjakov, M.J.F.T. Cabbolet.** RENORMALIZED NEWTONIAN CONSTANT AGAINST EQUIVLENCE PRINCIPLE (203).
- N.D. Kolpakov.** POLARIZATION WAVES AND PROBLEM OF THE GRAVITATION (207).
- M.F. Ozerov, A.E. Kochetov, L.V. Verozub.** ABOUT GRAVITY FORCE EXPERIMENTAL TESTING IN THE METRIC-FIELD GRAVITATION EQUATIONS (215).
- O.V. Sharypov, E.A. Pirogov, S.G. Grishin.** RELATIVISTIC QUANTUM-GRAVITATIONAL HYPOTHESES AND SPACE-TIME STRUCTURE (219).
- F.T. Shumakov.** CREATION OF THE RELATIVISTIC GRAVITATIONAL CONCEPT OF MODEL OF THE UNIVERSE (224).
- A.V. Snagoschenko, S.V. Bondarenko.** PHILOSOPHICAL PROBLEMS OF FUNDAMENTAL CONCEPTS: "PERPETUITY," "GRAVITATION" (229).
- V.R. Terrovere.** KLEIN'S FUNDAMENTALS OF THE SPECIAL RELATIVITY (233).
- N.A. Zhuck.** COSMOLOGICAL EFFECTS IN BULKY MICHELSON INTERFEROMETERS (235).
- I.I. Zima, G.F. Bogdanov.** CORONAL OF THE HOLE AND ROTOR MAGNETIC WAVES (238).

Vol. 2 (2001), No. 1 (6)

- L.I. Petrova.** THE ROLE OF CONSERVATION LAWS IN EVOLUTIONARY PROCESSES (1).
- N.A. Zhuck.** FIELD FORMULATION OF THE GENERAL RELATIVITY AND PROBLEMS OF COSMOLOGY (24).
- N.D. Kolpakov.** POLARIZATIONS WAVES AND PROBLEM OF GRAVITATION (31).
- Arbab I. Arbab.** A COASTING UNIVERSE WITH VACUUM ENERGY (39).
- Jo. Guala-Valverde.** THE IDENTITY OF GRAVITATIONAL MASS/INERTIAL MASS. A SOURCE OF MISUNDERSTANDINGS (42).
- Sergey Siparov.** COSMIC MASER AS A REMOTE QUANTUM DETECTOR OF THE GRAVITATIONAL WAVES: ON THE POSSIBILITIES OF THE OMPR-BASED METHOD (44).

Vol. 2 (2001), No. 2 (7)

- Afsar Abbas.** ON THE ORIGIN OF THE UNIVERSE (49).
- Arbab I. Arbab.** THE EVOLVING UNIVERSE AND THE PUZZLING COSMOLOGICAL PARAMETERS (51).
- Arbab I. Arbab.** LARGE SCALE QUANTIZATION AND THE ESSENCE OF THE COSMOLOGICAL PROBLEMS (55).
- W.B. Belayev.** COSMOLOGICAL MODEL WITH MOVEMENT IN FIFTH DIMENSION (63).
- L.C. Garcia de Andrade.** METRIC AND DENSITY PERTURBATIONS IN WORMHOLE GEOMETRY WITH SPIN-TORSION DENSITY IN FRW UNIVERSES AND THE VIOLATION OF THE WEC (66)
- M.E.X. Guimarães, L.P. Colatto and F.B. Tourinho.** ON THE WEAK-FIELD APPROXIMATION IN GENERALIZED SCALAR-TENSOR GRAVITIES (71).
- V.L. Kalashnikov.** X-MATTER INDUCED COSMOLOGICAL SCENARIOS IN THE RELATIVISTIC THEORY OF GRAVITY (75).
- Jozef Šima and Miroslav Súkeník.** BLACK HOLES — ESTIMATION OF THEIR LOWER AND UPPER MASS LIMITS STEMMING FROM THE MODEL OF EXPANSIVE NONDECELERATIVE UNIVERSE (79).
- V.R. Kurbanova and A.B. Balakin.** EXACTLY INTEGRABLE MODEL OF DYNAMICS OF VECTOR BOSONS AND BIREFRINGENCE INDUCED BY CURVATURE (82).
- I.M. Galitsky.** ABOUT NEW PHYSICS (PRINCIPLES) (84).
- DISCUSSION** (95).

Vol. 2 (2001), No. 3 (8)

- V.L. Rvachev and K. Avinash.** QUADRATIC RED SHIFT LAW AND THE NON-ARCHIMEDEAN UNIVERSE (97).
- B. Dragovich and Lj. Nešić.** ADELIC QUANTUM COSMOLOGY (100).

- A.K. Mittal, Daksh Lohiya.** CONDITIONAL COSMOLOGICAL PRINCIPLE AND FRACTAL COSMOLOGY (104).
- Alexandre Baranov and Dmitri Baranov.** STATIC STAR MODEL AND MATHIEU FUNCTIONS (108).
- H. Chávez, L. Masperi, M. Orsaria.** SUPERHEAVY PARTICLES EITHER FOR UHECR OR FOR MUON ANOMALY (111).
- Jacques Moret-Bailly.** POINTLESSNESS AND DANGEROUSNESS OF THE QUANTUM MECHANICS (116).
- Miroslav Súkeník and Jozef Šima.** PODKLETNOV'S PHENOMENON — GRAVITY ENHANCEMENT OR CESSATION? (124).
- G.B. Alaverdyan, A.R. Harutyunyan, Yu.L. Vartanyan.** ON SMALL MASS HYBRID STARS WITH QUARK CORE (129).
- M.M. Abdildin, M.E. Abishev, N.A. Beisehova.** ON SUBSTANTIATION OF RELATIVISTIC EQUATION OF ROTARY MOTION IN GR MECHANICS (132).
- Ali Shojai and Fatimah Shojai.** QUANTUM EFFECTS AND CLUSTER FORMATION (134).
- Jorge Guala-Valverde and Pedro Mazzoni.** THE UNIPOLAR MOTOR: A TRUE RELATIVIST ENGINE (140).
- DISCUSSION** (143).
- NEW BOOKS** (144).

Vol. 2 (2001), No. 4 (9)

The 1-st International Scientific Seminar

“THE THEORETICAL PREMISES AND EXPERIMENTAL FACTS OF GRAVITATIONAL SCREENING OF A SUBSTANCE”

(April 26–27, 2001, RTI TTR, Kharkov, Ukraine)

The Seminar Proceedings

- PROGRAM OF THE 1-ST SCIENTIFIC SEMINAR** (145).
- V.R. Terrovere.** KLEIN'S FOUNDATIONS OF THE UNITED THEORY OF FUNDAMENTAL INTERACTIONS AND PROBLEM OF GRAVITATIONAL SCREENING (147).
- N.A. Zhuck.** PROPERTIES OF THE YUKAWA POTENTIAL AND GRAVITATIONAL SCREENING OF A SUBSTANCE (153).
- A.A. Chernitskii.** DIRECT VARIATION OF SPACE-TIME METRIC BY ELECTROMAGNETIC FIELD (161).
- K.N. Sinitsyn.** ON THE IDEA OF GRAVITATIONAL SHIELDING OF MATTER IN BINARY MODEL (164).
- Volodymyr Krasnoholovets.** ON THE MASS OF ELEMENTARY CARRIERS OF GRAVITATIONAL INTERACTION (169).
- S.A. Sannikov-Proskuryakov, M.J.T.F.Cabbolet.** TOWARDS THE ETHER THEORY (APOLOGY OF THE ETHER) (171).
- N.A. Zhuck.** ON THE UNITED NATURE OF GRAVITATIONAL, ELECTROMAGNETIC AND NUCLEAR INTERACTIONS (175).
- V.I. Balabay.** DIFFUSION MODEL OF THE PHYSICAL VACUUM AND ITS EXPERIMENTAL CONFIRMATION (181).
- V.Ph. Tihonov.** POLARIZATION MODEL OF HYDROGEN ATOM (189).

Spacetime & Substance

International Physical Journal

INFORMATION FOR AUTHORS

The Editorial Council accepts the manuscripts for the publication only in an electronic variant in the format for LATEX 2.09. They should be completely prepared for the publication. The manuscripts are accepted by e-mail or on diskettes (3.5"). The manuscripts can be adopted in other view only for familiarization.

The original manuscripts should be preferably no longer than 6 pages. They should contain no more than 4 figures. Length of the manuscript can be up to 10 pages only in exclusive cases (at arguing problems of primary importance). If the length of the manuscript exceeds 10 pages, it should be divided by the author into two or more papers, each of which should contain all pieces of a separate paper (title, authors, abstracts, text, references etc.). The Editorial Council accepts for the publication the brief reports too.

The payment for the publication of the manuscripts is not done. Each author gets the electronic version of that Journal edition, in which his paper was published free of charge.

An E-mail message acknowledging the receipt of the manuscript will be sent to the corresponding author within two working days after the manuscript receipt. If a message is not received please contact *krasnoh@iop.kiev.ua* to inquire about the manuscripts.

The Style File and Instructions for its use can be found at <http://spacetime.narod.ru> (sample.zip, 19 kb).

An abstract (within 20 lines) must be submitted. This one should be concise and complete regardless of the paper content. Include purpose, methodology, results, and conclusions. References should not be cited in the abstract. The abstract should be suitable for separate publication in an abstract journal and be adequate for indexing.

If the argument of an exponential is complicated or long, "exp" rather than "e" should be used. Awkward fractional composition can be avoided by the proper introduction of negative degrees. Solidus fractions (l/r) should be used, and enough enclosures should be included to avoid ambiguity in the text. According to the accepted convention, parentheses, brackets, and braces are in the order { [()] }. Displayed equations should be numbered consecutively throughout the paper; the number (in parentheses) should be to the right of the equation.

Figures (black-and-white) should be of minimal size providing clear understanding. Breadth of the figure should not exceed 84 mm or 174 mm (in exclusive cases). Figures should be made out as separate files in the format of *.pcx (300 dpi/inch) or *.eps (minimum of kb).

Each figure must be cited in numerical order in the text and must have figure legend.

Tables should be typed as authors expect them to look in print. Every table must have a title, and all columns must have headings. Column headings must be arranged so that their relation to the data is clear. Footnotes should be indicated by reference marks ¹, ² etc. or by lowercase letters typed as superiors. Each table must be cited in the text.

The Editorial Council accepts also response on papers, published in the Journal. They should be no more than 1 journal page in length and should not contain figures but only to refer to the already published materials. But they can contain the formulas. The recalls are publishing in section "Discussion."

The list of references may be formed either by first citation in the text, or alphabetically.

Only works cited in the text should be included in the reference list. Personal communications and unpublished data or reports are not included in the reference list; they should be shown parenthetically in the text: (F.S. Jones, unpublished data, 1990).

The title of paper is permissible not to indicate. It is permissible to give only the initial page number of a paper. The format of the reference list is as indicated below.

References

- [1] F.W. Stecker, K.J. Frost, *Nature*, **245**, 270 (1973).
- [2] V.A. Brumberg, "Relativistic Celestial Mechanics", Nauka, Moskow, 1972 (in Russian).
- [3] S.W. Hawking, in: "General Relativity. An Einstein Centenary Survey", eds. S.W. Hawking and W. Israel, *Cambr. Univ. Press*, Cambridge, England, 1979.

Read the Journal before sending a manuscript!

CONTENTS

N.A. Zhuck, V.V. Moroz, A.M. Varaksin. QUASARS AND THE LARGE-SCALE STRUCTURE OF THE UNIVERSE 193

Yu.M. Galaev. ETHERAL WIND IN EXPERIENCE OF MILLIMETRIC RADIOWAVES PROPAGATION 211

Alexandre Baranov and Michael Lukonenko. BROAD STATIC STARS CLASS MODELLING WITHIN ONE APPROACH 226

Alexandre Baranov and Sergei Tegai. ON FIXED SINGULARITIES IN KERR-SCHILD SPACES 230

Alexandre Baranov and Nikolai Bardushko. ALGEBRAIC CLASSIFICATION OF 5D KRISHNA RAO WAVE SOLUTION 233

Spacetime & Substance. Contents of issues for 2000–2001 years 236